#### STOCHASTIC REPRESENTATION OF SURFACE ROUGHNESS AND ITS RELATION TO MANNING "n" FRICTION COEFFICIENT

Dissertation for the Degree of Ph. D.
MICHIGAN STATE UNIVERSITY
GUROL DINC
1975



This is to certify that the

thesis entitled

STOCHASTIC REPRESENTATION OF SURFACE ROUGHNESS AND ITS RELATION TO MANNING "n" FRICTION COEFFICIENT

presented by

has been accepted towards fulfillment of the requirements for

Ph.D. degree in Agricultural Engineering

Major professor

Date Feb 20, 1975

0-7639

•

#### **ABSTRACT**

#### STOCHASTIC REPRESENTATION OF SURFACE ROUGHNESS AND ITS RELATION TO MANNING "n" FRICTION COEFFICIENT

By

### Gürol Dinç

For steady state fully rough turbulent flow, the Manning equation, which relates the average velocity of flow to hydraulic radius of the conveyance system and the slope of the energy grade line, is widely used. One of the parameters of the Manning equation, the "n" friction coefficient, is related to the boundary characteristics of conveying surfaces. A concise way of relating the "n" values to a particular boundary configuration has not been available up to the present.

The current investigation proposes an approach to defining the relationship between the friction coefficient and the surface boundary. Spatial distribution of surface boundary protrusions is related to the resistance to flow. The surface protrusions are assumed to be a realization of a stochastic process with respect to distance. The techniques of autocorrelation and power spectrum analysis were used to describe the process.

The power spectrum functions of various surfaces with known "n" values, used in previous investigations, were analyzed. For each surface, a parameter, K, exponential decay coefficient, related to the spectrum function, was determined. A parabolic relationship is hypothesized between the decay coefficient and the corresponding Manning friction coefficient.

The power spectrum functions of several conveying surfaces commonly encountered in practice were experimentally determined in the laboratory. From their spectrum decay coefficients, corresponding Manning "n" friction coefficients were predicted by using the parabolic relationship. The predicted values of "n" agree well with the approximate "n" values given in the literature.

The methodology proposed appears to provide a good estimate of the Manning "n" for surfaces having high or medium roughness concentrations. The accuracy of the estimates is less for surfaces of low roughness concentrations.

BA Stort George & Merra Maja Professa

# STOCHASTIC REPRESENTATION OF SURFACE ROUGHNESS AND ITS RELATION TO MANNING "n" FRICTION COEFFICIENT

Ву

Gürol Dinç

#### A DISSERTATION

Submitted to
Michigan State University
in partial fulfillment of the requirements
for the degree of

DOCTOR OF PHILOSOPHY

Department of Agricultural Engineering

#### ACKNOWLEDGMENTS

The author wishes to thank Dr. George E. Merva (Agricultural Engineering) for serving as guidance committee chairman and for his tireless efforts and understanding in the completion of this study. A very special thanks is also extended to Dr. Dennis R. Heldman for his constructive contributions and guidance.

The author also expresses his sincere appreciation to the committee members, Dr. David C. Wiggert, Dr. Richard C. Dubes, and Dr. Ben J. Holtman, for their guidance during this study.

A thank you is also extended to my friends for their help in the experimental part of this project.

# TABLE OF CONTENTS

																Page
LIS	r of	TABLES	•	•		•	•	•	•	•	•		•	•	•	v
LIS	r of	FIGURE	s.	•	•	•	•	•	•	•	•	•	•	•	•	vi
LIS	r of	APPEND	ICES	•	•	•	•	•	•	•	•	•	•	•	•	ix
LIST	r of	SYMBOL	s.	•	•	•	•	•	•	•	•	•	•	•	•	x
1.	INT	RODUCTI	ON	•	•	•		•	•	•	•			•	•	1
2.	REVI	EW OF	LITE	RAT	JRE	•		•		•	•	•	•	•	•	5
	2.1.	Expe	rime	ntai	l St	tud:	ies	on	Roi	ıgh	nes	s of	=			
	2.2.	Dete Roug							on	Co	nce	ots	Fro	· om	•	12
	2.3.	Boun Stat							tic	Ro	ughi	ness	•	•	•	20
	2.4.	Stud Roug		s St		ies	on	Ai	rpoi	· ct	Runv	vays	•	•	•	28 33
3.	THEC	DRY .	•		•	•	•	•	•	•	•	•	•	•	•	36
	3.1.											•		•	•	38
	3.2.	Auto Func			tior •	n ar •	nd I	•	er S	Spe •	ctr	mı •	•	•	•	40
4.	EXPE	ERIMENT.	AL SI	ETUI	? A1	ND I	PROC	CEDU	JRE	•	•	•	•	•	•	44
	4.1.	-						:е	•		•	•				45 50
5.		· PUTATIO							ESUI	LTS	•	•	•	•	•	53
	5.1.						tiga	atio	ons	on	Spe	ectr	al			
		Esti	matic	on	•	•	•	•	•	•	•	•	•	•	•	54
	5.2.		othir							•	•	•	•	•	•	56
	5.3. 5.4.	Conf	idend	ce ]							ral	•	•	•	•	57
		Esti			•	•		•	•	•	• .	•	•	•	•	87
	5.5.										EST:	ımat	es	•	•	87
	5.6.	Pred.	rcrec	J Mic	ınnı	ıng	11	٧ć	ı ı ue	: S	•	•	•	•	•	90

																	Page
	5.7.	fac Ele	ces emer	Wit nts	th an	Rec d I	tan hei	rum gula r Co	ar omp	Rou ari	ghn son	ess Wi	th			•	92
6.	DISC	USSI	NC	•	•	•	•	•	•	•	•	•	•	•	•	•	105
7.	CONCI	LUSI	ONS	•	•	•	•		•	•	•	•	•	•	•	•	111
8.	RECO	MMENI	CTAC	ONS	s F	OR	FUT	URE	WO	RK	•	•	•	•	•	•	112
APPI	ENDIC	ES	•	•	•	•	•	•	•	•	•	•	•	•	•	•	113
LIST	r of i	REFEI	RENC	CES									•	•	•		134

# LIST OF TABLES

Table		Page
5.3.1.	Type of surfaces whose actual roughness profiles were obtained in the experimental procedure, their available Manning "n" friction coefficients, and the summary of computations and their results	59
5.3.2.	Type of surfaces whose actual profiles were obtained from previous research, their available Manning "n" friction coefficients, and the summary of computations and their results	60
5.4.1.	Confidence intervals on spectral estimates	87
5.6.1.	Comparison between predicted and literature values of Manning "n" friction coefficients .	92
A-1.	The surfaces and their corresponding Manning "n" coefficients obtained from the investigations of Dinc et al. (1971)	115
A-2.	The surfaces and their corresponding Manning "n" coefficients obtained from the investigations of Johnson (1944)	116
A-3.	The surfaces and their corresponding Manning "n" coefficients obtained from the investigations of E. A. LeRoux, reported by Johnson (1944)	116
A-4.	The surfaces and their corresponding Manning "n" coefficients obtained from the investigations of C. A. Smith and C. Warren, reported by Johnson (1944)	117
A-5.	The surfaces and their corresponding Manning "n" coefficients obtained from the investigations of Powell (1946)	117

# LIST OF FIGURES

Figure		Page
4.1.1.	Overall view of the experimental setup	48
4.1.2.	Corrugated plastic tubing	48
4.1.3.	Coarse gravel	51
4.1.4.	Fine gravel	51
5.3.1.	Roughness type, estimated autocorrelation, and power spectral density functions of surface 34	61
5.3.2.	Roughness type, estimated autocorrelation, and power spectral density functions of surface 36	62
5.3.3.	Roughness type, estimated autocorrelation, and power spectral density functions of surface 37	63
5.3.4.	Roughness type, estimated autocorrelation, and power spectral density functions of surface 18	64
5.3.5.	Roughness type, estimated autocorrelation, and power spectral density functions of surface 21	65
5.3.6.	Roughness type, estimated autocorrelation, and power spectral density functions of surface 23	66
5.3.7.	Roughness type, estimated autocorrelation, and power spectral density functions of surface 24	67
5.3.8.	Roughness type, estimated autocorrelation, and power spectral density functions of surface 20	68
5.3.9.	Roughness type, estimated autocorrelation, and power spectral density functions of surface 27	69

Figure		Page
5.3.10.	Roughness type, estimated autocorrelation, and power spectral density functions of surface 30	. 70
5.3.11.	Roughness type, estimated autocorrelation, and power spectral density functions of	
5.3.12.	surface 32	. 71
	and power spectral density functions of surface 39	. 72
5.3.13.	Roughness type, estimated autocorrelation, and power spectral density functions of surface 44	. 73
5.3.14.	Roughness type, estimated autocorrelation, and power spectral density functions of	_,
5.3.15.	Roughness type, estimated autocorrelation,	. 74
	and power spectral density functions of surface 40	. 75
5.3.16.	Roughness type, estimated autocorrelation, and power spectral density functions of surface 42	. 76
5.3.17.	Roughness type, estimated autocorrelation, and power spectral density functions of surface 45	. 77
5.3.18.	Roughness type, estimated autocorrelation, and power spectral density functions of	
5.3.19.	Roughness type, estimated autocorrelation,	. 78
	and power spectral density functions of surface 17	. 79
5.3.20.	Roughness type, estimated autocorrelation, and power spectral density functions of surface 15	. 80
5.3.21.	and power spectral density functions of	
	surface 10	. 81

Figure		Page	
5.3.22.	Roughness type, estimated autocorrelation, and power spectral density functions of surface 12	. 82	
5.3.23.	Roughness type, estimated autocorrelation, and power spectral density functions of surface 6	. 83	
5.3.24.	Roughness type, estimated autocorrelation, and power spectral density functions of surface 5	. 84	
5.3.25.	Roughness type, estimated autocorrelation, and power spectral density functions of surface 4	. 85	
5.3.26.	Roughness type, estimated autocorrelation, and power spectral density functions of surface 1	. 86	
5.5.1.	Behavior of the Manning "n" friction coefficient with respect to the cutoff frequency	. 89	
5.5.2.	Behavior of the Manning "n" friction coefficient with respect to the decay coefficients	. 91	
5.7.1.	Sampling function, $X_k(l)$	. 93	
5.7.2.	General correlation function of $X_k(l)$ .	. 93	
5.7.3.	The theoretical and estimated spectral density functions of surface 30	. 100	
5.7.4.	The theoretical and estimated spectral density functions of surface 23	. 101	
5.7.5.	The theoretical and estimated spectral density functions of surface 40	. 102	
5.7.6.	The theoretical and estimated spectral density functions of surface 39	. 103	

# LIST OF APPENDICES

Appen	ndix	Page
A.	Identification of surfaces obtained from previous investigations	114
В.	FORTRAN IV program for estimation of autocorrelation and power spectrum density functions	118
С.	FORTRAN IV program for estimation of decay coefficients	125
D.	FORTRAN IV program for calculation of theoretical power spectrum density functions	130

# LIST OF SYMBOLS

Symbol	Meaning
a	= Height of artificial roughness elements
b, B	= Constants
c	= Constant
c <sub>1</sub> , c <sub>2</sub> , c <sub>3</sub>	= Constants
$c_{_{ m D}}$	= Drag coefficient
C <sub><b>x</b></sub> (τ)	= Autocovariance function
C(T)	= Correlation function
đ	= Mean depth of flow
d <sup>1</sup>	= Detention
d <sub>16</sub> , d <sub>50</sub> , d <sub>84</sub>	= Percentile sizes
dw	= Weighted percentile size
dx	= Sampling interval
D	= Diameter of pipe
е	= Base of the natural logarithms
E	= Measure of roughness
Ex	= Diffusion coefficient
f	= Frequency
f <sub>c</sub>	= Cutoff frequency
fo	= Folding frequency
$f^1$	= Darcy-Weisbach friction factor
g	= Acceleration of gravity

Symbol	Meaning
G <sub>x</sub> (f)	= Power spectral density function
G(f)	= Estimated power spectral function
G <sub>x</sub> (Ω)	= Estimated spectra based on reduced frequency
<b>G (ω)</b>	= Energy spectrum
<b>G'(ω)</b>	= Normalized spectrum function
G'	= Measure of roughness
h	= Bed elevation
Н	= Head loss
H <sub>1/3</sub>	<pre>= Average amplitude of highest one-third of   waves</pre>
Η (ω)	= Spectrum of first wave form
ī, ţ, k	= Unit vectors in $x$ , $y$ , and $z$ directions
ks	= Mean diameter of sand
K	= Decay coefficient
$K_0, K_1$	= Constants
k	= Von Karman constant
l	= Distance
L	= Length of conveying system
$^{\mathtt{L}}_{\mathtt{h}}$	= Average wave length
m	= Maximum lag value
<sup>m</sup> 1	= Constant
$Mom_{O}$	= First moment of spectra
n	= Manning friction coefficient
N	= Number of data points
P	= Lag number
p •	= Constant

Symbol	Meaning
P(h,x)	= The probability of the elevation of the channel bed being ≤ h at x
Q	= Discharge
r	= Radius
R	= Hydraulic radius
R <sub>e</sub>	= Reynolds number
R <sub>χ</sub> (τ)	= Autocorrelation function
s	= Standard deviation
S	= Slope of energy grade line
s <sub>p</sub>	= Slope per unit length
t	= Time
u	= Velocity component in x-direction
v	= y component of the velocity
v	= Average velocity
$\vec{v}$	= Velocity vector
v <sub>*</sub>	= Friction velocity
w	= Width of roughness elements
x, y, z	= Directions of cartesian coordinates
x '	= Lateral distance
χ	= Roughness parameter
x	= Body forces in x-direction
x(l <sub>i</sub> )	= Random variable
x <sub>k</sub> (l)	= Sample function
y¹	= Vertical distance from the rigid boundary
Y	= Body forces in y-direction
Yn	= Normal depth

Symbol	Meaning
Yo	= Roughness parameter
z	= Body forces in z-direction
δ	= Boundary layer thickness
δ (ω)	= Delta function
λ	= Distance between roughness elements
μ <sub>χ</sub> (k)	= Mean value
ν	= Kinematic viscosity
ρ	= Density of fluid
σ <b>2</b>	= Variance
τ	= Lag distance
$\tau_{\omega}$	= Shear stress at wall
ω	= Angular frequency
ω'	= Velocity component in z-direction
Ω	= Reduced frequency

#### 1. INTRODUCTION

Three classical formulas have been widely used in engineering practice to model the average velocity of turbulent steady state fluid flow at a cross section of a water conveying system. The three formulas are: the Darcy-Weisbach equation, the Chezy equation, and the Manning equation. The Darcy-Weisbach equation is mainly used for flow in closed conduits whereas the latter two are used for open channel flow.

One of the variables involved in defining the average velocity in all three formulas is attributed to the boundary roughness characteristics of the conveying surfaces and is known as resistance or friction factor. Initially, with the acceptance of these formulas by engineers and scientists early in this century, it was thought that the friction coefficients were constant for a particular surface boundary regardless of the type of flow condition. Later, however, it was shown by many investigators that the friction coefficients would vary as much as 50 percent from their designated constant values, depending upon the nature of the flow. It thus became necessary to understand the hydraulic mechanism relating

a type of boundary roughness and the nature of flow occurring over the roughness.

The first rational formulas for hydraulic roughness were established by Nikuradse (1933) who utilized the boundary layer theory concepts of Prandtl and VonKarman, in his experimental work in pipe flow. He discovered that the friction coefficients are not functions of surface boundary characteristics alone, but are also functions of Reynolds numbers for partly rough turbulent flow while the friction factors remain constant only for fully rough turbulent flow. His definition for relative roughness in terms of sand grain height and validity ranges of the friction coefficients, as well as his proposed formulas, have been universally accepted and have led many researchers to determine an artificial standard for roughness in open channels.

Probably due to impracticality involved in regenerating Nikuradse's sand grain roughness in open channels, the investigators in this field have attempted to determine an artificial standard for roughness by using idealized geometric configurations as roughness elements in either one-dimensional form (strip roughness), or two-dimensional form (patterned roughness). For both cases, the data obtained were so scattered that the resultant derivations were either unreliable or too complex for any practical usage. Some researchers (Herbich and Shulits, 1964)

pointed out correctly that the magnitude of artificial roughness elements used in previous investigations were greater than the laminar boundary layer thickness. Because of this, the use of Nikuradse's assumptions, as discussed in Section 2.2, to correlate the roughness elements to the resistance was erroneous. Many different ways of correlation were offered instead, such as roughness concentration, projected roughness area, drag coefficient, etc. However, for each case, the results presented were beyond the simplicity that practical applications deem necessary.

There is no doubt that previous investigations on this subject contributed much toward understanding the mechanism involved between surface roughness elements and flow resistance. The previous work has been sufficient to describe friction factors in practice provided that the surface is the same form as the investigated surface from which the experimental data were obtained. Since a general and concise way of defining roughness has not been developed, difficulty arises especially when new surfaces are encountered in practice. In such a case, the engineer either determines the friction factor in the field or in the laboratory, using experiments, a practice which has been proven to be costly, or he estimates the roughness, a practice requiring a high degree of engineering judgment and one which is often risky.

A concise way of explaining a functional relationship between the concentration of roughness elements and the resistance caused by those elements can be proposed if one visualizes certain quantitative aspects of the roughness. It is fairly evident that increasing roughness element concentration increases resistance up to a maximum point, beyond which an increase in concentration decreases resistance. A quantitative way of evaluating this physical phenomenon would be to consider the contribution to the variance resulting from specific special frequencies since the distribution of the frequencies is a measure of the concentration of the roughness elements.

The method used in this study is to obtain frequency decompositions of the variance for particular surfaces for which Manning "n" friction coefficients have already been known, and to correlate the decomposition to corresponding friction factors.

#### 2. REVIEW OF LITERATURE

For three-dimensional incompressible fluid motion, the flow field is described by the pressure P, and by the velocity vector

$$\vec{V} = \vec{i}u + \vec{j}v + \vec{k}w' \qquad (2.0.1)$$

where

- u, v, w'are the three orthogonal components of
   the velocity vector in x, y, and z directions
   of cartesian coordinates, and
- $\vec{1}$ ,  $\vec{j}$ ,  $\vec{k}$  are the unit vectors in x, y, and z directions.

To determine the four quantities there exist four equations; namely, three equations of motion, and the continuity equation.

The equation of continuity states that the mass of a unit volume is constant and equal to summation of the mass entering and leaving the unit volume per unit time.

The equations of motion are directly derived from Newton's Second Law which states that the sum of the external forces acting on a body equals the product of the body's mass and its acceleration. There are two types of forces encountered in fluid motion; namely, gravitational

forces, acting throughout the mass of the body, and the pressure and friction forces acting on the boundaries of the body.

If the condition of equilibrium is assumed in fluid motion such that for each particle there exists equilibrium between body, surface forces and friction forces, then the equations of motion for incompressible fluids can be written,

$$\rho \left[ \frac{\partial \mathbf{w}}{\partial \mathbf{t}} + \mathbf{u} \frac{\partial \mathbf{u}}{\partial \mathbf{x}} + \mathbf{v} \frac{\partial \mathbf{u}}{\partial \mathbf{y}} + \mathbf{w'} \frac{\partial \mathbf{u}}{\partial \mathbf{z}} \right] = \mathbf{x} - \frac{\partial \mathbf{P}}{\partial \mathbf{x}} + \mu \left[ \frac{\partial^2 \mathbf{u}}{\partial \mathbf{x}^2} + \frac{\partial^2 \mathbf{u}}{\partial \mathbf{y}^2} + \frac{\partial^2 \mathbf{u}}{\partial \mathbf{z}^2} \right]$$

$$\rho \left[ \frac{\partial \mathbf{v}}{\partial \mathbf{t}} + \mathbf{u} \frac{\partial \mathbf{v}}{\partial \mathbf{x}} + \mathbf{v} \frac{\partial \mathbf{v}}{\partial \mathbf{y}} + \mathbf{w'} \frac{\partial \mathbf{v}}{\partial \mathbf{z}} \right] = \mathbf{Y} - \frac{\partial \mathbf{P}}{\partial \mathbf{y}} - \mu \left[ \frac{\partial^2 \mathbf{v}}{\partial \mathbf{x}^2} + \frac{\partial^2 \mathbf{v}}{\partial \mathbf{y}^2} + \frac{\partial^2 \mathbf{v}}{\partial \mathbf{z}^2} \right]$$

$$\rho \left[ \frac{\partial \mathbf{w'}}{\partial \mathbf{t}} + \mathbf{u} \frac{\partial \mathbf{w'}}{\partial \mathbf{x}} + \mathbf{v} \frac{\partial \mathbf{w'}}{\partial \mathbf{y}} + \mathbf{w'} \frac{\partial \mathbf{w'}}{\partial \mathbf{z}} \right] = \mathbf{z} - \frac{\partial \mathbf{P}}{\partial \mathbf{z}} - \mu \left[ \frac{\partial^2 \mathbf{w'}}{\partial \mathbf{x}^2} + \frac{\partial^2 \mathbf{w'}}{\partial \mathbf{y}^2} + \frac{\partial^2 \mathbf{w'}}{\partial \mathbf{z}^2} \right]$$

(2.0.2. a, b, c)

where

 $\rho$  = density of the fluid,

t = time,

X = body forces in x-direction,

Y = body forces in y-direction,

Z = body forces in z-direction, and

 $\mu = viscosity.$ 

These are the well-known differential equations of the fluid mechanics, namely, Navier-Stokes equations. The continuity equation

$$\frac{\partial \mathbf{u}}{\partial \mathbf{x}} + \frac{\partial \mathbf{v}}{\partial \mathbf{y}} + \frac{\partial \mathbf{w'}}{\partial \mathbf{z}} = 0 \tag{2.0.3}$$

along with the Navier-Stokes equations with known body forces consist of a set of four equations for the four unknowns u, v, w, and p. The solutions to these equations should satisfy the boundary and initial conditions for a particular physical flow phenomenon. For viscous fluids, the condition of no slip on solid boundaries must be satisfied, i.e., tangential and normal components of the velocity must be equal to zero.

There exists no general technique for the integration of the Navier-Stokes equations due to the complex mathematical difficulties encountered in the process (Schlichting, 1968). However, for some special cases such as Covette flow between two parallel walls, Poiseville flow through a circular pipe, etc., the exact solutions of the differential equations are known.

In the general sense, the approach to a solution of the Navier-Stokes equations has been to first consider the two limiting cases of viscosity, namely, very large and very small viscosities. In this manner the required mathematics are considerably simplified.

For motions with very large viscosity, or with very small Reynolds number, the viscous forces are far greater than the inertia forces. Inertia terms in the Navier-Stokes equations can therefore be neglected and only the terms containing the viscous forces must be retained. This results in a considerable mathematical simplification and solutions to these equations for certain cases exist.

For motions with very large Reynolds number, or with very small viscosities, viscous terms in the Navier-Stokes equations cannot be omitted, since such an assumption implies the elimination of the essential boundary condition (no slip at the wall). The resultant simplified Navier-Stokes equations have no physical meaning. In order to retain the boundary condition, Prandtl (1904) introduced the concept that the viscous effect for this type of motion is confined in a thin layer adjacent to the wall and the rest of the motion field is free from the effects of viscous forces. In the first region, which is known as the boundary layer, the motion satisfies the Navier-Stokes equations whereas in the external region the motion is defined by the equations of potential flow theory. The division of the flow field into two distinct flow regimes considerably reduces the mathematical complexities and increases the applicability of the equations to a wide spectrum of flow cases. This concept contains the

essence of the boundary layer theory approach. Pertinent portions of this theory will be reviewed in the forthcoming sections.

For very large Reynolds numbers at which turbulent fluid motion exists, the velocity and pressure components of the fluid motion do not remain constant at a fixed point with time in the flow domain. Rather, they exhibit irregular fluctuations with respect to time. Consequently, the velocity and pressure variables of the motion are described in mathematical terms as consisting of two components; namely, the average component and the fluctuating component.

The same Navier-Stokes equations (2.0.2) are used to describe fluid motion for turbulent flow, except that the velocity and pressure terms are interchanged with their time averaged components and additional stress terms, caused by the velocity fluctuation component, are introduced in the right-hand side of the equations. The "turbulent" Navier-Stokes equations, in addition to being extremely complex, cannot be solved rationally, since the relation between the mean and the fluctuation components are not known mathematically (Schlichting, 1968). Such relations are obtained only empirically and are actually the basis of turbulent boundary layer theory.

As will be discussed in the following sections, boundary layer theory is not valid for certain types of

turbulent flow (i.e., fully rough) conditions. For such flows, the relationship between the pressure gradient and the velocity can only be determined empirically (Schlichting, 1968).

For this reason, numerous empirical formulas were developed to describe fluid flow through closed or open conveying systems in the late 19th century. Among these only three have been recognized and widely used by the modern engineer. The head loss or slope of the energy grade line for a length L for fully developed uniform flow in open channels and smooth flow and partly rough flow in closed conduits has been expressed by the Darcy-Weisbach formula:

$$H = f' \frac{L}{4R} \frac{V^2}{2g}$$
 (2.0.4)

where

H = total head loss, change in elevation of the
 energy grade line over the length L,

f' = Darcy-Weisbach friction factor,

L = length of the conveying system,

V = velocity,

R = hydraulic radius, and

g = acceleration of gravity.

For closed conduits, 4R in equation (2.0.4) is replaced by the diameter of the conduit.

Another widely used equation for uniform flow in open channels is the Chezy formula:

$$V = C\sqrt{RS}, \qquad (2.0.5)$$

where

C = Chezy friction coefficient, and

S = slope of the energy grade line.

Perhaps the most well-known and used formula for relating the average velocity of flowing water to the hydraulic radius and slope of the energy grade line for uniform flow in open channels and for rough flow in closed conduits is the Manning equation which is wrongly credited to Robert Manning (1891). The relation is

$$V = \frac{1.486}{n} R^{2/3} s^{1/2}$$
 (2.0.6)

where

n = Manning friction coefficient.

The origin, development, and evolution of these formulas, as well as others, will not be reviewed in this study. Comprehensive studies on this subject were done by Houk (1918), and especially on Manning by Chow (1955), Powell (1968), and Williams (1970).

With the appearance of these formulas in hydraulics, an eagerness developed among scientists to understand the

physical interpretation of the relationships between the variables involved. This was motivated by a lack of confidence in these formulas because no one knew the flow conditions for which the equations were valid in the early part of this century. Once the ranges of application of the equations were determined, scientists and engineers began to wonder about the mathematical relationships between the friction coefficients and the surface over which flow occurred. Although numerous studies have been conducted, a concise mathematical description of the resistance coefficients has yet to be developed.

Most of the research on resistance coefficients to date has been carried out by creating artificial roughness elements and determining the behavior of coefficients under controlled conditions, or by attempting to determine behavior of the coefficients through application of boundary layer theory, or through a combination of both of these approaches. Selected, important papers will be reviewed in the pertinent sections of this chapter, and the resistance coefficients C, f, and n will be referred to as they appear in the original papers.

# 2.1. Experimental Studies on Roughness of Deterministic Surfaces

The concept of relative roughness was initiated by the famous work of Nikuradse (1933) who determined values of f over the range of laminar flow to fully turbulent flow with Reynolds numbers exceeding 100,000 for three different sizes of pipes. Sand of uniform diameter was used as a roughness element. The mean diameter  $k_{\rm S}$  of sand was chosen such that  $k_{\rm S}/r$  was the same for the three different pipes, where r is the radius of the pipe. He defined the relative roughness as  $k_{\rm S}/r$ . From a logarithmic plot of each  $r/k_{\rm S}$ , the reciprocal of the relative roughness, versus the Reynolds number and friction coefficients f', he identified three stages of flow: the first stage covered the laminar flow region and that part of the turbulent flow region in which the relative roughness has no effect on the resistance. For the laminar flow region, the friction coefficient was defined by the following relation:

$$f' = \frac{64}{Re}$$
 (2.1.1)

where

Re = the Reynolds number.

For the part of the turbulent flow unaffected by relative roughness, the Blasius (1913) law of resistance applies:

$$f' = \frac{0.316}{Re^{1/4}} \tag{2.1.2}$$

In the second range, termed the transitory range, where a comparatively abrupt transition takes place from

smooth flow to rough flow, the effect of relative roughness on resistance is noticeable in that the friction coefficient increases with increasing Reynolds numbers.

In the third range, the roughness coefficient is independent of the Reynolds number. In this range the friction factor is expressed by the following relationship given by Nikuradse (1933):

$$\frac{1}{\sqrt{f'}} = 1.74 + 2 \log_{10} \frac{r}{k_s}. \tag{2.1.3}$$

The equivalent sand-grain roughness, k<sub>s</sub>, suggested by Nikuradse as a relative measure of surface roughness, has served as a reference for numerous subsequent investigations of frictional resistance in closed conduits and open channels for partly rough and fully rough flow conditions.

The transition zone between smooth and rough flow, where the resistance depends on both the Reynolds number and the relative roughness, was not conclusively explained by Nikuradse and was the subject of studies done by Colebrook and White (1937) and Colebrook (1939). It was experimentally determined that the transition process is gradual rather than abrupt. Colebrook suggested as a transition formula for pipes:

$$\frac{1}{\sqrt{f''}} = -2 \log_{10} \left( \frac{k_s}{3.7D} + \frac{2.51}{Re \sqrt{f''}} \right)$$
 (2.1.4)

where

D = the diameter of the pipe.

Streeter (1936) used several roughness elements consisting of grooves cut spirally into pipes, to determine the effect of the shape of roughness elements on the frictional resistance. Converting the roughness elements to their equivalent sand-grain roughness by the law of similitude, Streeter concluded that the shape of the roughness elements have as much effect on the resistance as the depth of the roughness elements. Working with the Streeter type artificial roughness element on rectangular channels, Skoglund (1936) confirmed the applicability of a Nikuradse type equation (2.1.3) for predicting the friction factors for fully developed turbulent flow under the range of conditions used in his tests.

Adopting Nikuradse's methodology for pipes and using Bazin's (1865) experimental data on open channel flow, Keulegan (1938) derived a formula for fully developed turbulent channel flow. He confirmed that the resistance to flow in a rough channel having a defined degree of roughness is equivalent to the resistance to flow in a pipe having the same degree of roughness and hydraulic radius. Keulegan's formula is:

$$\frac{C}{\sqrt{g}} = 6.25 + 5.75 \log_{10} (R/k_s). \tag{2.1.5}$$

Using square steel strips across the sides and bottom of a channel as roughness elements, Powell (1946, 1950) conducted a series of experiments on eleven types of roughness configurations. From his experimental findings he concluded that the resistance to flow in a channel is not the same as that in a pipe because of the effect of the free surface and of the angles between the walls and the bottom of the channel, and between the side walls and the free surface. Considering these facts along with (2.1.5), Powell developed an expression for fully developed rough flow in open channels:

$$C = 42 \log_{10} (R/E)$$
 (2.1.6)

where

E = measure of roughness.

Although the roughness parameter E was assumed as the same as Nikuradse's  $k_{\rm S}$ , it was speculated that it would be 4 to 10 times greater than Nikuradse's  $k_{\rm S}$ , depending upon the nature of the channel. For the transition zone between smooth and rough channels where the resistance depends both on Reynolds number and the relative roughness, Powell (1950) proposed the formula

$$C = -42 \log_{10} (C/Re + E/R).$$
 (2.1.7)

Similar experiments were performed by Johnson (1944) using rectangular sills as roughness elements. He found that the spacing and the height of the elements had a considerable effect on resistance. The maximum resistance was obtained when the longitudinal spacing-to-height ratio was between 2 and 10. Robinson and Albertson (1952), keeping this ratio at 10, experimented on various sizes of geometrically similar roughness baffles in open channels. For a particular roughness, they demonstrated that Chezy's resistance coefficient C depends only on the ratio of flow depth to baffle height assuming the presence of fully developed turbulent flow conditions. A resistance formula for this particular flow type was proposed with

$$C = 26.65 \log_{10} (1.891 d/a)$$
 (2.1.8)

where

d = mean depth of flow, and

a = height of artificial roughness elements.

For natural channels, in which resistance to flow is caused by more than one type of roughness element, Nikuradse's grain-type roughness definition has been found inadequate. The relative size and the arrangement of the roughness elements play an important role in the boundary characteristics of the channel. Investigations on this type of roughness started as early as the late 1940s. Einstein and Banks (1950), using concrete blocks and metal

pegs as roughness elements in a flume, found that the total resistance exerted by combined types of roughness is equal to the sum of the resistance forces exerted by each type individually. A series of equations was developed for resistance exerted by the bed of the channel in terms of the density of roughness elements and the square of the average velocity of the flow.

Flow conditions for both the submerged and protruding cubical roughness elements with various arrangements were considered by Herbich and Shulits (1964). It was found that systematic relationships exist among Manning's n, Reynolds number, Froude number, and a special quantitative parameter of the roughness pattern. This parameter was said to be the ratio of the projected area of the roughness elements in the direction of mean flow to the horizontal area of the channel. The relationship is given in graphical form.

Rouse (1965) and Koleseus and Davidian (1966) emphasized the nature of the concentration of roughness elements as a factor influencing surface resistance.

Koleseus and Davidian concluded from the result of an extensive investigation on previous definite roughness studies that the ratio of projected roughness areas to the total floor area is, within some range of density, a satisfactory measure of roughness concentration. Furthermore, it was claimed that a simple relationship,

independent of roughness shape, exists between the roughness coefficient and the concentration which is applicable to both turbulent open and closed conduit flow. For various values of roughness concentration, Roberson and Chen (1970) obtained plots of the functions

$$1/\sqrt{f'}$$
 -2 log (R/a) versus Re $\sqrt{f'}$  (R/a). (2.1.9)

For sand-bedded channels in which the roughness is principally related to the formation of ripples, Vanoni and Hwang (1967) introduced the areal concentration of ripples as an important variable in computing the total resistance. They expressed the friction factor f' in terms of the height of the ripples, the hydraulic radius, and the areal concentration of ripples. Chang (1970), assuming the same principles, divided the total resistance into two parts, a portion due to grain-roughness and a portion due to form-roughness. He suggested that grain-roughness may be determined directly by using Nikuradse's formula (2.1.3) while form-roughness could be calculated by procedure similar to that proposed by Vanoni and Hwang.

Resistance to flow in corrugated pipes produces a different type of friction factor-Reynolds number relationship. This phenomenon was first demonstrated by Neil (1962) who found that the magnitude of f' was proportional to the number of square feet of the relative corrugation depth. Working with corrugated plastic tubing, Dinc et al.

(1971) demonstrated that depth, spacing, and shape of corrugations affect the resistance, and even in fully developed turbulent flow they observed that the Manning n varied to some extent, contrary to the common belief that the friction factor is constant at that region.

# 2.2. Roughness Studies Based on Concepts From Boundary Layer Theory

Prandtl (1904) discovered that for most applications of fluid flow, the influence of viscosity is confined to an extremely thin region adjacent to the rigid boundary surface. This region is known as the boundary layer. The fundamental assumption of the boundary layer approximation is that the fluid particles next to the rigid boundary are at rest. Hydrodynamically, the velocity boundary layer is defined as that region within which the flow velocity ranges from zero, at the rigid boundary, to a constant value, the free stream velocity. Boundary layers may be either laminar or turbulent. The laminar boundary layer is always present over a rigid body when the Reynolds number in a pipe flow situation is less than 2000 and this type of flow is termed laminar flow. At Reynolds numbers greater than 2000, the laminar boundary tends to become unstable and a new type of boundary layer develops simultaneously with a transition to turbulent flow. layer is called the turbulent boundary layer. Since most flows in engineering practice are turbulent, no attempts

will be made to discuss the concept of the laminar boundary layer theory in this review. The turbulent boundary layer theory is not completely formulated in the mathematical The theory is based on semi-empirical relationships derived from correlating experimental observations. Researchers have observed that the turbulent boundary layer consists of two principal regions: an inner and an outer region. In the inner region, the characteristics of the rigid surface are important factors in determining the form of the velocity profile, whereas in the outer region the velocity profile surface and the history of the layer are important. The velocity distribution in the boundary layer may be expressed in either a logarithmic or a power law form. In the inner boundary layer, the logarithmic law takes the general form given by the ASCE Task Force Report (1963),

$$\frac{\mathbf{V}}{\mathbf{V}_{\star}} = \frac{1}{\mathbf{k}} \log_{\mathbf{e}} \frac{\mathbf{Y}'}{\mathbf{Y}_{\mathbf{O}}} + \mathbf{b} \tag{2.2.1}$$

whereas the logarithmic law for the outer layer is

$$\frac{\mathbf{V} - \mathbf{v}}{\mathbf{V}_{\perp}} = -\frac{1}{k} \log_{\mathbf{e}} \frac{\mathbf{y'}}{\delta} + \mathbf{c}$$
 (2.2.2)

where

v = y component of the velocity,

k = Von Karman constant,

y' = vertical distance from the rigid boundary,

V = free stream velocity,

b, c = constants,

 $\delta$  = boundary layer thickness,

$$V_{\star}$$
 = friction velocity =  $\sqrt{\frac{\tau_{\omega}}{\rho}}$ ,

 $\tau_{ii}$  = shear stress at the wall,

 $\rho$  = density of the fluid, and

Y = roughness parameter.

The constants k and b are believed to be universal constants. Von Karman's constant is usually assumed to be 0.4 while b is assigned the value 5.5. However, Vononi (1953) and Sayre and Albertson (1961) found evidence that k is not a constant, but is influenced by such factors as suspended-sediment concentration and boundary roughness. The constant c varies with the nature of the flow and frequently with the characteristics of the surface boundary.

The power law (ASCE Task Force Report, 1963), when the Reynolds number is less than 100,000 for the inner and outer regions, takes the form, for the inner region

$$\frac{\mathbf{v}}{\mathbf{V}_{\star}} = 8.74 \left( \mathbf{Y} \frac{\mathbf{V}_{\star}}{\mathbf{v}} \right)^{1/7} \tag{2.2.3}$$

in which  $\nu$  is kinematic viscosity. For the outer region

$$\frac{\mathbf{v}}{\mathbf{v}} = \left(\frac{\mathbf{y}}{\delta}\right)^{1/7}.\tag{2.2.4}$$

In an examination and reinterpretation of the extensive measurements of Nikuradse, Martinelli (1947) discovered three distinct regions associated with the logarithmic representations of the boundary layer. For  $v/V_{\star} < 5$ , he found that the data showed a linear dependence between  $v/V_{\star}$  and  $y'/Y_{o}$  and he termed this region the laminar sublayer. For 5 <  $v/V_{\star} < 30$  and  $v/V_{\star} > 30$  the general logarithmic laws for the inner and outer regions appeared to hold and these regions were termed the buffer layer and the turbulent core, respectively. Martinell's interpretation of the boundary layer is widely accepted.

The term  $Y_0$  in (2.2.1) is attributed to the roughness parameter of the rigid boundary. It is frequently defined:

$$Y_{O} = k_{S} f\left(\frac{k_{S} V_{*}}{V}\right). \qquad (2.2.5)$$

From his experiments with sand grains as roughness elements, Nikuradse (1933) discovered that for fully rough turbulent flow  $f(k_S V_*/v)$  in (2.2.1) can be written in the more general form:

$$\frac{v}{v_{*}} = \frac{1}{k} \log_{10} \frac{y'}{k_{s}} + B$$
 (2.2.6)

where

B = constant.

From his experimental data Nikuradse found that B is 8.5 for the flow condition used.

Nikuradse's sand grain definition of roughness and his proposed equation, (2.2.6), have been widely accepted by scientists and engineers and have been used to determine the friction coefficient of the rigid boundary for the particular flow under consideration.

Some scientists have argued, however, that since the surface resistance is related to the development of the boundary layer, the equations, derived on the assumption that the boundary layer is fully developed, could not be applied to types of flow for which developing boundary layers exist. These types of flow commonly occur in practice when the properties of bed materials change drastically; i.e., for joints on concrete-lined channels, changes from concrete to natural channels, changes in surface materials on natural channel beds, etc. Another type of problem arises from the application of universal boundary layer equations when the surface protrusions are the same or are of greater magnitude than the laminar sublayer thickness. Here the protrusions tend to disturb or break up the laminar sublayer and consequently increase the shear stress on the wall. It has been experimentally demonstrated (Herbich and Shulits, 1964) that for sufficiently rough surfaces no predominantly viscous region exists. The apparent shear forces are transmitted to the

wall in the form of pressure drag on the protrusions.

Hence the basic assumptions of the boundary layer theory

collapse for this type of surface.

Realizing the fundamental fact that the main source of friction loss in a fluid flowing over a sufficiently rough surface comes from the generation, separation, and subsequent dissipation of vortices from the wake and separation zones behind each roughness element, Morris (1955) concluded that the longitudinal frequency of each element is a significant parameter in the definition of the turbulence structure and energy dissipation phenomena. Morris suggested that k can be determined in a more fundamental way than that given by (2.2.6). define the surface geometry, two new parameters were introduced: the roughness index, defined as  $\lambda/a$ , the ratio of the roughness element spacing to the height of the projections; and the relative roughness spacing, defined as  $r/\lambda$ , the ratio of radius to the spacing of the roughness elements. Based on these parameters, he classified three types of roughness:

(1) Isolated roughness, where the surface protrusions are far apart, as are the joints in concretelined channels. The friction factor results from the form
drag on the roughness elements plus the friction drag on
the surface between elements. Thus, the roughness index

 $\lambda/a$  is a significant correlating factor for this type of flow.

- (2) Wake-interference roughness, where the roughness elements are close enough to each other so that the zones of separation and vortex generation and dissipation associated with each element are intermingled. The friction drag on the wall does not contribute to the total friction. Therefore the height, a, of the elements is unimportant but the spacing  $\lambda$  is of major importance, making the relative roughness spacing  $r/\lambda$  an important friction correlating factor.
- (3) Quasi-smooth roughness, where the roughness elements are so close together that between the elements, regions of dead water containing stable vortices exist. The energy loss for this type of flow is largely due to the width or depth of the elements. Hence, the roughness index expressed either by  $\lambda/a$  or  $\lambda/w$  (w is the width of the elements) is an important factor influencing the apparent friction. Morris presented different formulas for each type of flow.

Raju and Garde (1970), using the data collected from their investigation along with those of Sayre and Albertson (1961), and Basha (1961), checked the reliability of the method suggested by Morris. They found that the agreement of the experimental data with Morris' approach is valid for certain types of flow although in

some cases it may either over- or under-predict the resistance. It was therefore concluded that the method was not sufficiently reliable. Rather, Raju and Garde proposed a more general form of flow equation on the assumption that the total resistance is equal to the form drag resistance of the roughness elements. Their empirical relation is

$$\frac{1}{C_D} = C_1 \log \frac{d}{a} + C_2, \qquad (2.2.7)$$

where

C<sub>D</sub> = drag coefficient based on free stream
 velocity,

 $C_1$   $C_2$  = constants, and

a = height of roughness elements.

The coefficients  $C_1$  and  $C_2$  were independently determined for each roughness index,  $\lambda/a$ .

For hydrodynamically rough surface boundaries where roughness elements are protruding above the laminar sublayer, Sayre and Albertson (1961) introduced a new roughness parameter  $\chi$ , which is considered a function of both the relative size and the relative spacing of the roughness elements. It was experimentally found that for open channels, a logarithmic relationship exists between the Chezy coefficient C, and the general roughness parameter  $\chi$ . The relationship is

$$\frac{C}{\sqrt{q}} = 6.06 \log_{10} \frac{Y_n}{\chi},$$
 (2.2.8)

where

Y<sub>n</sub> = normal depth; i.e., depth of flow occurring when the slopes of the energy gradient, the water surface, and the bed are equal.

It was found that (2.2.8) gave more accurate results than the Manning formula for the range of roughness and flow conditions of the experiment. Sayre and Albertson's (1961) approach was extended to study the natural roughness effects in open channels by Mirajgaoker and Charlu (1963). Using 2.5-3 in. average diameter stones as roughness elements, they obtained a logarithmic expression similar to (2.2.8) for their particular flow conditions. The relationship found was

$$\frac{C}{\sqrt{g}} = 5.72 \log \frac{Y_n}{\chi} + 1.72. \tag{2.2.9}$$

## 2.3. Statistical and Stochastic Roughness Studies

In considering the irregularity of natural channel beds and their variation with respect to time and space, some investigators (Limerinos, 1970; Nordin and Algert, 1966) have reasoned that the application of the results of roughness studies based on geometrically deterministic surfaces to stochastic surfaces would be erroneous; hence,

the correct way to analyze nondeterministic roughnesses would be to utilize the methods of statistics. The concept of statistical analysis in roughness studies is relatively new and consequently only a limited number of works are available in the literature.

Statistical parameters for roughness studies were first used by Leopold and Wolman (1957) who described the Darcy-Weisbach friction factor, f', as a function of a parameter, percentile size, which is defined as an intermediate diameter of particle size that equals or exceeds that of an arbitrarily chosen percentage of the stream bed particles. Am empirical equation for the friction factor, f', was developed in the form

$$\frac{1}{\sqrt{f!}} = 1.00 + 2.0 \log \frac{R}{d_{RA}}$$
 (2.3.1)

where

d<sub>84</sub> = the particle size, that equals or exceeds
 the diameter of 84 percent of the stream
 bed particles.

Similar equations were derived by Limerinos (1970) using  $d_{16}$ ,  $d_{50}$ , and  $d_{84}$  as particle size parameters. In addition, Limerinos introduced a weighing parameter,  $d_w$ , which was defined by assigning a weight of 0.1 to  $d_{16}$ , a weight of 0.3 to  $d_{50}$ , and a weight of 0.6 to  $d_{84}$ . The

relations best fitting the experimental data were obtained by using either  $d_{84}$  or  $d_w$ .

Stochastic processes in roughness studies in hydraulics were first used by Nordin and Algert (1966). They assumed that the elevations of a dune bed along an alluvial channel are random variables which are realizations of a stochastic process with respect to distance. The techniques of autocovariance and spectral density analysis were used to describe the properties of the process. Based on the experimental observations, it was reasoned that the velocity near the bed is influenced only by the properties of the bed profile in the adjacent Therefore, the stochastic process was upstream area. represented by a Markov second-order linear model. first three values of the covariance function were used to model the process. It was experimentally found that the significant wave height for the dunes was related to the variance by the following model:

$$H_{1/3} = 3(\sigma^2)^{1/2} \tag{2.3.2}$$

where

 $H_{1/3}$  = average amplitude of the highest onethird of the waves, and

 $\sigma^2$  = variance of the dune elevation.

It was concluded that  ${\rm H}_{1/3}$  values, obtained from the first three values of the covariance function for several discharges, correlate well with the flow parameter of unit discharge. However, Squarer (1970) demonstrated that a second-order Markov model did not fit the bed configurations in his investigation. Instead, parameters of roughness elements, height, and length were obtained directly from the autocorrelation and spectral density function. The height parameter was given in terms of the standard deviation of the bed elevation and the length was given in terms of the moments of the spectrum.

The concept of using moments of the spectra to define the roughness parameters was also introduced by Burney and Higgins (1973). From their experimental results a general model was developed to describe average runoff depth from a watershed in the form

$$d^1 = .004 \sqrt{Q} S_p^{\chi},$$
 (2.3.3)

where

d<sup>1</sup> = average flow depth,

Q = discharge,

 $S_p = slope per unit length, and$ 

 $\chi$  = roughness parameter.

The roughness parameter  $\chi$  was postulated to be a function of grain and form roughness and was obtained from the area

spectrum of the watershed. It was suggested that  $\chi$  could be described by the expression,

$$\chi = \frac{\text{Mom}_0^{1/2}}{L_h}, \qquad (2.3.4)$$

in which  $L_h$  is the average wave length perpendicular to both the flow direction and flow depth, and  ${\rm Mom}_{\rm O}$  is the first moment of the spectra. In terms of roughness configurations the  ${\rm Mom}_{\rm O}^{1/2}$  value reflects a parameter of grain roughness whereas  $L_h$  describes a parameter for the distribution of the roughness elements.

Assuming bed elevations of an irregular channel are random variables, Chiu (1968) claimed that the Brownian motion process is a suitable stochastic model to stimulate roughness elements satisfying the following diffusion type equation:

$$\frac{\partial P(h,x)}{\partial x} = E_x \frac{\partial^2 P(h,x)}{\partial h^2}, \qquad (2.3.5)$$

where

x = lateral distance,

h = bed elevation, and

 $E_{y}$  = diffusion coefficient.

The diffusion coefficient,  $E_{\chi}$ , was claimed to be a parameter defining channel roughness. Furthermore, it was concluded that the probability  $P(h,\chi)$  could be obtained by a Monte Carlo simulation without actually solving equation (2.3.5).

### 2.4. Roughness Studies on Airport Runways

Another extensive type of surface roughness study, unrelated to fluid mechanics, has been completed by aeronautical scientists. The studies are conceived with runway roughness problems encountered by aircraft during taxiing operations. In all the studies mentioned here, the height of surface roughness elements along longitudinal cross-sections of runways were assumed to be a random variable and the techniques of autocorrelation and spectral density analysis were used to describe the contribution to the variance of the roughness elements as a function of the spatial frequencies.

The use of power spectrum techniques in roughness analysis was pioneered by Walls et al. (1954) who selected two runways which were known to possess very different degrees of roughness. The spectrum of the runways showed that the rougher runway had 10 times the power of the smooth runway at the longer wave lengths and about twice the power at the shorter wave lengths. From this observation it was concluded that the behavior of the power spectrum provided an important guide toward the establishment

of criteria for runway roughnesses. In order to increase the amount of data available for studies of this nature, additional contributions were made by Potter (1957) and Thompson (1958) who obtained the power spectrums of several different runways.

Reviewing previous investigations on runway roughness, Houbolt et al. (1955) concluded three significant points: (1) The power spectrum is a very concise way of presenting runway characteristics. (2) A means is suggested for establishing a criterion for judging the severity of runway roughness. By holding the spectra of satisfactory runways as references, a spectrum criterion may be established for the construction of future runways or for maintenance of existing runways in order to insure satisfactory operations. (3) A "design spectrum" might also conceivably be established which provides the basis for solving taxiing problems.

Houbolt (1961) assumed a general model to represent the power spectrum function

$$G_{\mathbf{x}}(\Omega) = \frac{C_3}{m_1} \tag{2.4.1}$$

where

 $G_{\mathbf{X}}(\Omega)$  = roughness spectrum (ft<sup>2</sup>/radian/ft),  $C_{3}$ ,  $m_{1}$  = constants, and  $\Omega$  = reduced frequency (radians/ft). Integrating (2.4.1) produces an expression for the variance of roughness elements present in a wave length  $\mathbf{L}_{h}$  and yields an expression for standard deviation

$$s = \left(\frac{K_1}{p'-1}\right)^{1/2} \left(\frac{x'}{2\pi}\right)^{\frac{p'-1}{2}}.$$
 (2.4.2)

The maximum deviations of the roughness elements about a mean line in length x' were assumed to be of  $\sqrt{2}$  times s and the resulting equation was regarded as a criterion of smoothness,

$$G^{1} = \sqrt{2} \left( \frac{K_{1}}{p'-1} \right) \left( \frac{x'}{2} \right)^{\frac{p'-1}{2}}.$$
 (2.4.3)

By using a very good commercial runway as a criterion, values of  $K_1$  and p' in (2.4.3) were obtained. After arithmetical simplifications, (2.4.3) was converted to the form

$$G^1 = 0.00146 \sqrt{x^{\dagger}}$$
 (2.4.4)

It was concluded that good, acceptable runways should meet this criterion.

#### 3. THEORY

A hydrodynamically rough or fully turbulent flow condition over a surface occurs either if the Reynolds number is large causing the laminar sublayer to shrink, causing the roughness elements to protrude through the laminar sublayer, or if the roughness elements are initially large enough so that they already protrude through the sublayer regardless of the Reynolds number. For this type of flow, for which Manning's formula or Chezy's formula are mainly used as models, the friction factors are independent of the Reynolds number. The independence of the friction factors for the first type of fully turbulent flow mentioned above was discovered by Nikuradse (1933), and that for the latter type has been accepted by most researchers after Nikuradse. The independence of the friction factors on the Reynolds number plays an important role in defining the relationship between the roughness characteristics of a surface and the corresponding flow resistance. The independence hypothesis implies that the only variable affecting the resistance to flow is the roughness makeup of the surface; i.e., the concentration of the roughness elements constituting a surface. One possible way to correlate the friction factor to the surface configuration would be to first describe the surface realistically, then analyze the frequency distribution of the concentration of the surface elements.

The Review of Literature stated that some researchers have concluded that the roughness of a water conveying surface is made of local elevation of surfaces which are, in nature, nondeterministic. For this reason, a mathematical description of the roughness cannot be achieved with artificial deterministic surfaces. tistical methods, which have been employed in the past in the analysis of various nondeterministic phenomena, can be more properly adopted to analyze and characterize surface roughness than can deterministic methods. Standard tools for describing and analyzing the characteristics of nondeterministic phenomena are the autocorrelation and spectral density functions. Herein, the definitions, assumption, and mathematical background related to autocorrelation and power spectrum functions are briefly outlined and the application of these techniques to surface roughness is described. More detailed theoretical background and information on the application of these techniques to other fields can be found in Blackman and Tukey (1958), Jenkins and Watts (1969), Taub and Schilling (1971), Lee (1960), and Bendat and Piersol (1966).

#### 3.1. Theoretical Development

If the longitudinal or transverse cross-section of any water conveying surface is sampled, one can conclude that the height of the surface protrusions are random. All profile samples of the cross-section will be differ-In other words, each observation will be only one of many possible results which might have occurred. Thus, if the surface protrusion height, X, is considered to be a function of length, \( \ell \), along any cross-section, then at any given distance,  $l_i$ , the quantity  $X(l_i)$  is considered to be a random variable. A set of values for the random variables spaced along the distance parameter defines a realization of a stochastic process. of all random functions of length form the class of all possible processes and is known as an ensemble. water conveying surface encounted in practice defines its own distinct realization from the ensemble.

The process  $X(\ell_j)$  can be characterized by any one of four main types of statistical functions depending upon the objectives of the study. These are (1) the variance, (2) the probability density function, (3) the autocorrelation function, and (4) the power spectral density function. The variance or the mean square value furnishes information on the intensity of the process. The probability density function defines the amplitude domain of the process, while the autocorrelation function

and the power spectral density function define distribution of "power" in the space domain and frequency domain, respectively. For a stationary process, the power spectral density function provides the same information as the autocorrelation function since the two functions are Fourier transforms of each other. However, the two functions display the information in different formats. One format may be more suitable for a specific application than the other. It is especially convenient to use the power spectral density function when raw data occurs periodically.

The process  $X(\ell_j)$  must be stationary and ergodic in order to utilize the standard techniques of autocorrelation and power spectrum analysis. The stationary property means that the joint distribution of any two random variables in the process depends on the difference between the two distances rather than on the distances themselves. For example, the mean value (first moment),  $\mu_X(\ell)$ , of the random process is the same for all  $\ell$ . An ergodic process is stationary. In addition,  $\ell_X(k)$  and the autocorrelation function can be computed from any sample functions of the ensemble. Consequently, if the process is stationary and ergodic, one sample function  $X_k(\ell_1)$  defines the whole process.

The stationary and ergodic properties of the process could not be verified for the ensemble which

was analyzed in this study because of the time involved in accomplishing such an undertaking. However, Squarer (1970) working on bed forms in fluvial channels and Hutchinson (1965) whose studies concerned the pavement roughness of highways verified that the random processes which they studied were indeed stationary and ergodic. Throughout this study the process is assumed to be stationary and ergodic as was assumed by Nordin and Algert (1966), Houbolt (1961), and by Burney and Higgins (1973).

# 3.2. Autocorrelation and Power Spectrum Functions

If the sample function  $\mathbf{X}_{\mathbf{k}}(l)$  is normally distributed, the function itself is completely characterized in the statistical sense by its mean and autocovariance functions. These two functions are:

$$\mu_{x}(k) = \lim_{L \to \infty} \frac{1}{L} \int_{-L/2}^{L/2} x_{k}(\ell) d\ell$$
 (3.2.1)

and

$$C_{\mathbf{x}}(\tau) = \lim_{L \to \infty} \frac{1}{L} \int_{-L/2}^{L/2} X_{\mathbf{k}}(\ell) X_{\mathbf{k}}(\ell + \tau) d\ell \qquad (3.2.2)$$

where

L = the profile length under consideration,

 $\tau$  = a lag distance, and

 $\mu_{\mathbf{x}}(\mathbf{k})$  = mean value of the sample function.

When  $\tau=0$ , (3.2.2) gives the mean square or variance of the sample function. The autocovariance function is commonly normalized when several autocovariance functions are to be compared with each other. This normalization process is accomplished by dividing the autocovariance function by the variance R(0). The resulting function is called the autocorrelation function, and is frequently denoted symbolically as  $R_{\mathbf{v}}(\tau)$ .

The autocorrelation function describes the general dependence of the roughness at one point on that at another point separated by a distance τ. Therefore, if the roughness amplitudes of a surface profile are represented as positive and negative deviations about a zero mean value, the roughness profile can be characterized by the autocorrelation function provided that roughness amplitudes are normally distributed and the process is ergodic. The autocovariance or autocorrelation function defined in (3.2.2) can be written in a form as given by Blackman and Tukey (1958):

$$R_{\mathbf{X}}(\tau) = \int_{-\infty}^{\infty} G_{\mathbf{X}}(f) e^{-i2\pi f} df \qquad (3.2.3)$$

and

$$G_{X}(f) = \lim_{L \to \infty} \frac{1}{L} \left| \int_{-L/2}^{L/2} X(l) e^{-i2\pi l f} dl \right|^{2}$$
(3.2.4)

where

f = spatial frequency (cycles per inch), e = the base of the natural logarithms, and  $i = \sqrt{-1}$ .

The function  $G_{X}(f)$  is known as the power spectral density function. The spectral density function and the autocorrelation functions form a Fourier transform pair. Hence, (3.2.4) is equivalent to

$$G_{\mathbf{x}}(f) = \int_{-\infty}^{\infty} R_{\mathbf{x}}(\tau) e^{-i2\pi f \tau} d\tau. \qquad (3.2.5).$$

Since the functions  $G_{\mathbf{x}}(f)$  and  $R_{\mathbf{x}}(\tau)$  are real and even functions, the relationships between them can be put into a simpler form:

$$R_{\mathbf{x}}(\tau) = 2 \int_{0}^{\infty} G_{\mathbf{x}}(\tau) \cos 2\pi f \tau df \qquad (3.2.6)$$

and

$$G_{\mathbf{x}}(f) = 2 \int_{0}^{\infty} R_{\mathbf{x}}(\tau) \cos 2\pi f \tau d\tau. \qquad (3.2.7)$$

The power spectral density function for random surface expresses the frequency composition of the surface roughness elements. Thus, the value of  $G_{\mathbf{x}}(f)df$  indicates the roughness power present between frequencies f and f+df.

The above expressions for autocorrelation and power spectrum functions are approximated in practice.

One set of digital approximations are given by Blackman and Tukey (1958):

$$R_{X}(p) \approx \frac{1}{N-p} \sum_{q=1}^{N-p} X(q) X(q+p)$$
 (3.2.8)

and

$$G_{x}(f) \approx R_{x}(0) + 2 \sum_{q=1}^{m-1} R_{x}(q) \cos \frac{q\pi f}{m} + R_{y}(m) \cos \pi f$$
 (3.2.9)

where

N = number of data points,

p = lag index (p = 1, 2, ... m), and

m = maximum lag value.

The spectral density function can be computed by first computing the autocorrelation function  $R_{\chi}(p)$  because the autocorrelation function is generally a rapidly converging function.

In practice,  $R_{\chi}(p)$  and  $G_{\chi}(f)$  are derived from finite length of records. Special attention must therefore be given to the expected statistical errors in the experimental estimates.

#### 4. EXPERIMENTAL SETUP AND PROCEDURE

The main objective of the experimental phases of this investigation was carried out in two parts. In the first part, the goal was to obtain Manning's "n" friction coefficients for several one-dimensional deterministic surfaces. This was accomplished by using results from previous investigations in which resistance to flow was studied by using deterministic artificial roughness elements. More than 30 different types of surfaces, along with corresponding friction coefficients, were obtained in this manner. Details of the surfaces, their origins, and a descriptive analysis of these will be given in the next chapter.

The chief objective of the second part was to measure magnitudes of surface roughness elements along longitudinal profiles of several rough water conveying surfaces which are commonly encountered in practice. The conveying surfaces selected for this investigation were 11 different types of corrugated plastic tubing, with their inside diameters ranging between 4 and 8 inches, one 6 in. diameter corrugated metal tube, one rough open channel surface and two gravel beds, one having coarse gravel, and another fine gravel as surface materials. A

section of a length of 40 inches for each conveying surface was sampled and the profiles of each were recorded for future analysis.

### 4.1. Experimental Setup

The instrumentation used for surface profile measurement consisted of four main components: (a) a sensitive measuring device which produces an output signal voltage proportional to the mechanical displacement of a sensing probe, (b) a voltage carrier amplifying system, (c) an analog-to-digital converter, and (d) a table with precise horizontal movement.

The measuring mechanism selected was a nominal to line linear displacement transducer. This instrument consists of a primary coil and two secondary coils which are symmetrically arranged to form a hollow cylinder.

Within the cylinder, a small magnetic core attached to a supportive nonmagnetic rod is constructed so as to be able to move axially in response to the mechanical input to the probe. When the primary coil is excited by an alternating current, a current is induced in the secondary coils. The output current which results from the phase differences between the outputs of the two secondary coils is linearly related to the position of magnetic core and, therefore, to the position of the probe. The original diameter of the probe was too large to measure the heights of the surface elements at the required sampling intervals for

this experiment. Hence, a much narrower extension to the probe (less than .05 in.) was constructed. A 4-48 type carbon steel tap was used. The shank portion of the tap was ground with a lathe grinder to form a .03 in. diameter proble with a 60° needle point.

A carrier amplifier instrument with a precision transducer indicator was used to amplify the signals from the linear displacement transducer. A differential transformer input module provided the "front end" circuitry and adjustments on the amplifier for calibrating the amplifier indicator with respect to output signals from the transducer. An output module with an adjustable (5 to 55 mv) recorder output unit was used for the amplifier.

A six channel analog-to-digital converter was used to convert the analog signal from the output module of the amplifier to digital data, which was punched on paper tape with ASKII binary code. All six channels were connected to the input source (amplifier); i.e., the same input exitation voltage was recorded simultaneously by each channel.

A level plane with horizontal movement was needed to obtain the required sampling displacements of the conveying surfaces. The feed table of a milling machine was used for this purpose. The table had a maximum 40 in. horizontal travel as well as vertical and cross travel.

The handwheel had 250 graduations, each corresponding to .001 in. of travel on the horizontal table.

Since the probe could not be moved across the rough profiles, the linear displacement transducer was fixed at a reference point above the level plane by building a special housing mechanism for the transducer. A 4  $\times$  3  $\times$  1.5 in. aluminum block was drilled with a 7/8 in. drill to obtain a 4 in. long hollow cylinder inside the block. A thin aluminum sleeve was placed at the approximate midpoint of the cylinder. The side of the block was threaded with a 10-32 tap at the same level as the sleeve for a hexagonal head screw as a tightening mechanism for the sleeve. The transducer was inserted in the cylinder and was held in place by tightening the sleeve via the hexagonal head screw. Then the block was bolted on one end of a 17 in. long, 1/4 in. thick and 4 in. wide metal piece, and the other end of the metal piece was bolted into the arbor arm of the milling machine. This type of flexible fastening mechanism provided tremendous convenience for the calibration of the system. Figure 4.1.1 shows the overall view of the experimental setup.

Calibration of the system was achieved by the following steps. The table was first lifted by the vertical lifting mechanism on the milling machine until the surface elevation of the table touched the tip of the transducer probe. A 3/4 in. square metal bar was laid



Figure 4.1.1.--Overall view of the experimental setup.



Figure 4.1.2.--Corrugated plastic tubing.

under the probe. The height of the bar was used as the zero elevation reference point for all measurements. The mechanical zero output of the transducer, while the probe was still on the metal reference bar, was obtained by sliding the transducer up and down in the housing to the point at which the output from the transducer equaled zero millivolts on the amplifier indicator. The position of the transducer was fixed by tightening the sleeve. After the position of the transducer was set with respect to the zero elevation reference point, micrometer calibration blocks ranging from 0.1 to 1.0 in. were used as known mechanical inputs to the transducer to calibrate the amplifier output. This was accomplished by assigning a millivolt value to the known mechanical input by adjusting the "front end" circuitry of the input module of the amplifier. The output from the amplifier was also coupled to the analog-to-digital converter by calibrating the converted over a working range of from 0 to 50 millivolts.

As previously mentioned, the table of the milling machine had a maximum horizontal travel distance of 40 inches. Therefore, the maximum length of the profile measurements of each sample was about 40 inches. A 12 × 40 in. base plate for the samples, made from 3/4 in. plywood, was built to provide a stationary support. This base plate was bolted down on the sides to the plate of the milling machine to prevent lateral movement of the sample.

The corrugated tubing had inside diameters of 6 inches or less. The tubing was divided into two equal parts. One-half was set upon the base plate with its bottom parallel to the sides of the base plate and was nailed in that position. The corrugated tubing with inside diameters greater than 6 inches was divided into four pieces. One piece was placed upon the base plate in the same manner as the smaller diameters, as illustrated in Figure 4.1.2 (on page 48).

To simulate gravel beds of a stream, two different types of gravel surfaces were constructed. One surface, made of coarse gravel, had an average diameter ranging between 1/2 to 1 in., as shown in Figure 4.1.3. The second surface was made from fine gravel as illustrated in Figure 4.1.4, with an average diameter which varied between 1/4 and 3/8 in. The gravel was fixed on the plate with a thin coat of industrial glue.

It was impossible to obtain a representative sample of the rough open channel. Instead, it was assumed that a foundation brick having a rough surface would have the same surface properties as a rough channel.

#### 4.2. Experimental Procedure

For the first step in the profile measurements of the samples, the table of the milling machine was moved to the end point. This end point was assumed to be the zero starting point. The base plate containing the sample



Figure 4.1.3.--Coarse gravel.



Figure 4.1.4.--Fine gravel.

was placed on the milling machine table. The probe was brought into contact with the sample. The signal from the transducer was recorded on a paper tape through six channels of the analog-to-digital converter. The probe was then lifted and the surface was moved .05 in. The process was repeated, continually maintaining the .05 in. interval as the sampling interval, until the profile measurements of the 40 in. sample were completed.

Originally, the converter was set to scan the data from the transducer through six channels at once. During the experiments, it was discovered that two of the channels were malfunctioning. The malfunctioning channels were taken out of the system and the rest of the experiments were continued using the remaining four channels. The data, punched onto paper in ASKII code, was interpreted by using a library FORTRAN IV computer program. The interpreted data was recorded on a permanent file for future analysis.

#### 5. COMPUTATIONAL PROCEDURE AND RESULTS

The surface roughness profiles and the corresponding Manning "n" friction coefficients were obtained from two sources. The first group of surface profiles was obtained from previous investigations on one-dimensional strip roughnesses by C. A. Smith, Jr., and C. Warren, J. W. Johnson, and E. A. LeRoux as reported by Johnson (1944) and R. W. Powell (1946). An attempt was also made to analyze an artificial roughness by Streeter (1936). The dimensionality involved in representing the surface and excessive computer space required made it impossible to perform a meaningful analysis on the surfaces. fore, Streeter's investigation was not included. All of the artificial surfaces in the first category were constructed from rectangular sills with different dimensions and different periodic arrangements. The corresponding friction coefficients were defined experimentally.

The second group of surface profiles was obtained from laboratory measurements as explained in Chapter 4. In this category of surfaces, actual Manning "n" friction coefficients were known only for those surfaces investigated previously by this author and reported by Dinc et al. (1971). For the remaining surfaces, friction coefficients

as cited in textbooks for design purposes were used.

These surfaces were investigated to verify the methodology developed in this study.

A total of 47 surfaces were analyzed. The identification numbers of the surfaces and the corresponding identifications of these surfaces as they appear in the original papers along with their Manning "n" coefficients are given in Appendix A, Tables A-1 through A-5.

## 5.1. Preliminary Investigations on Spectral Estimation

Estimating the spectral density of random data requires a pilot analysis in order to optimize the degree of accuracy and to reduce the labor and cost involved. This process requires converting continuous data into discrete values at some sampling interval. The sampling frequency must be large enough to properly describe significant high frequencies. The optimum sampling interval is assumed in practice to be the largest sampling interval which will avoid aliasing errors. Once the sample interval is established, the length of the sample record is determined in accordance with the number of values required to obtain a meaningful estimate of the spectrum.

If the sampled data points are too far apart, the points could represent either false low or false high frequencies not in the original data. This phenomenon is known as aliasing. The sample frequency below which

aliasing problems occur is termed the "folding frequency" or Nyquist frequency (cycles/in.) and defined as:

$$\frac{1}{dx} = 2 f_0$$
 (5.1.1)

where

 $f_0$  = the highest frequency in the sample, and dx = the sampling interval.

In order to overcome aliasing problems, the original data should not contain information above the folding frequency. In practice, two methods exist for handling this problem. The first method is to filter the original data prior to sampling so that information above the folding frequency does not exist in the filtered data. Such a technique requires some initial knowledge of the desired frequency range. The second method is to choose the sampling interval, dx, sufficiently small so that  $G_{\mathbf{x}}(\mathbf{f})$  is zero for  $\mathbf{f}_{\mathbf{O}} > 1/2$  dx. This technique requires an initial knowledge of the spectrum.

The second method was chosen for this study.

Initially, nothing was known of the spectrum functions of the surfaces' roughness and corresponding folding frequencies. To gain insight into the rough shape of spectrum functions and consequently of the anticipated folding frequencies, various rectangular surface roughnesses representing low, high, and intermediate roughness concentrations were selected for

preliminary analysis. A pilot FORTRAN IV computer program was developed by utilizing (3.2.8) and (3.2.9) to estimate the autocorrelation and power spectrum functions of the particular surfaces.

The height of the roughness elements were represented as positive and negative deviations from their mean values. Several values of sampling intervals, dx, maximum lag values, m, the number of data points, N, and their various combinations were analyzed in this manner. The sampling intervals chosen were 0.03125 in., 0.05 in., 0.0625 in., and 0.1 in. The maximum lag values were 50, 100, 200, and 400, and the number of data points were 500, 1000, 2000, 4000, and 8000.

From plots of the spectrum functions, it was visually determined that optimum sampling intervals were 0.3125 in. and 0.05 in. depending upon the surface roughness type. Corresponding folding frequencies for these two sample intervals were generally about 10 cycles per inch. Beyond this frequency no power was observed on the spectrum functions. Therefore, for final power spectrum estimations, 0.03125 and 0.05 in. were used as sampling intervals for the appropriate surfaces and 10 cycles per inch was used as the folding frequency.

#### 5.2. "Smoothing" Process

The preliminary spectrum function obtained by the procedure explained in Section 5.1 were raw estimates

of the true spectrum and are inefficient estimates. A general property of spectral estimates is that their variability does not decrease with increased record length. Smoothing or weighting the correlation function nonuniformly is used to obtain better estimates. A commonly used weighting function is called the "Hanning lag window" and is given by Bendat and Piersol (1958):

$$G_0 = 0.5 G_0 + 0.5 G^1$$
 (5.2.1a)

$$G_k = 0.25 G_{k-1} + 0.5 G_k + 0.25 G_{k+1}$$
 (5.2.1b)

$$G_{m} = 0.5 G_{m-1} + 0.5 G_{m}$$
 (5.2.1c)

where

$$k = 1, 2, ... m-1.$$

The Hanning lag window was used to obtain final power spectral density estimates in this study.

#### 5.3. Final Spectrum Estimations

The FORTRAN IV computer program used to calculate the final spectral density estimates is given in Appendix B, along with a sample output.

Approximately 40 inches of the surfaces which were constructed in the laboratory were used to estimate the power spectral density functions while for rectangular surfaces, 200 inch sections were analyzed. The latter

were generated in the main computer program to provide data for the spectral analysis.

The sampling interval, the number of data points, and the maximum lag values used in the computations for each surface along with the resultant spectral parameters are given in Tables 5.3.1 and 5.3.2. Table 5.3.1 summarizes the surface profile data obtained in the experimental procedure. Table 5.3.2 summarizes the data for rectangular surfaces.

Results of the autocorrelation and spectral estimates are given in Figures 5.3.1 through 5.3.26. Because of the similar estimates obtained from similar surfaces, only distinct representative samples of estimates are included in the figures.

The value of the autocorrelation function at zero displacement, 1, was not included in the original output of the autocorrelation estimates. This was later added during the plotting of figures.

Although extremely small, some negative values were obtained in some of the power spectral estimations. This was due to the window function used. Whenever negative data points were encountered they were assumed to have zero values during the plotting of power spectrum.

TABLE 5.3.1.--Type of surfaces whose actual roughness profiles were obtained in the experimental procedure, their available Manning "n" friction coefficients, and the summary of computations and their results.

	Number	Coefficient n	Interval dx (in.)	Data Points N	Lag Value M	Cutoff Frequency fc (Cycles/in.)	Coefficient
Coarse gravel (Run I)	1	1	0.05	725	100	2.0	1.23
Coarse gravel (Run II)	6	ł	0.05	725	100	1.6	1.48
Corrugated plas. tubing 4-in. ID	Э	ŀ	0.05	725	100	1.9	0.52
Fine gravel (Run I)	4	1	0.05	725	100	6.1	0.30
Corrugated plas. tubing 5-in ID	2	0.0178	0.05	719	100	2.8	0.88
Corrugated plas. tubing 4-in ID	9	1	0.05	725	100	1.5	3.13
Corrugated plas. tubing 8-in. ID	7	0.0150	0.05	725	100	1.8	0.93
Corrugated plas. tubing 5.7-in. ID	8	0.0159	0.05	705	100	2.6	0.44
Corrugated plas. tubing 4-in. ID	6	0.0178	0.05	710	100	4.1	0.43
Corrugated plas. tubing 8-in. ID	10	0.0151	0.05	725	100	1.9	0.25
Corrugated plas. tubing 8-in. ID	11	1	0.05	725	100	2.3	0.85
Corrugated plas. tubing 6-in. ID	12	0.0150	0.05	725	100	5.9	0.28
Corrugated plas. tubing 8-in. ID	13	0.0180	0.05	725	100	4.8	0.37
Corrugated plas. tubing 4-in. ID	14	0.0169	0.05	725	100	2.0	0.31
Brick (Run I)	15	;	0.05	725	100	7.6	0.21
Brick (Run II)	16	!	0.05	725	100	8.5	0.08
Corrugated metal tubing 6-in. ID	17	;	0.05	710	100	4.0	0.40

TABLE 5.3.2.--Type of surfaces whose actual profiles were obtained from previous research, their available Manning "n" friction coefficients, and the summary of computations and their results.

Type of Surface	Surface I.D. Number	Manning Friction Coefficient n	Sampling Interval dx (in.)	Number of Data Points N	Maximum Lag Value M	Cutoff Frequency fc (Cycles/in.)	Decay Coefficient K
Rectangular	18	0.0163	0.05	4000	200	1.50	0.47
Rectangular	19	0.0244	0.05	000 <b>+</b>	200	1.30	99.0
Rectangular	20	0.0208	0.05	4000	200	1.25	1.54
Rectangular	21	0.0194	0.05	4000	200	1.55	0.44
Rectangular	22	0.0236	0.05	4000	200	1.35	0.85
Rectangular	23	0.0229	0.05	4000	200	1.35	0.58
Rectangular	24	0.0223	0.05	4000	200	1.30	1.55
Rectangular	25	0.0240	0.05	4000	200	1.40	0.61
Rectangular	26	0.0240	0.05	4000	200	1.30	17.0
Rectangular	27	0.0158	0.05	4000	200	2.00	0.16
Rectangular	28	0.0222	0.05	4000	200	1.90	0.57
Rectangular	59	0.0198	0.05	4000	200	1.60	1.25
Rectangular	30	0.0204	0.05	4000	200	1.80	0.38
Rectangular	31	0.0219	0.05	4000	200	1.70	99.0
Rectangular	32	0.0177	9.05	4000	200	1.55	1.37
Rectangular	33	0.0222	0.03125	4000	200	1.80	0.48
Rectangular	34	0.0112	0.03125	4600	200	9.44	0.30
Rectangular	35	0.0185	0.03125	4600	200	4.80	0.28
Rectangular	36	0.0200	0.03125	4600	200	4.80	0.25
Rectangular	37	0.0170	0.03125	4600	200	4.72	0.25
Rectangular	38	0.0149	0.03125	4600	200	4.72	0.34
Rectangular	39	0.0185	0.05	4000	200	2.90	0.49
Rectangular	40	0.0231	0.05	4000	200	2.95	0.45
Rectangular	41	0.0264	9.05	4000	200	2.95	0.44
Rectangular	42	0.0264	0.05	4000	200	3.55	0.40
Rectangular	43	0.0217	0.05	4000	200	3.95	0.34
Rectangular	44	0.0238	0.05	4000	200	4.30	0.42
Rectangular	45	0.0217	0.05	4600	200	5.84	0.26
Rectangular	46	0.0186	0.05	4600	200	5.68	0.25
Rectangular	47	0.0156	0.05	4600	200	5.68	00

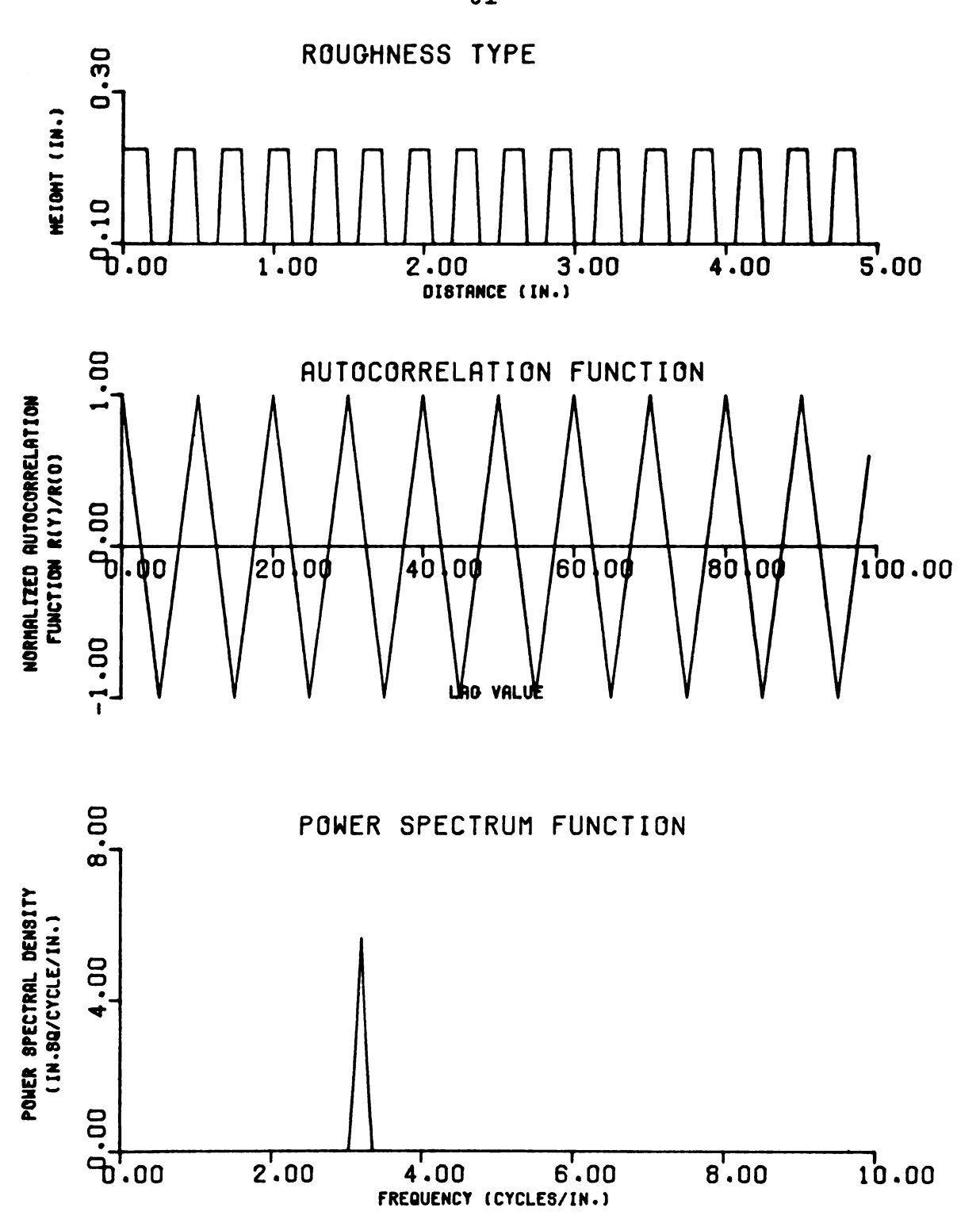


Figure 5.3.1.--Roughness type, estimated autocorrelation, and power spectral density functions of surface 34.

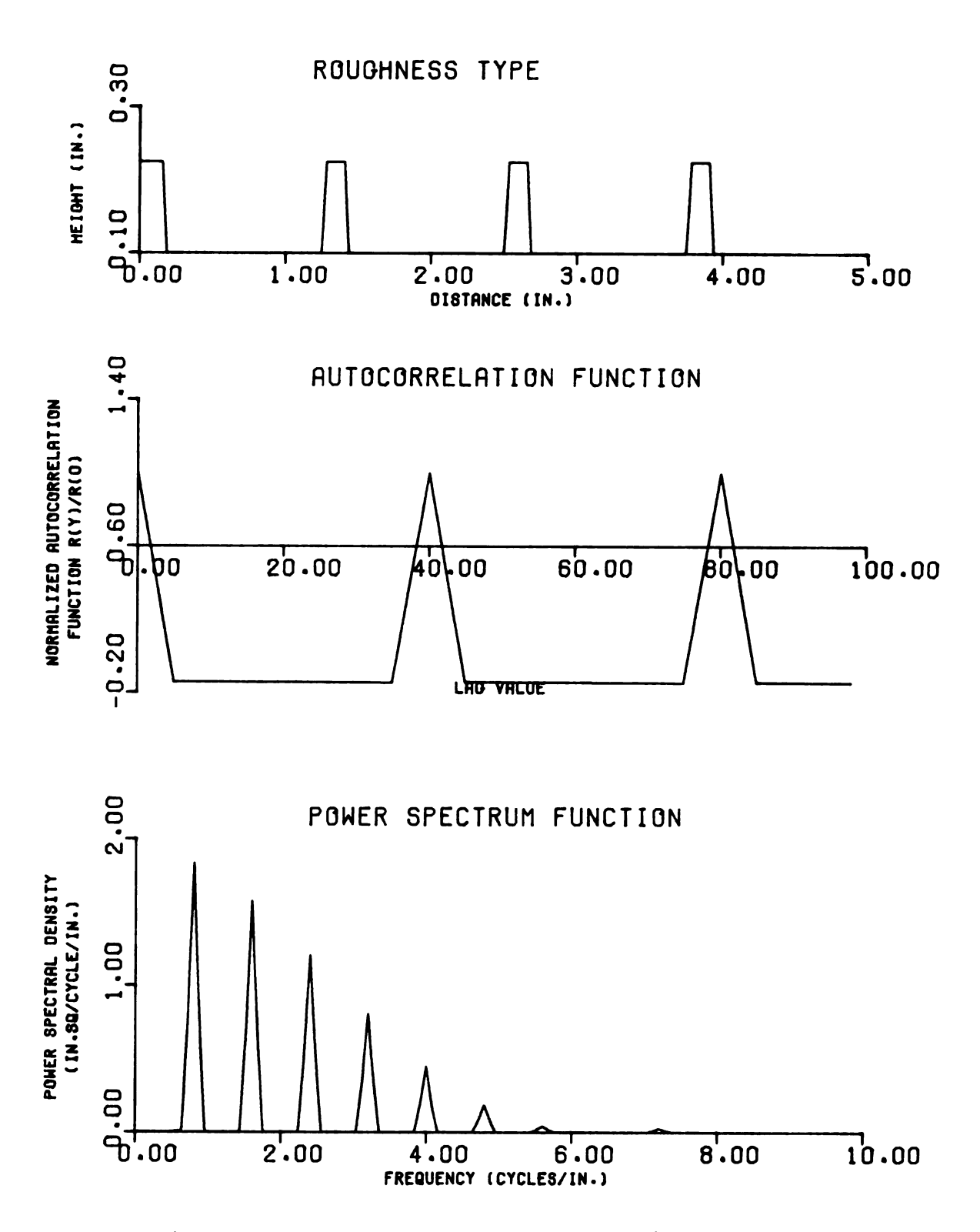


Figure 5.3.2.--Roughness type, estimated autocorrelation, and power spectral density functions of surface 36.

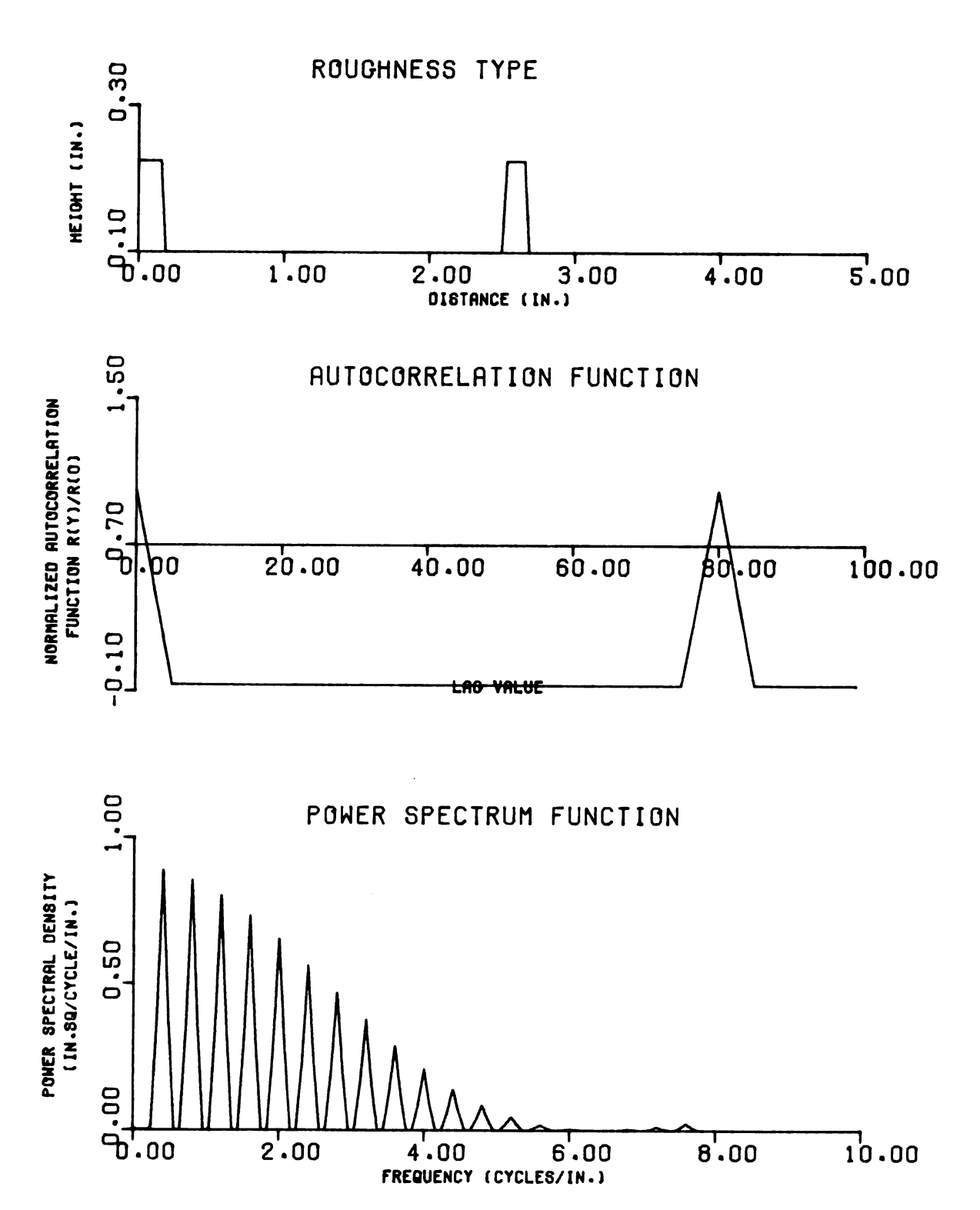


Figure 5.3.3.—Roughness type, estimated autocorrelation, and power spectral density functions of surface 37.

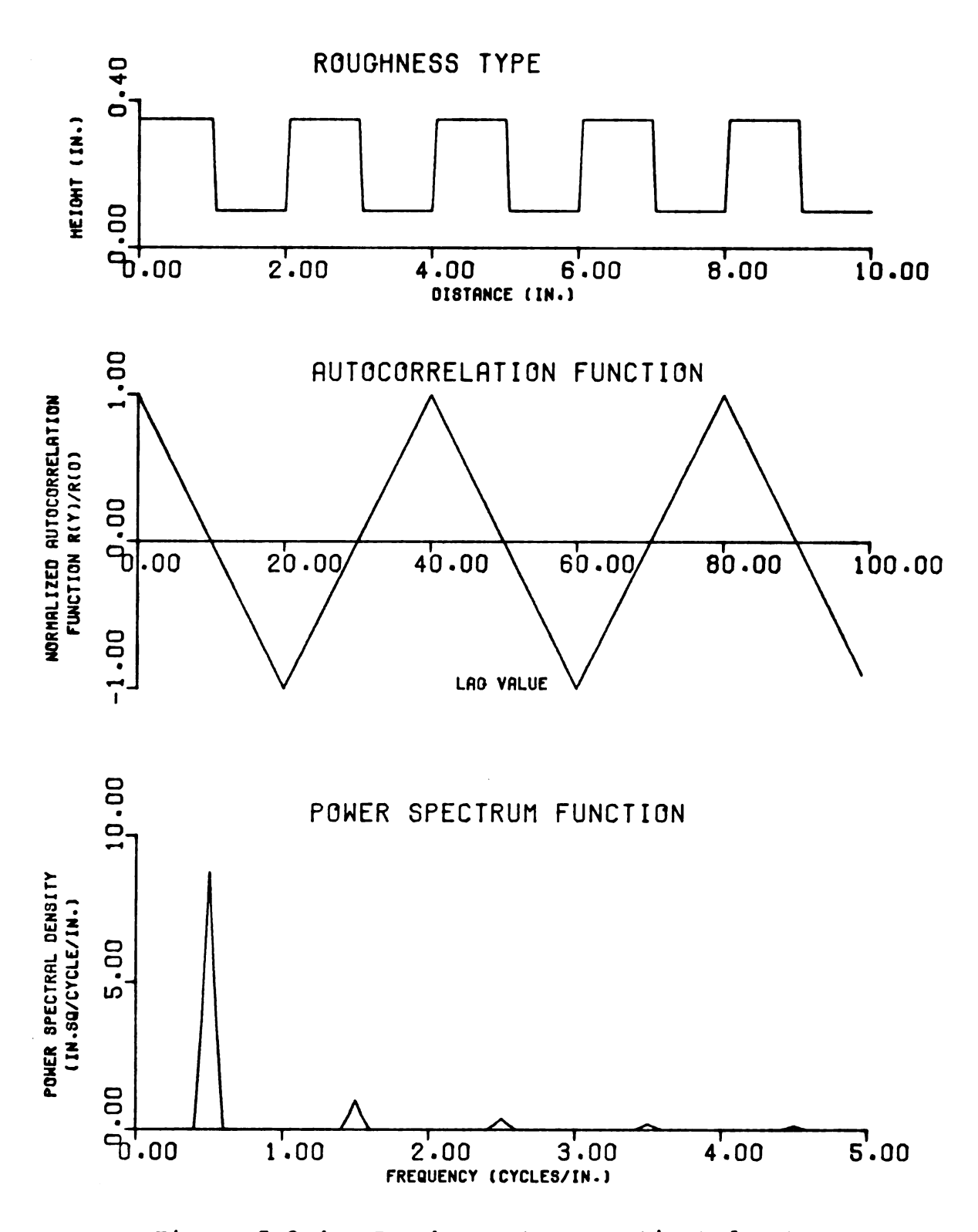


Figure 5.3.4.--Roughness type, estimated autocorrelation, and power spectral density functions of surface 18.

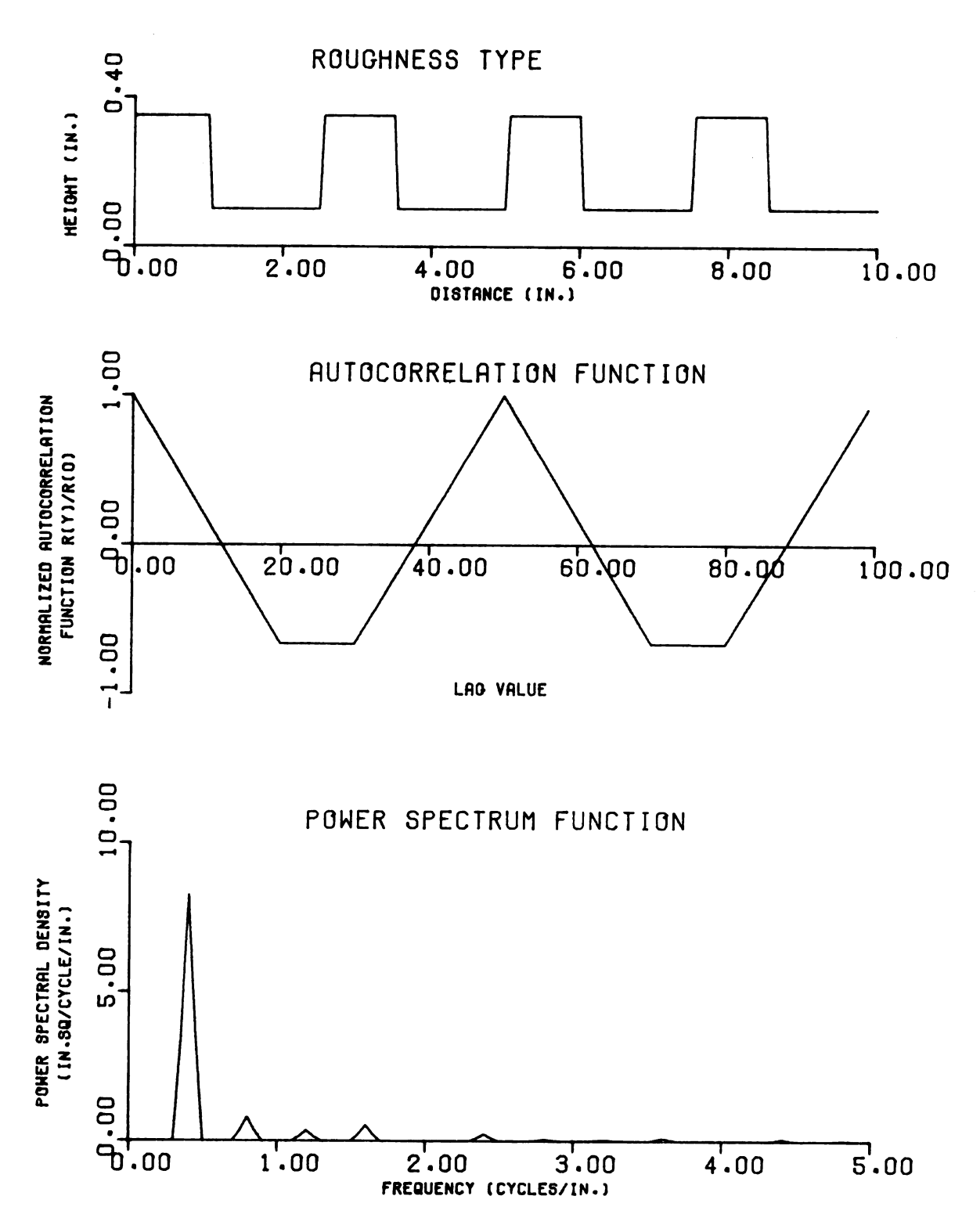


Figure 5.3.5.—Roughness type, estimated autocorrelation, and power spectral density functions of surface 21.

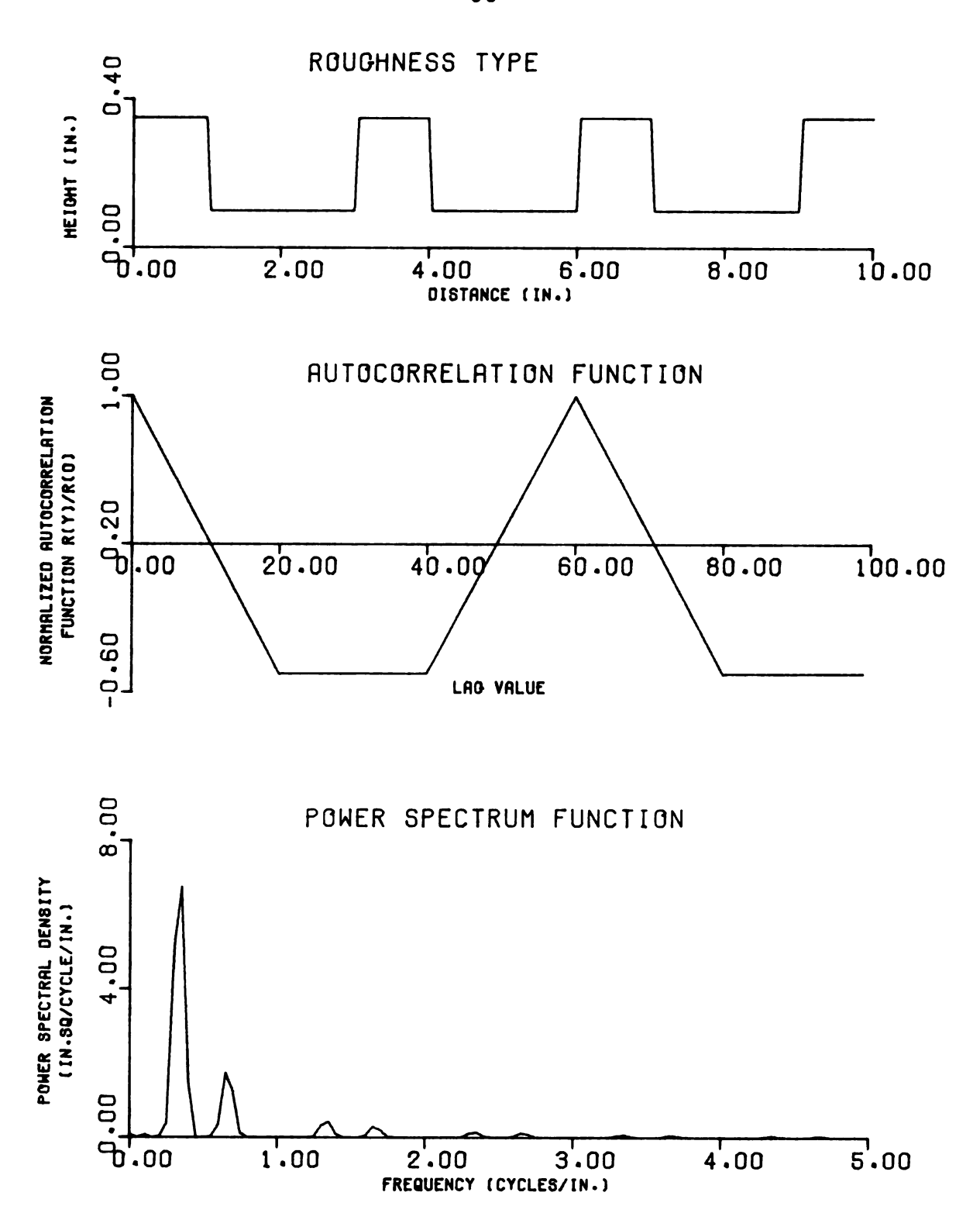


Figure 5.3.6.--Roughness type, estimated autocorrelation, and power spectral density functions of surface 23.

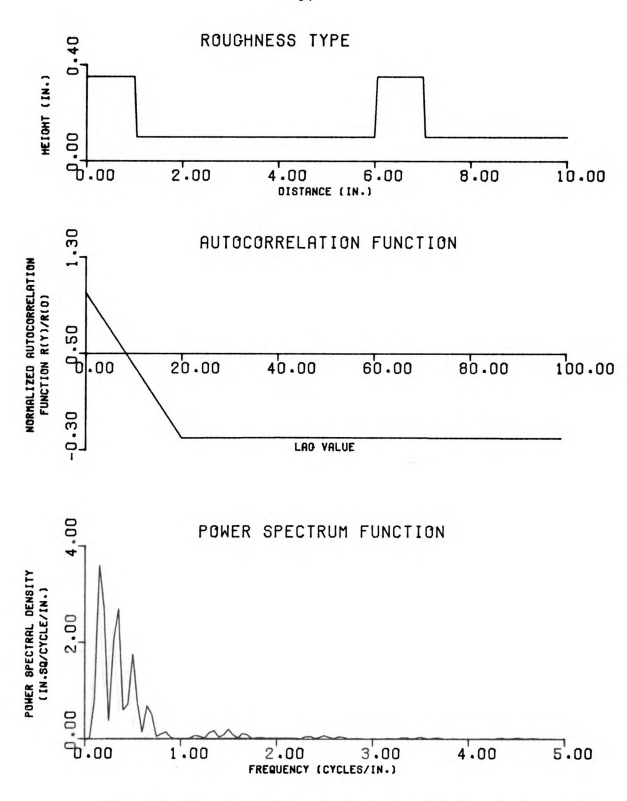


Figure 5.3.7.--Roughness type, estimated autocorrelation, and power spectral density functions of surface 24.

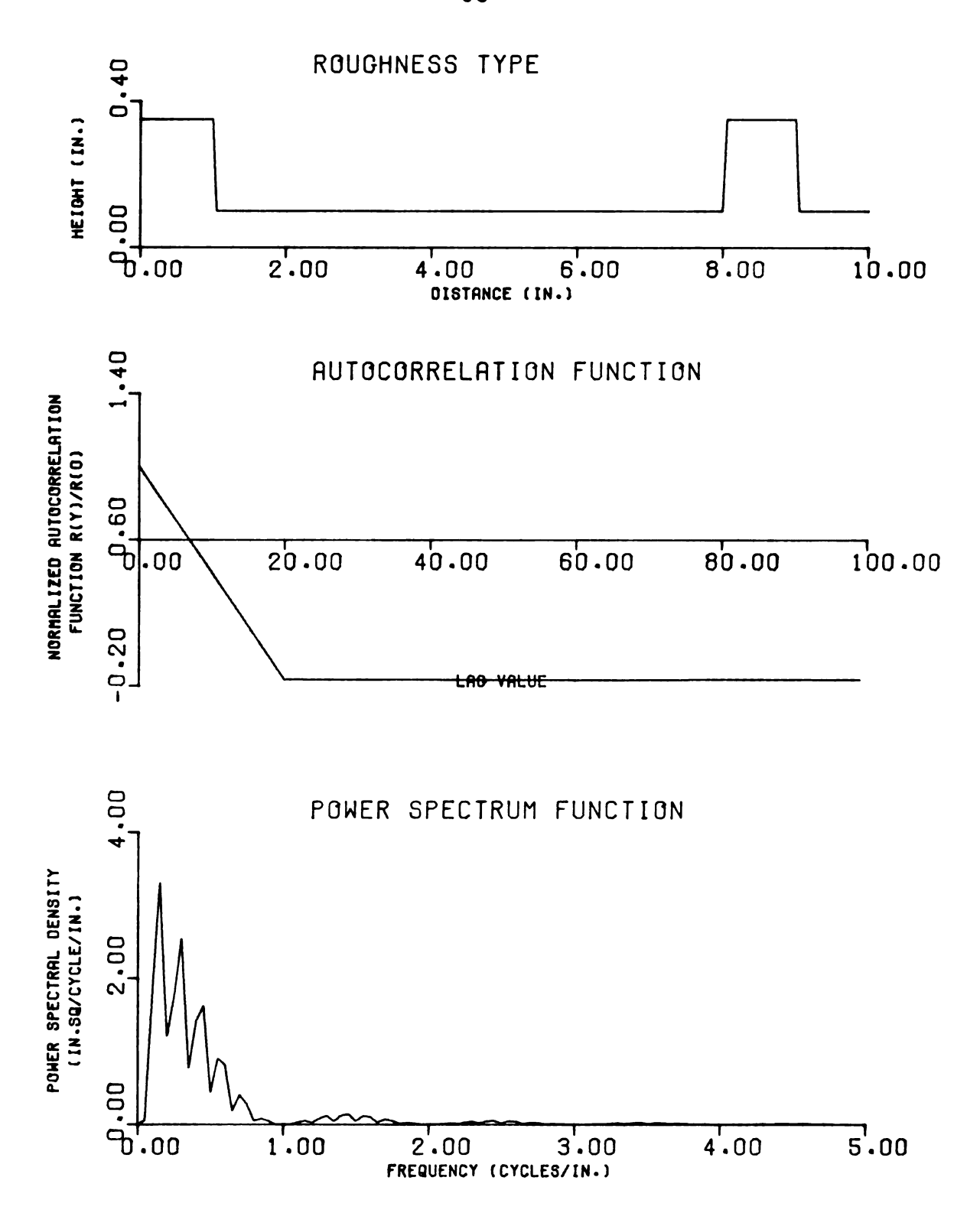


Figure 5.3.8.--Roughness type, estimated autocorrelation, and power spectral density functions of surface 20.

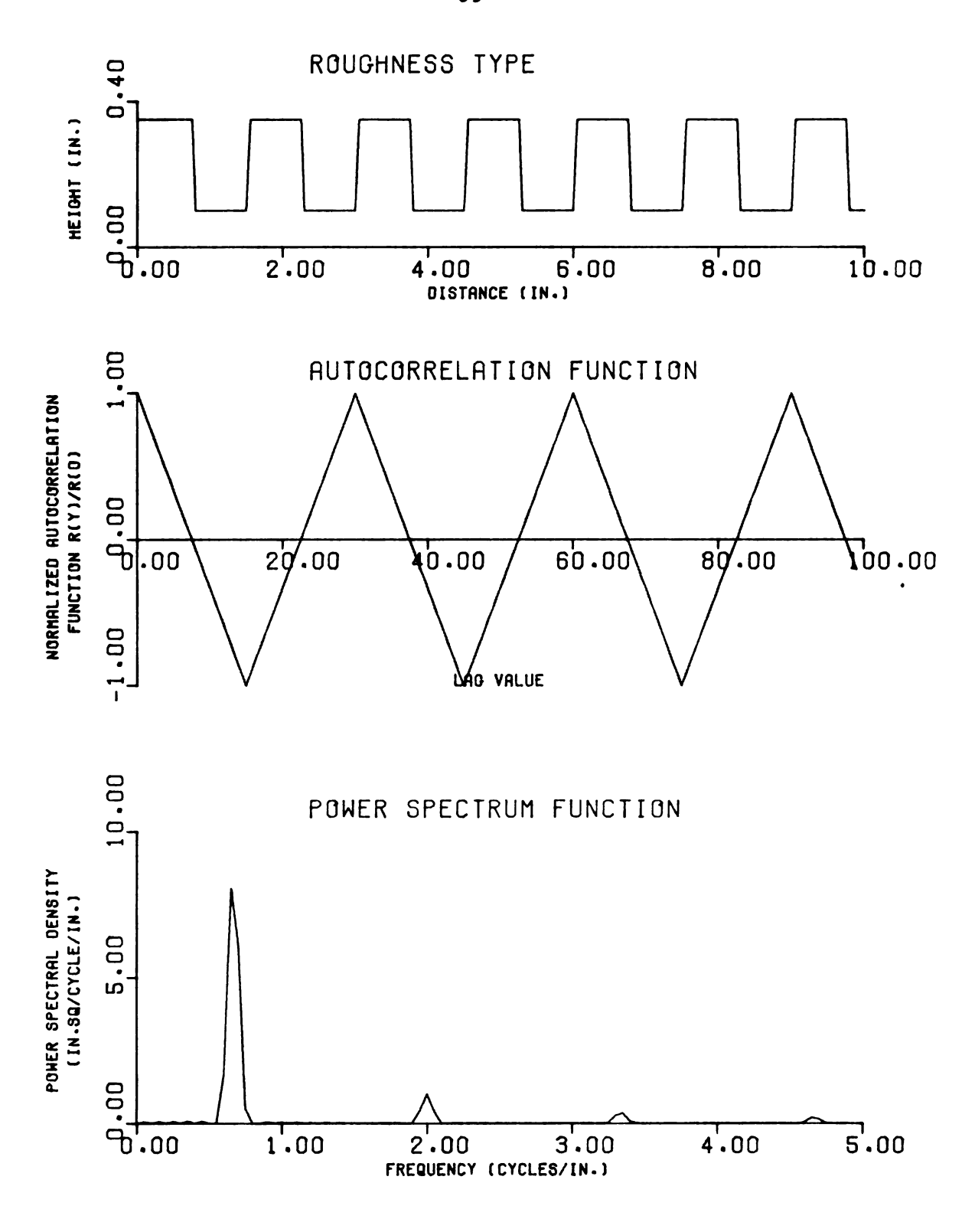


Figure 5.3.9.--Roughness type, estimated autocorrelation, and power spectral density functions of surface 27.

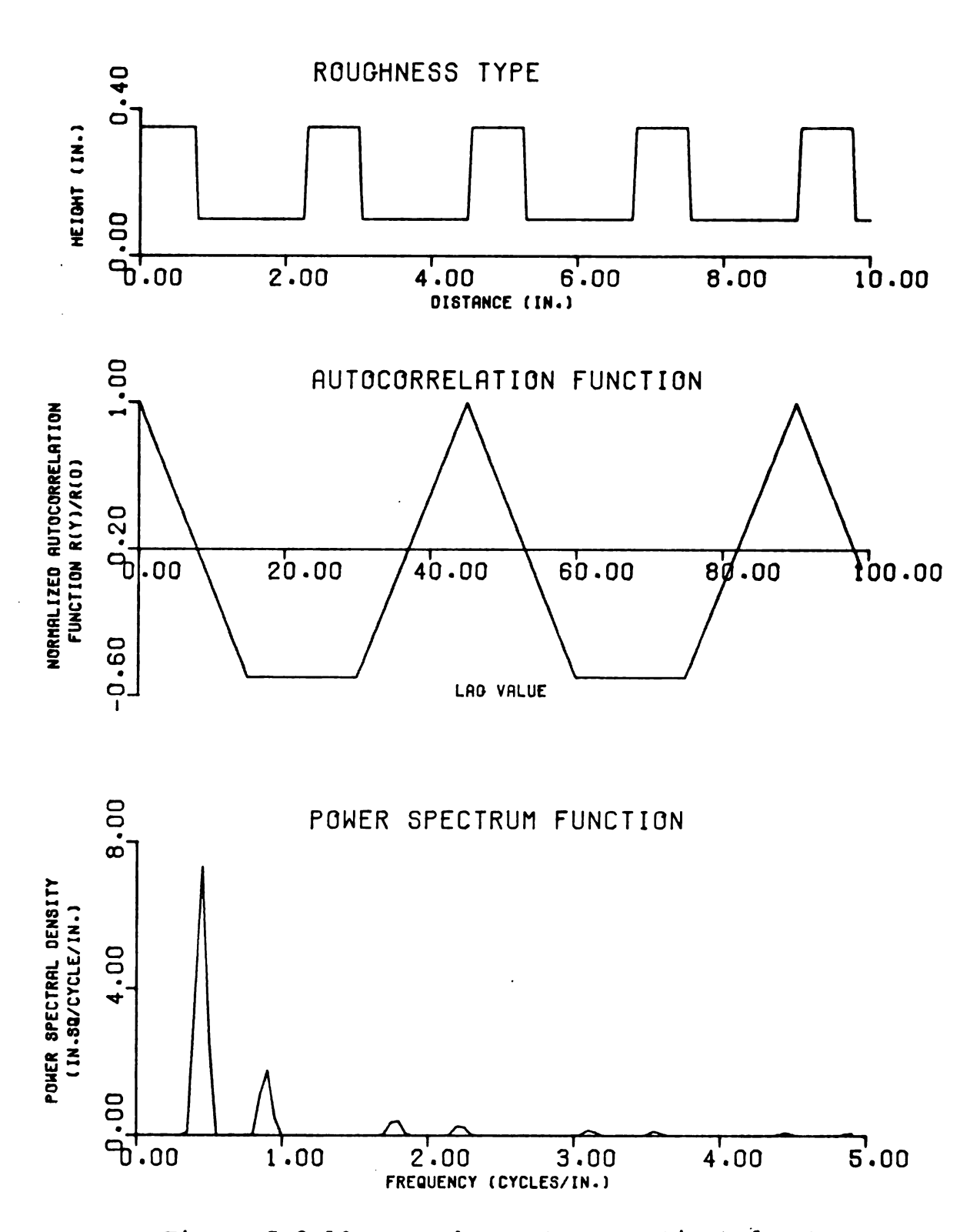


Figure 5.3.10.--Roughness type, estimated autocorrelation, and power spectral density functions of surface 30.

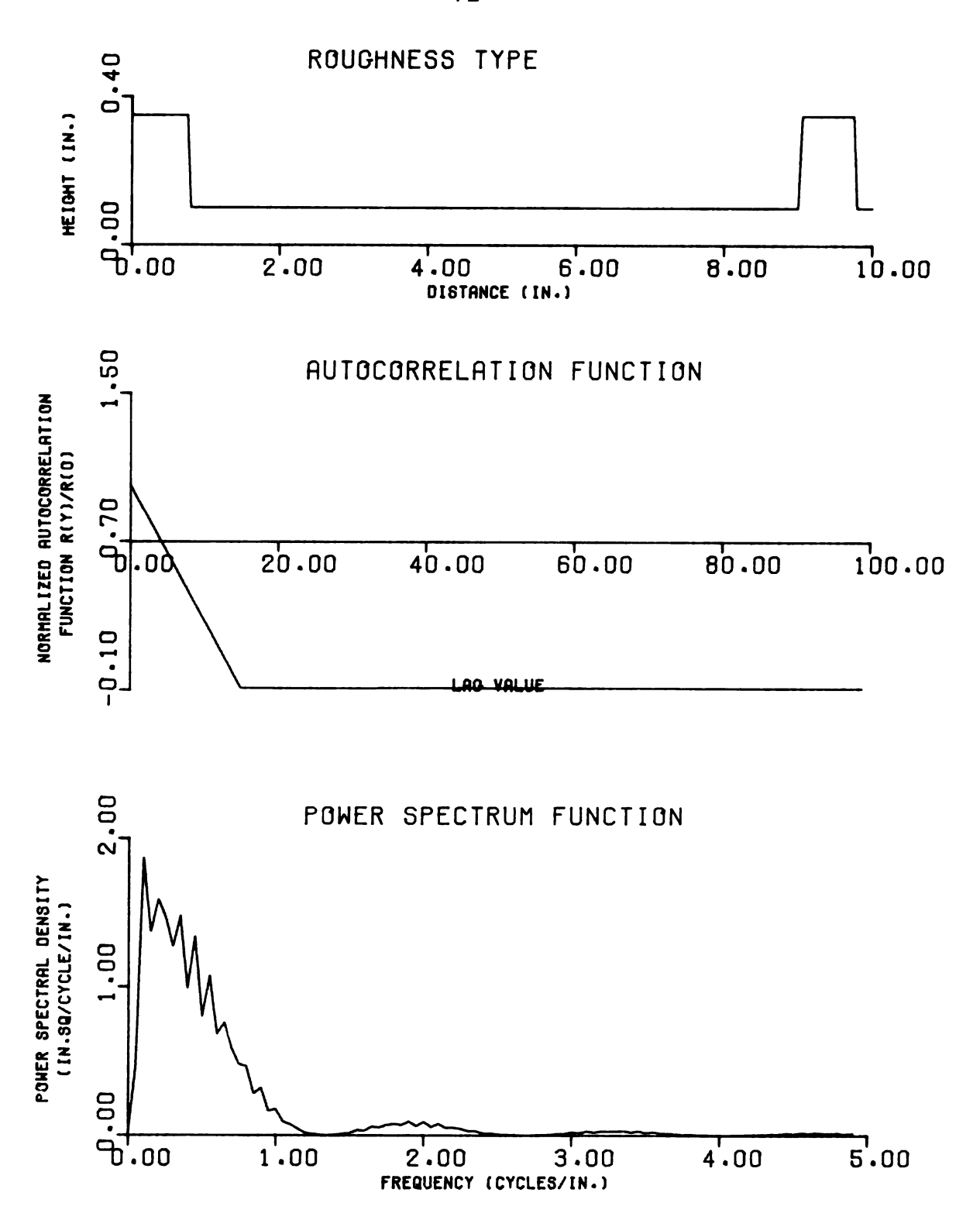


Figure 5.3.11.--Roughness type, estimated autocorrelation, and power spectral density functions of surface 32.

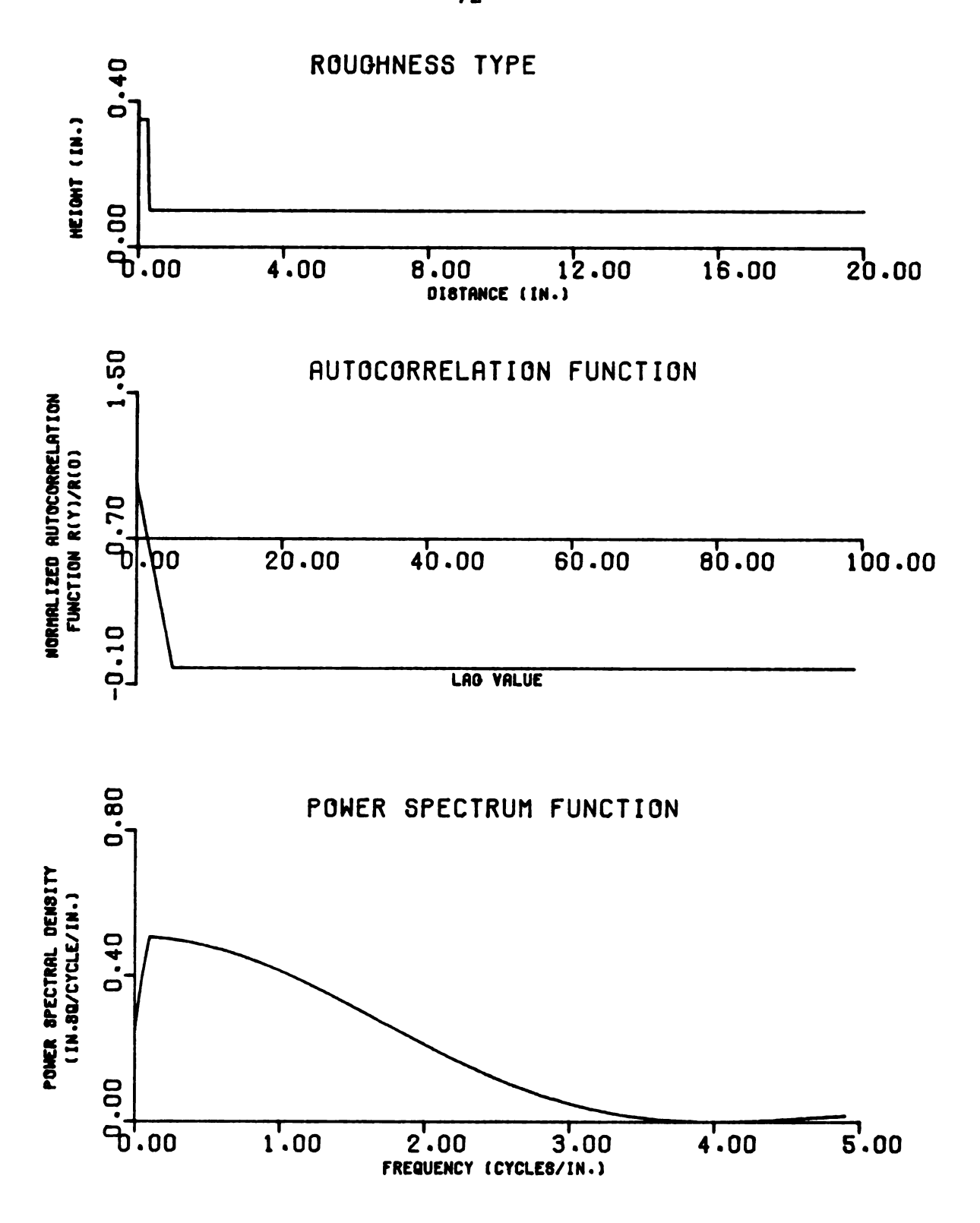


Figure 5.3.12.--Roughness type, estimated autocorrelation, and power spectral density functions of surface 39.

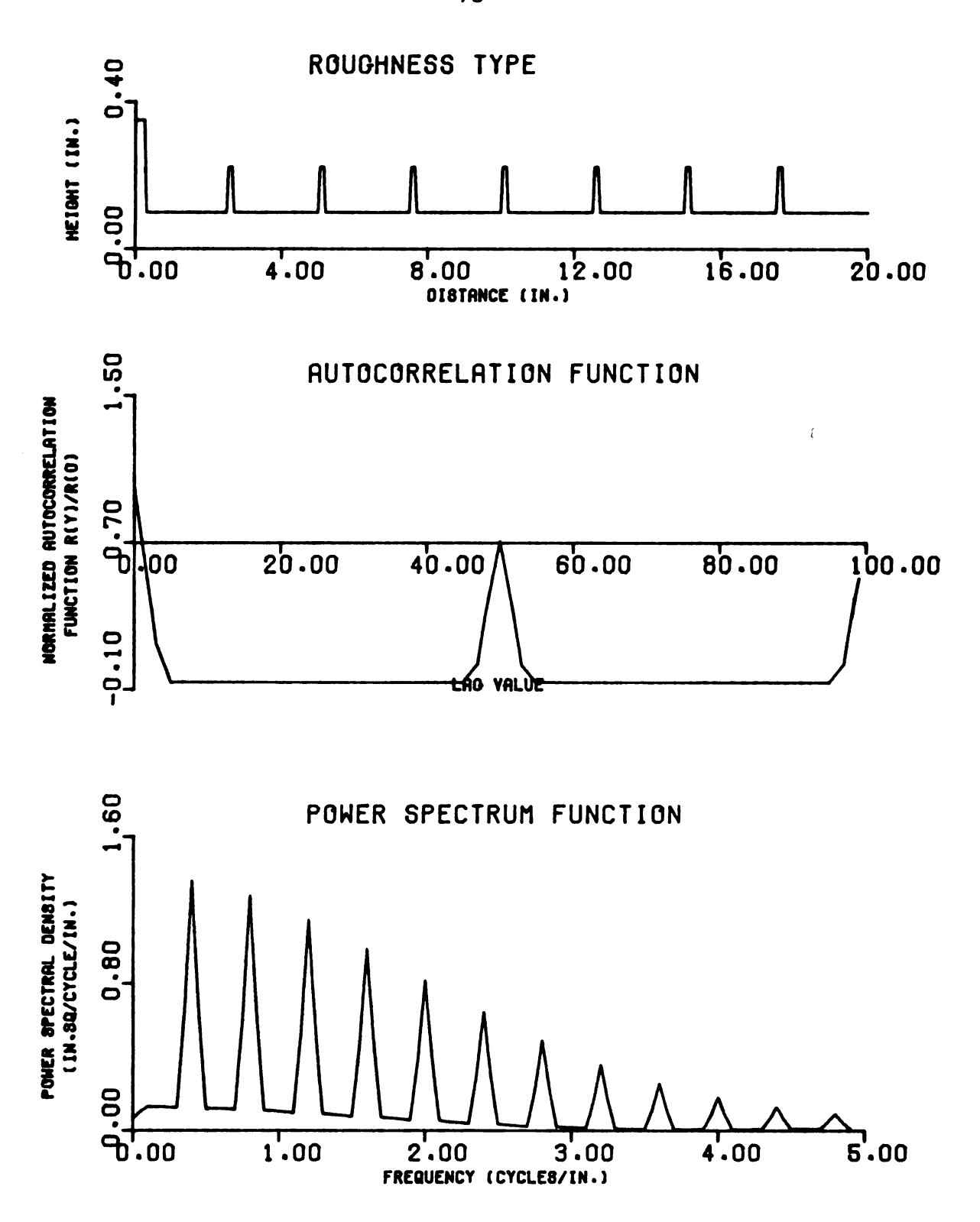


Figure 5.3.13.--Roughness type, estimated autocorrelation, and power spectral density functions of surface 44.

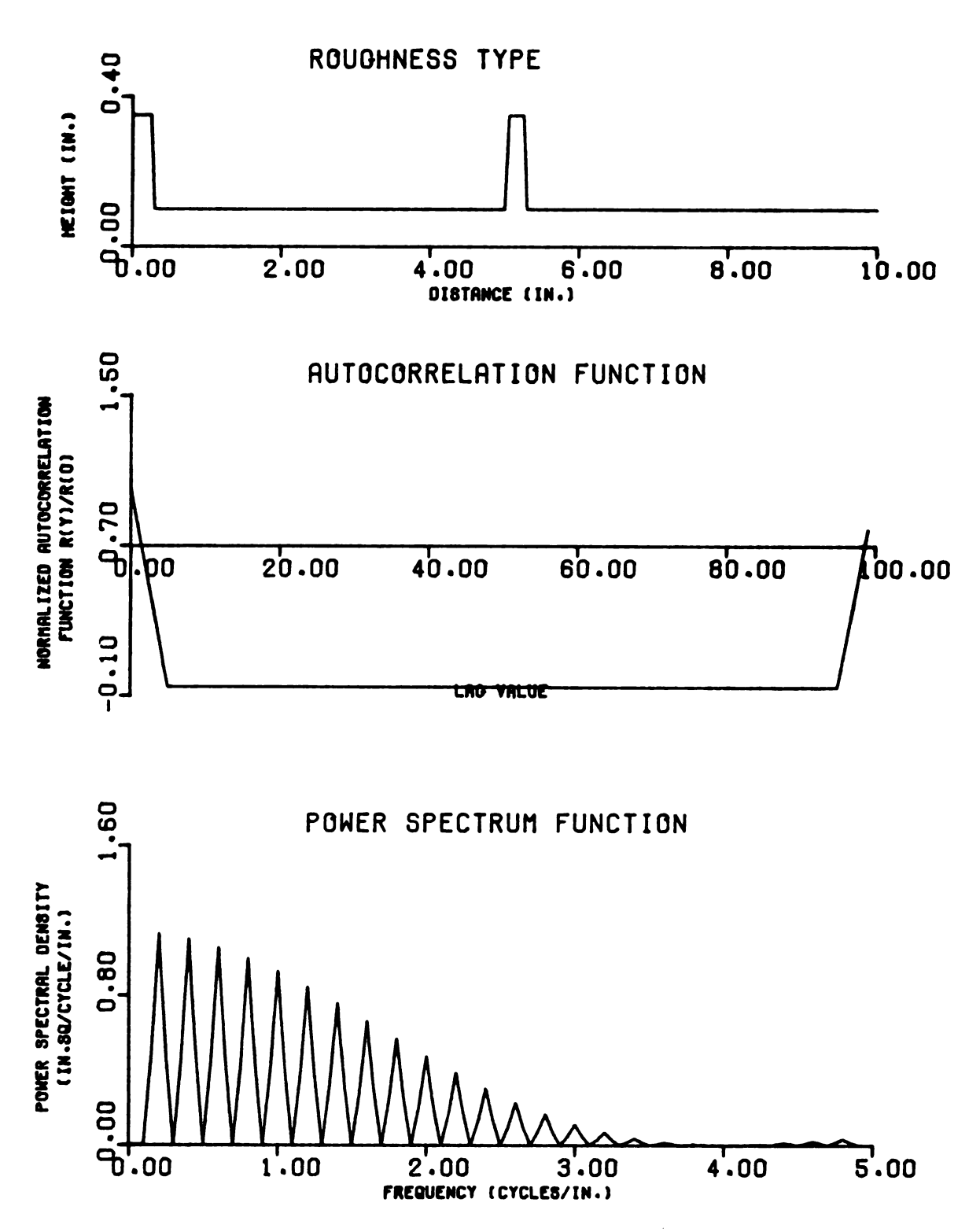


Figure 5.3.14.--Roughness type, estimated autocorrelation, and power spectral density functions of surface 41.

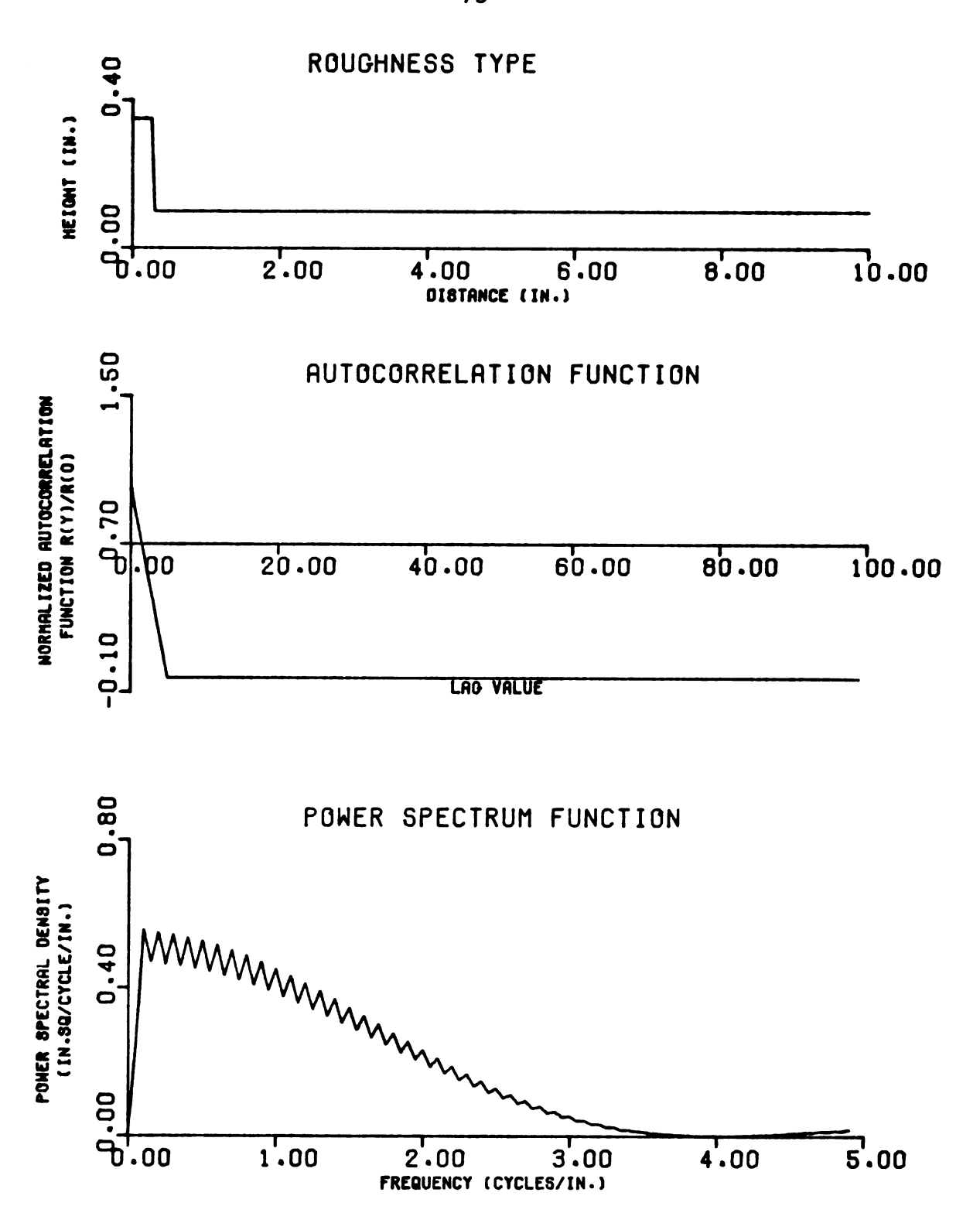


Figure 5.3.15.--Roughness type, estimated autocorrelation, and power spectral density functions of surface 40.

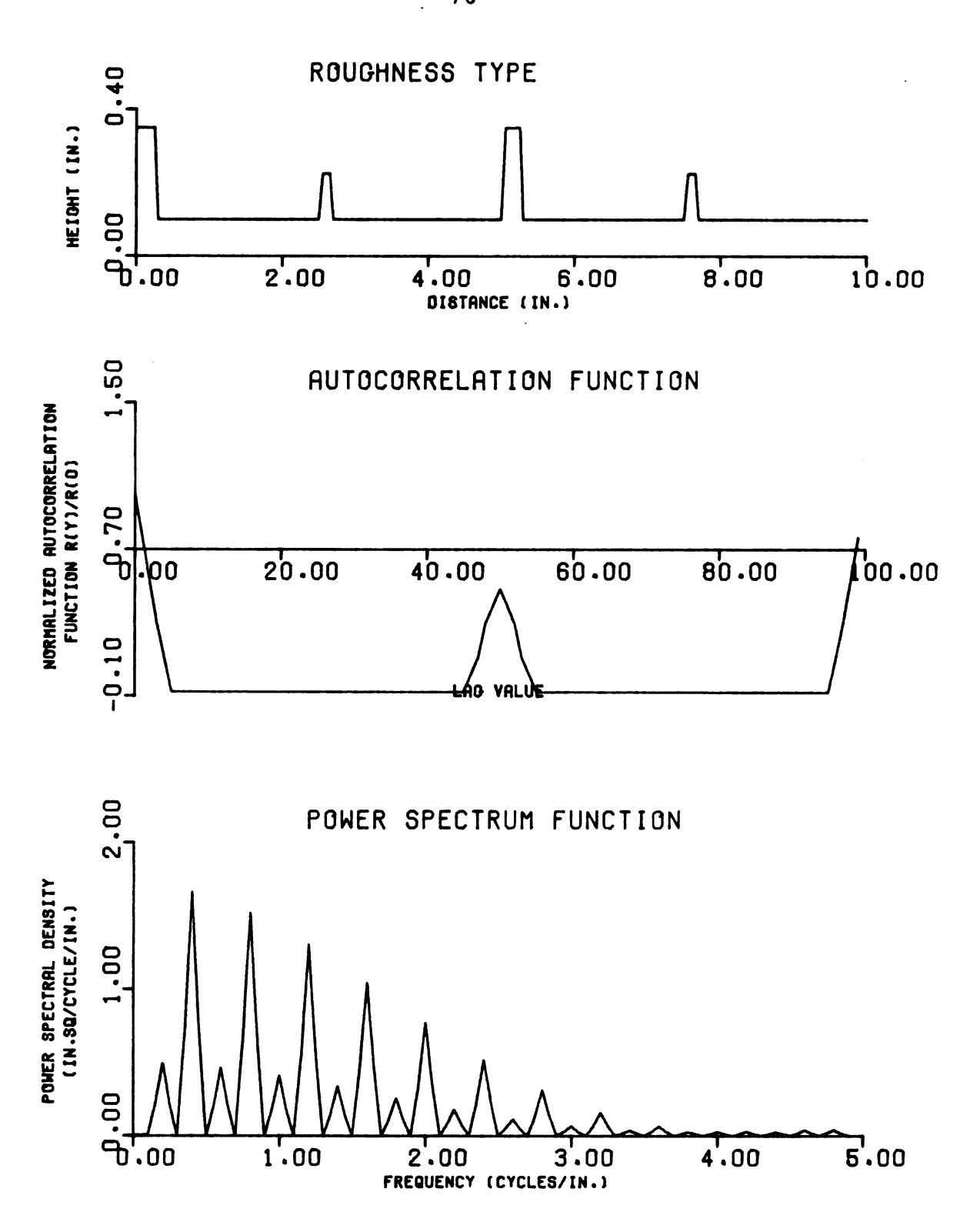


Figure 5.3.16.--Roughness type, estimated autocorrelation, and power spectral density functions of surface 42.

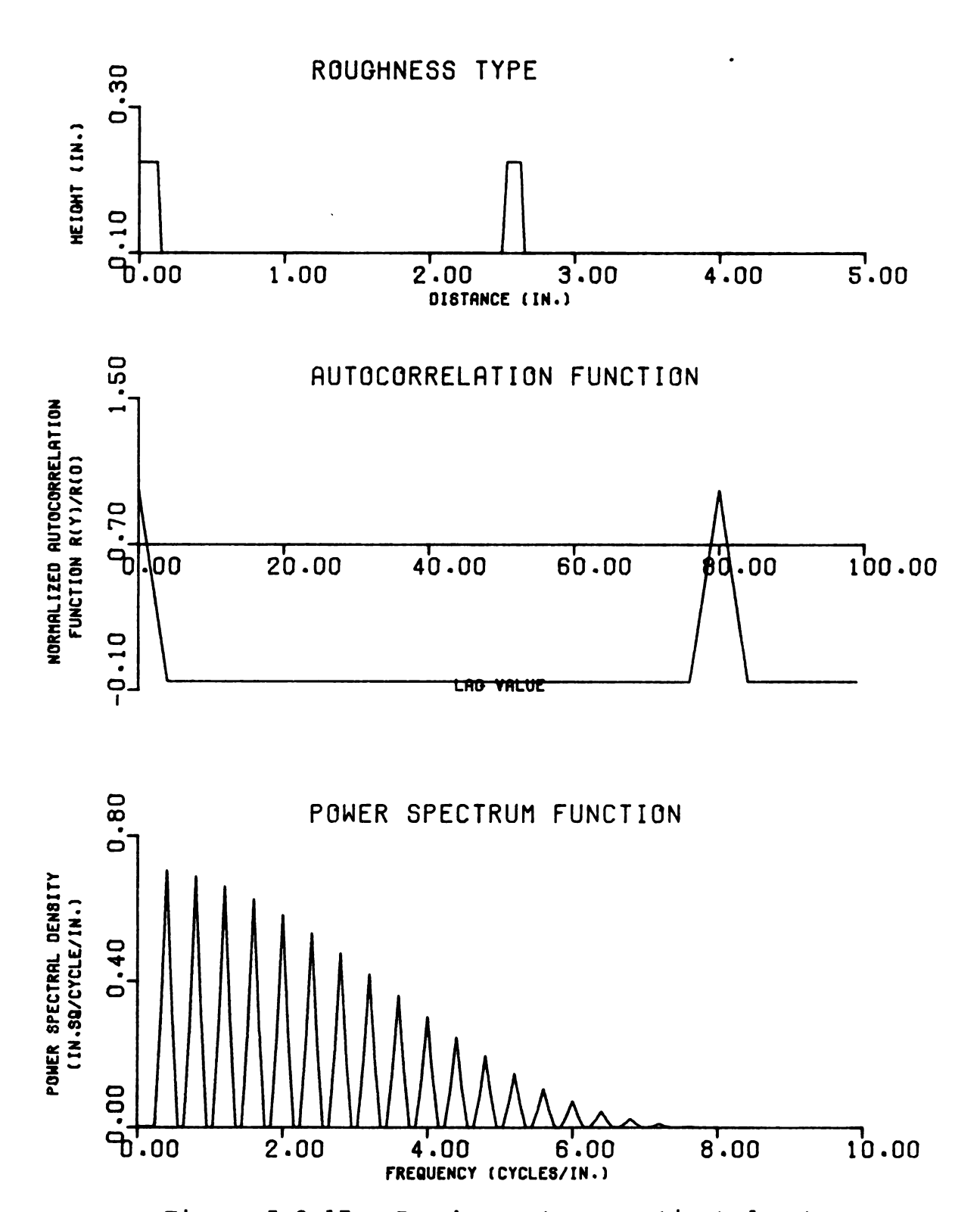
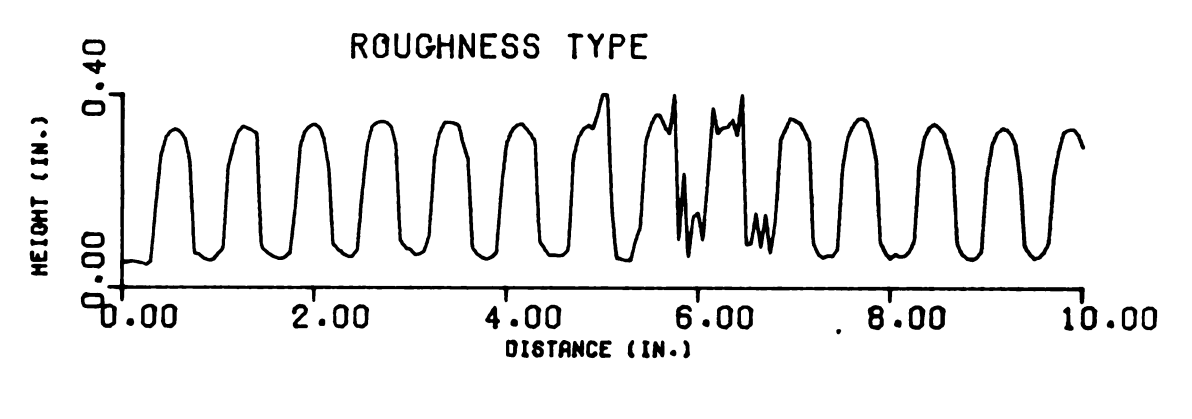
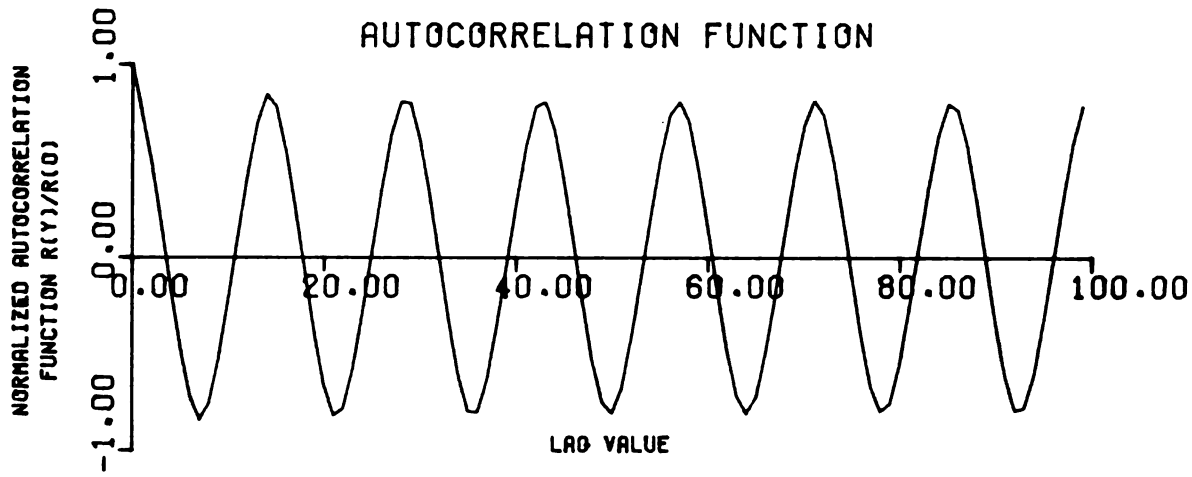


Figure 5.3.17.--Roughness type, estimated autocorrelation, and power spectral density functions of surface 45.





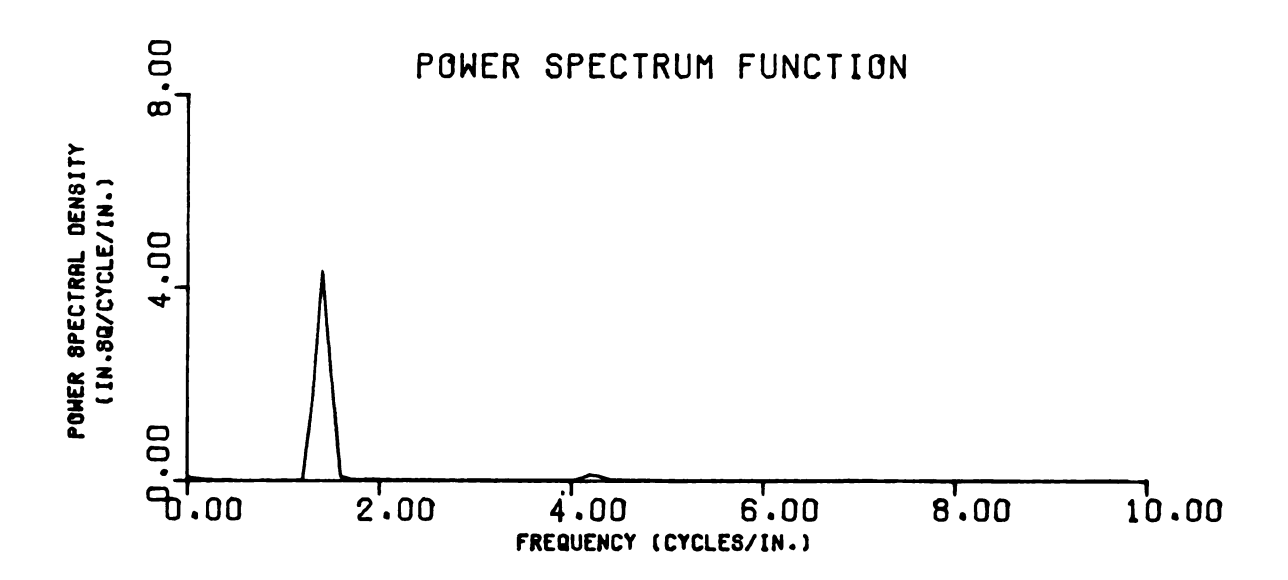


Figure 5.3.18.--Roughness type, estimated autocorrelation, and power spectral density functions of surface 9.

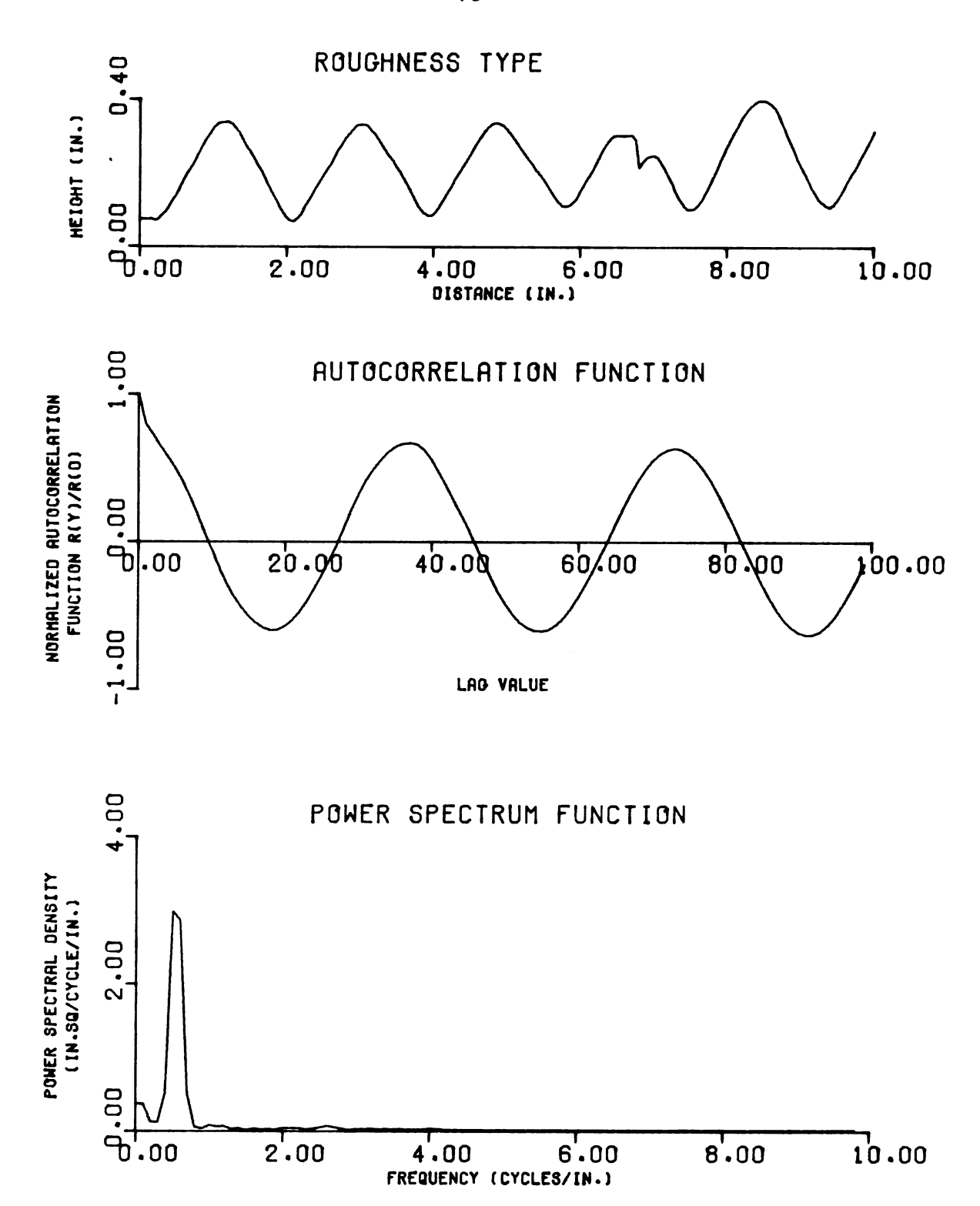


Figure 5.3.19.--Roughness type, estimated autocorrelation, and power spectral density functions of surface 17.

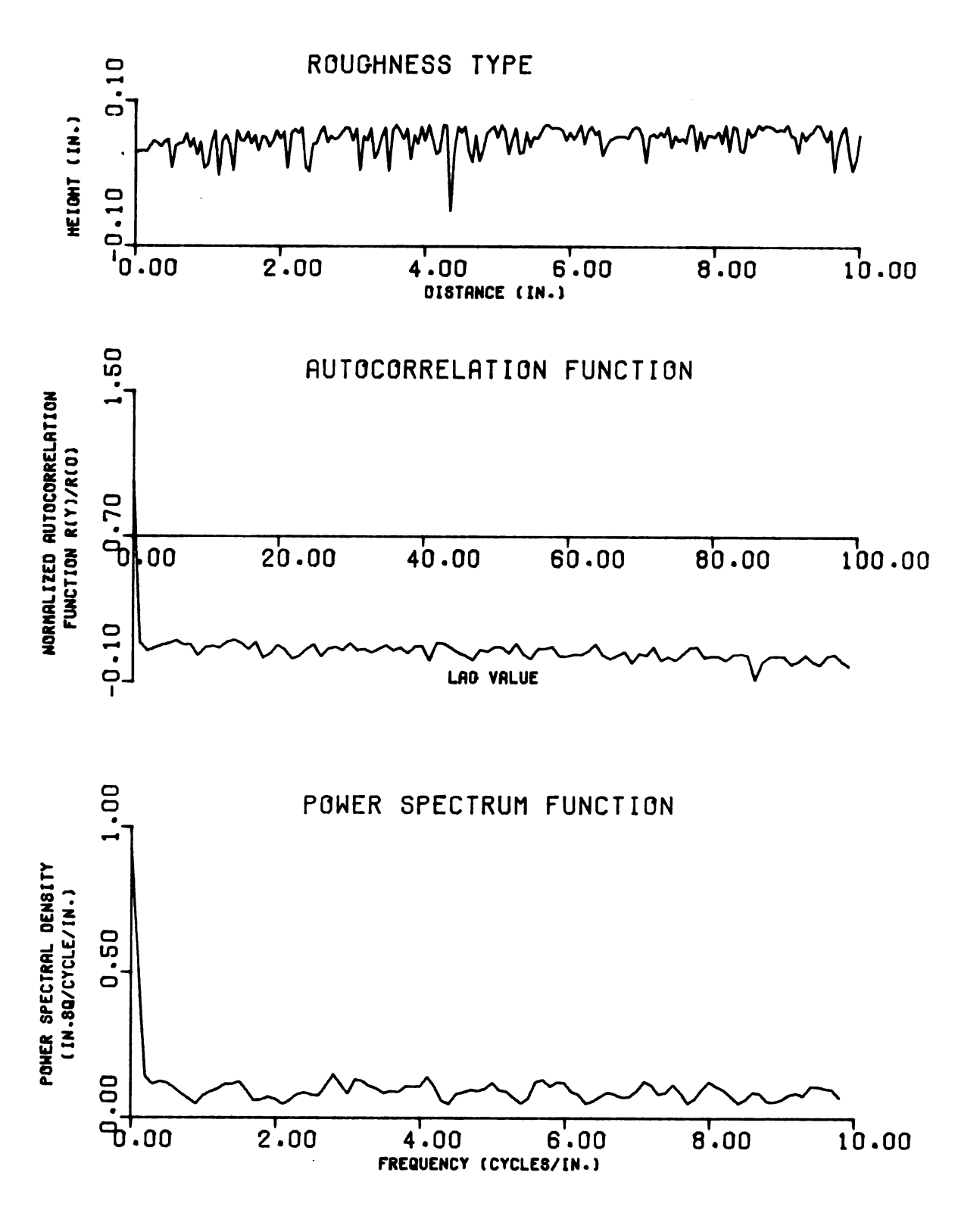
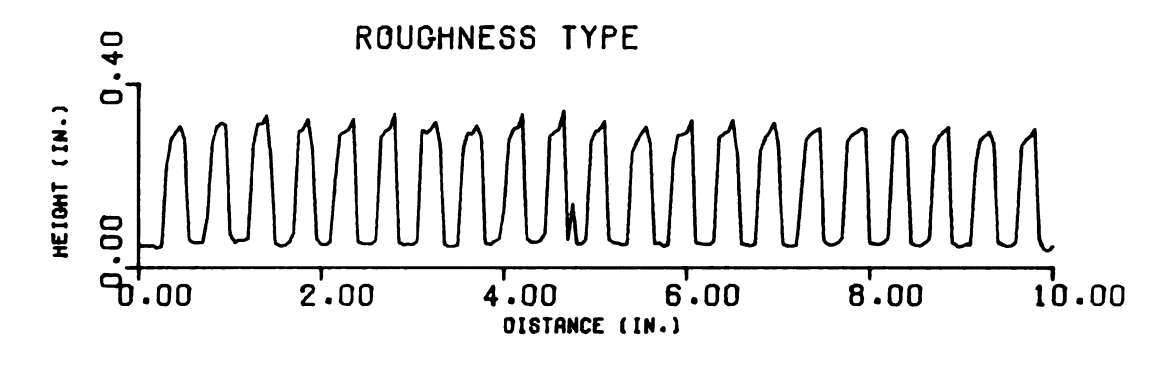
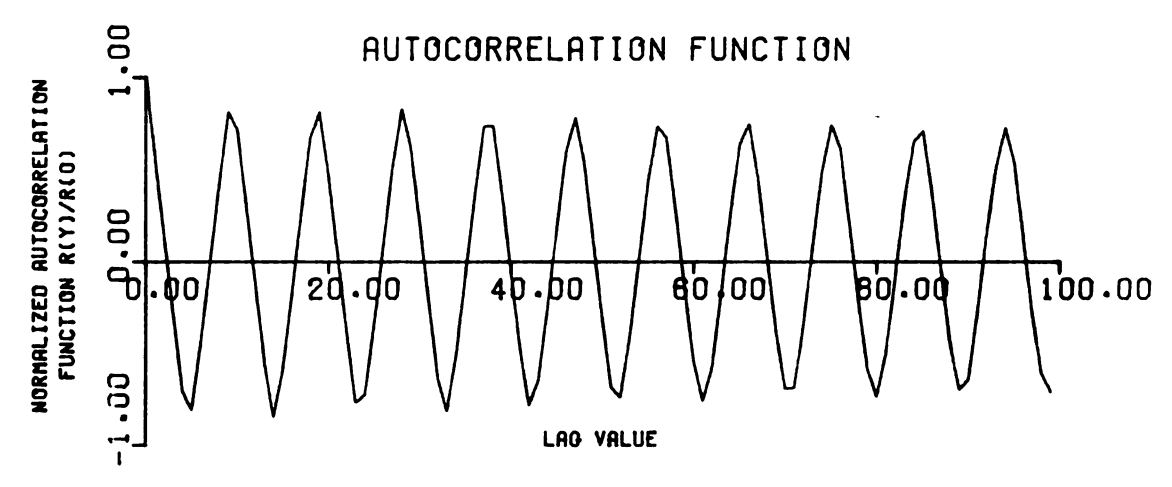


Figure 5.3.20.—Roughness type, estimated autocorrelation, and power spectral density functions of surface 15.





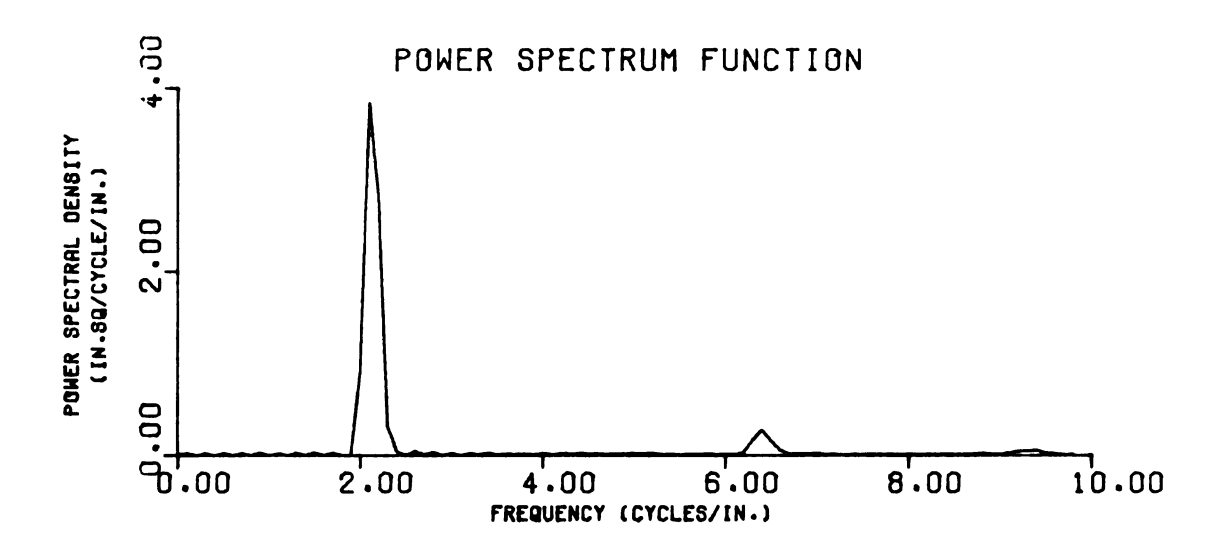
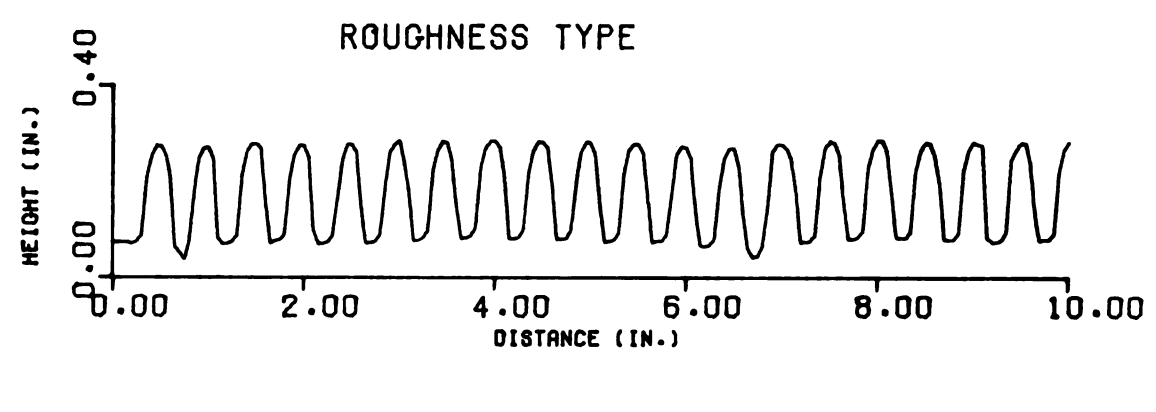
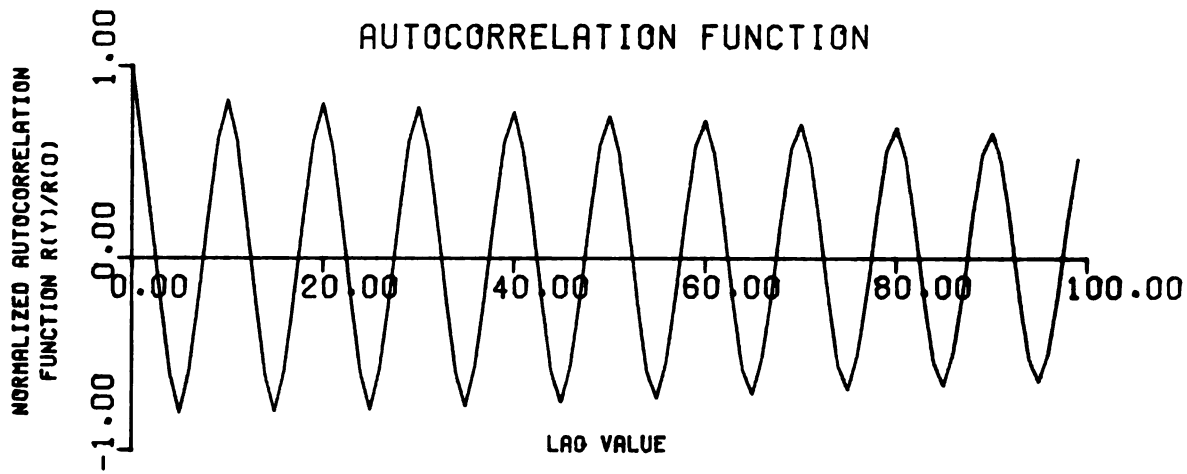


Figure 5.3.21.--Roughness type, estimated autocorrelation, and power spectral density functions of surface 10.





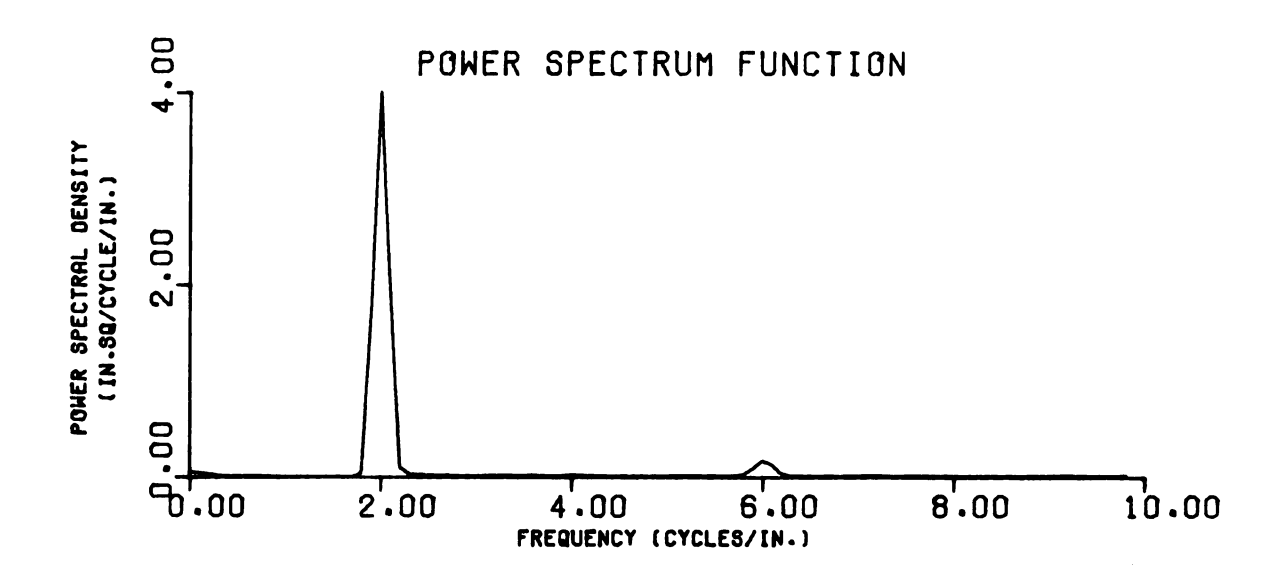


Figure 5.3.22.--Roughness type, estimated autocorrelation, and power spectral density functions of surface 12.

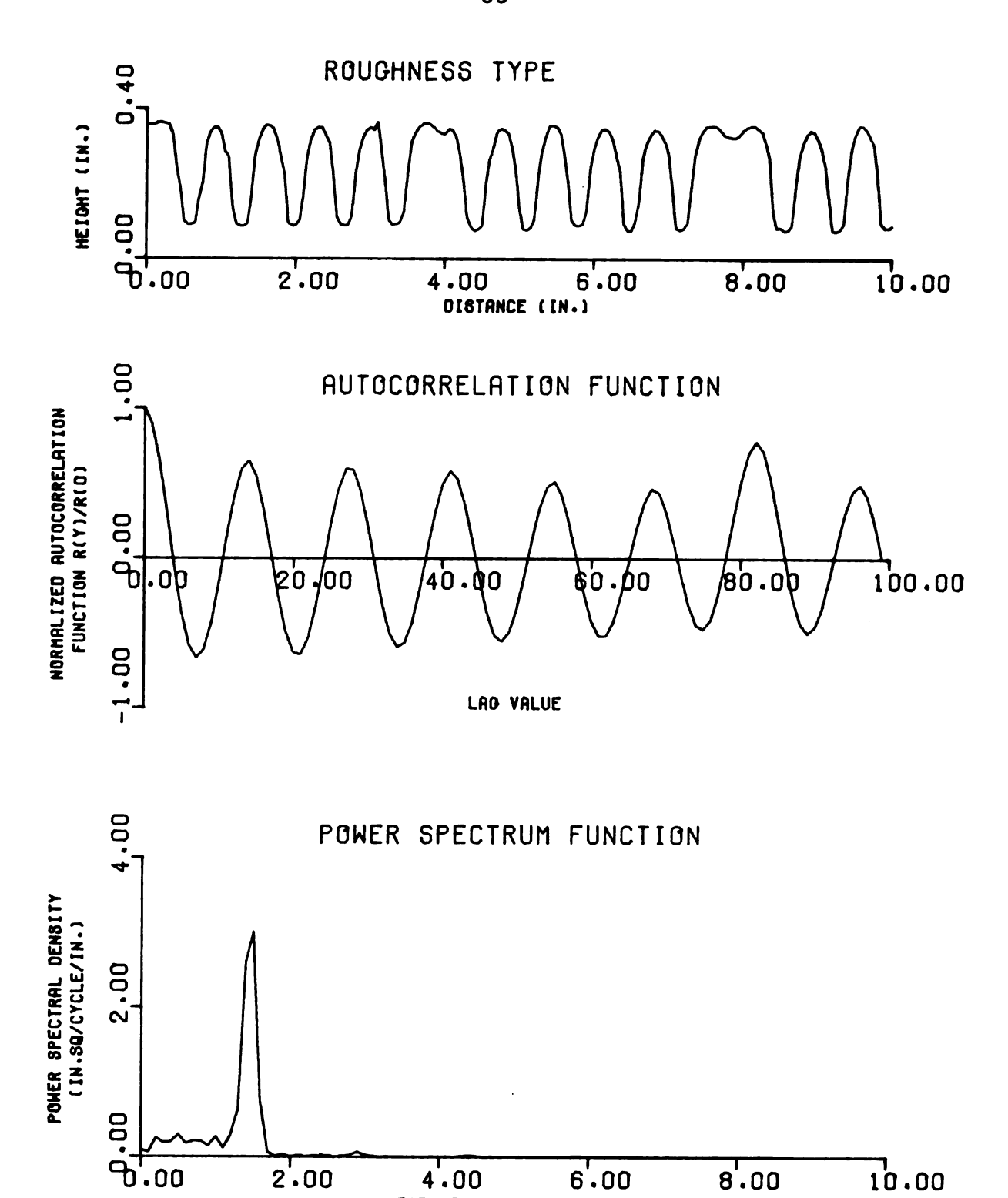
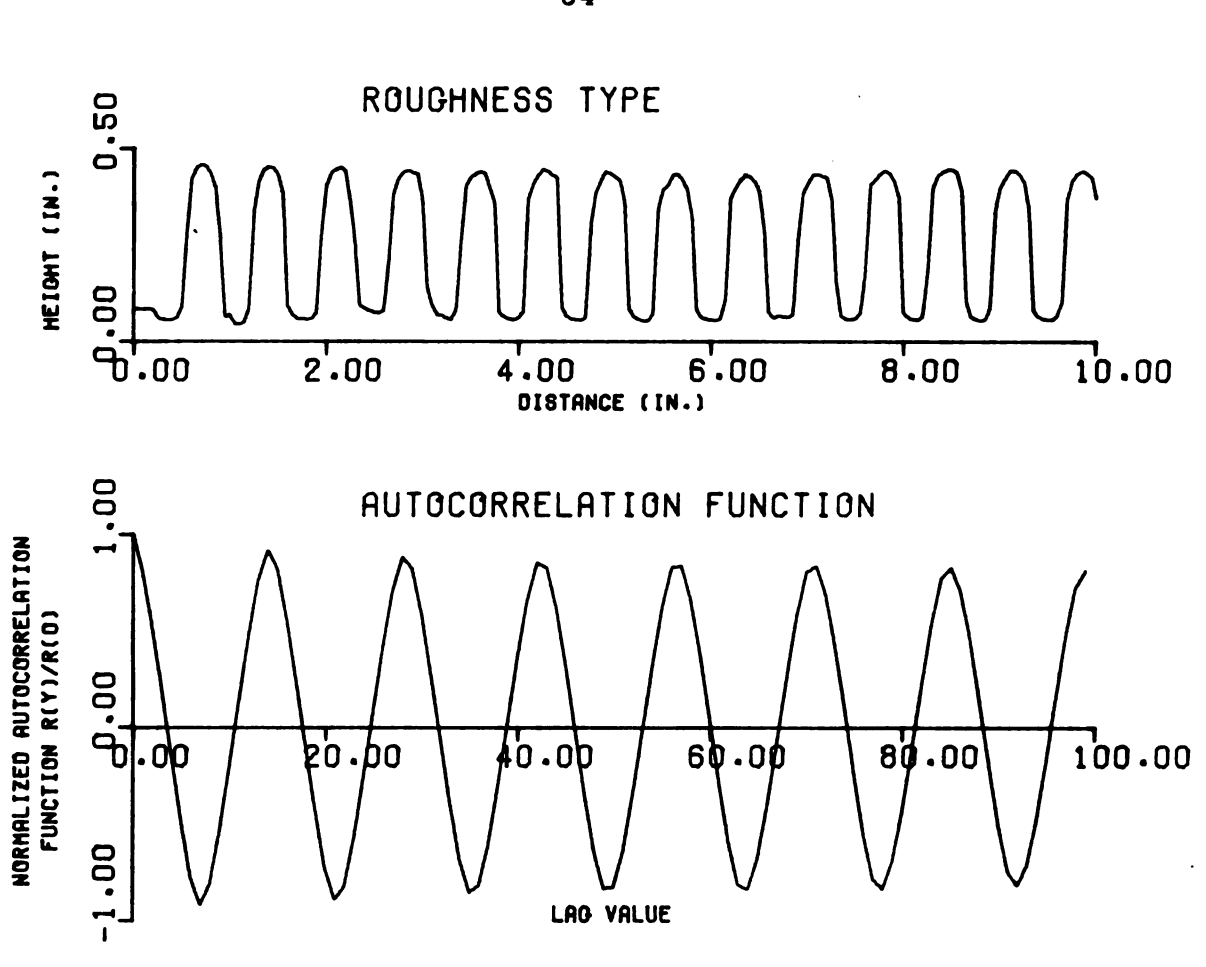


Figure 5.3.23.--Roughness type, estimated autocorrelation, and power spectral density functions of surface 6.

FREQUENCY (CYCLES/IN.)



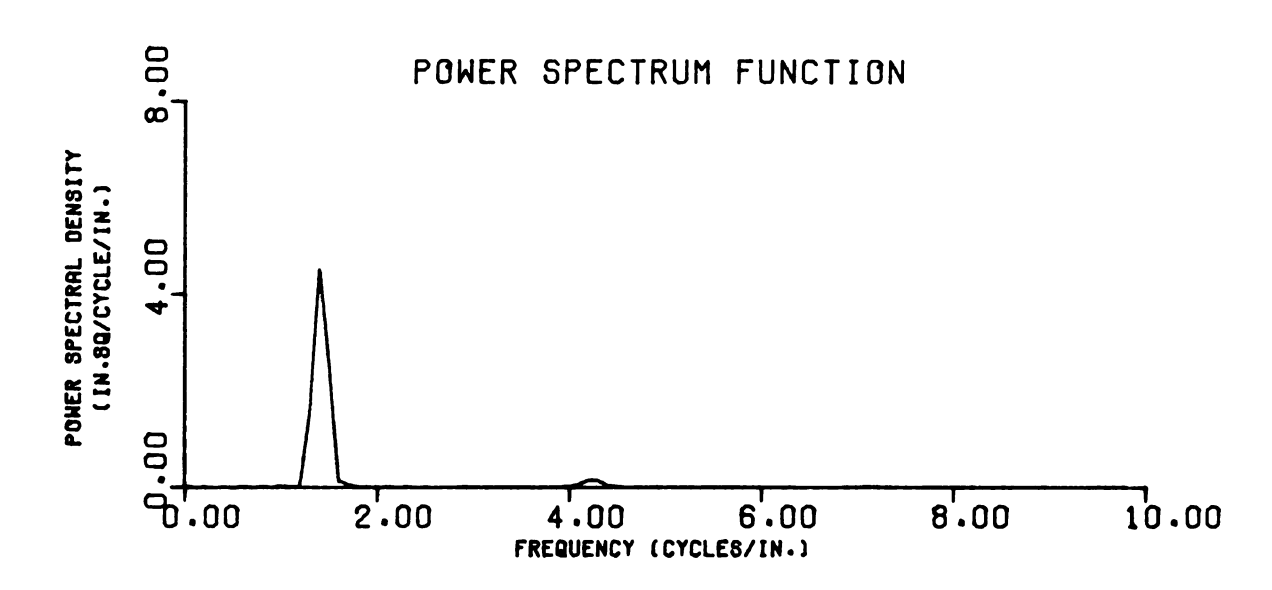


Figure 5.3.24.--Roughness type, estimated autocorrelation, and power spectral density functions of surface 5.

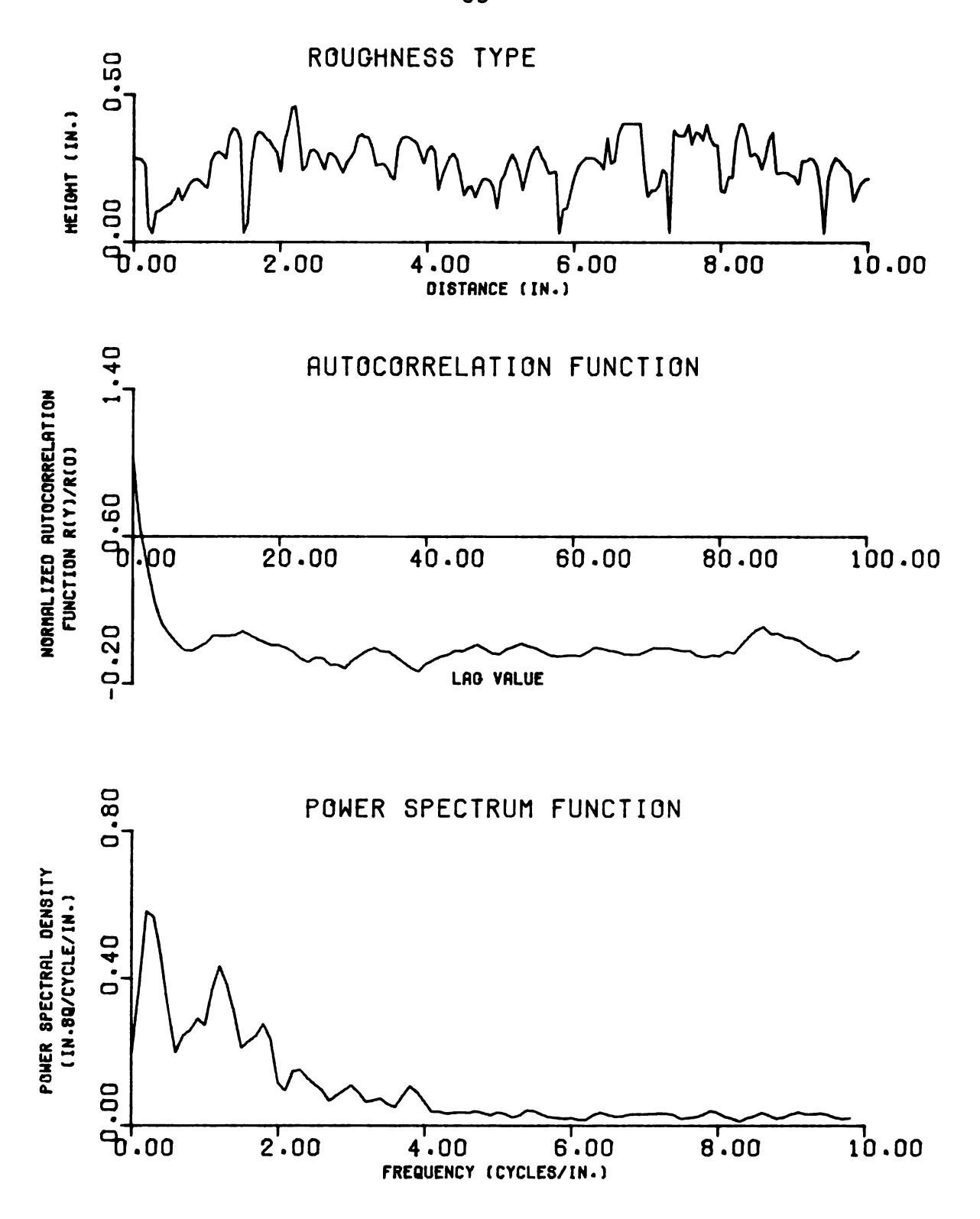


Figure 5.3.25.--Roughness type, estimated autocorrelation, and power spectral density functions of surface 4.

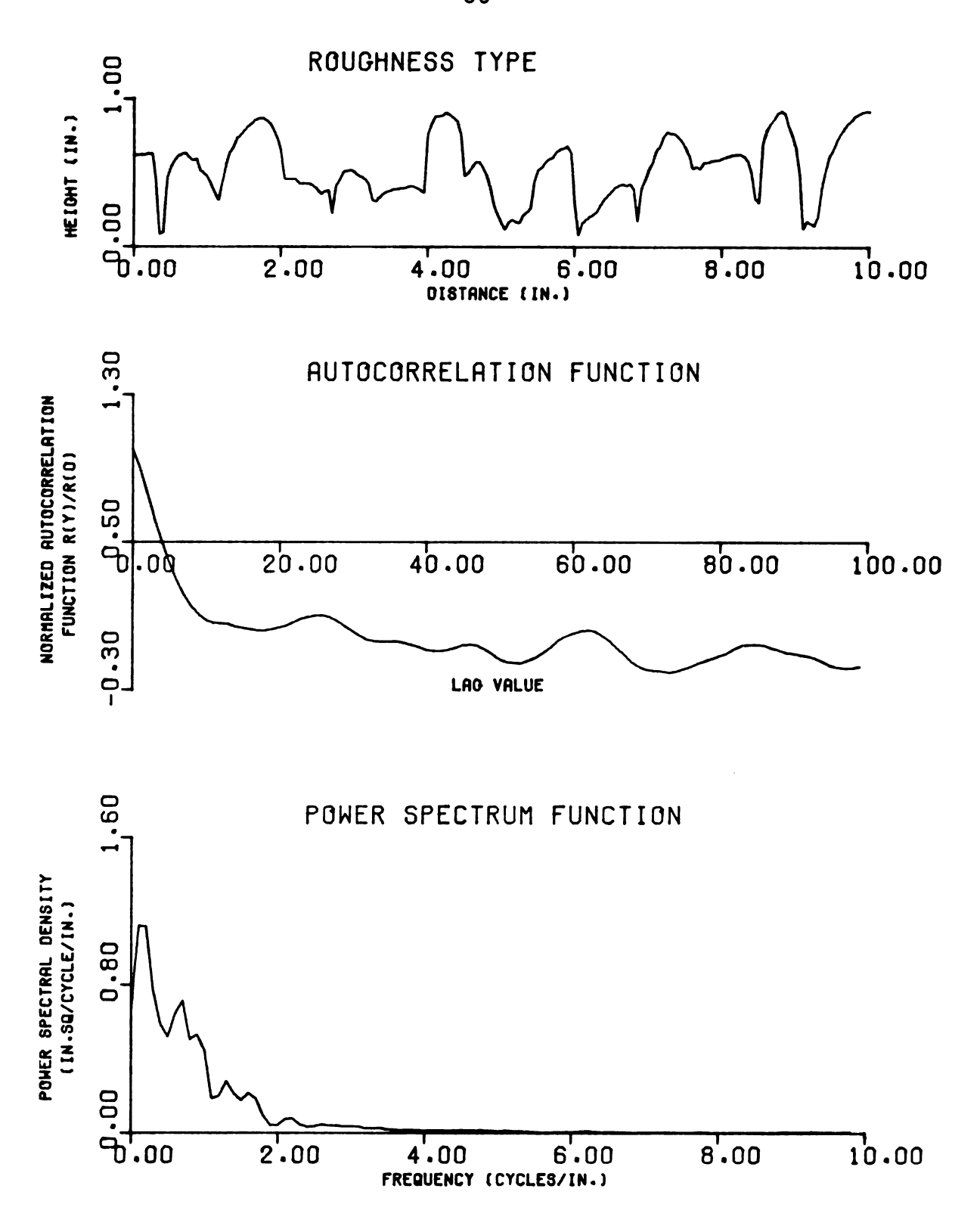


Figure 5.3.26.--Roughness type, estimated autocorrelation, and power spectral density functions of surface 1.

# 5.4. Confidence Intervals on Spectral Estimates

As was mentioned in Section 5.3, only 40-inch sections or, equivalently, 720 data points were used to obtain spectral estimates of the surfaces whose profiles were determined in the laboratory. Ninety-five percent confidence intervals at 10 cpi on the spectral estimates of these surfaces along with those of rectangular surfaces are given in Table 5.4.1.

TABLE 5.4.1.--Confidence intervals on spectral estimates.

Number of Da	ta Points	Associated Degrees of Freedom	95% Confidence Intervals
720	)	14	0.54-2.4
4000	)	40	0.67-1.65

# 5.5. Parameters Defining Spectral Estimates

One-dimensional strip roughnesses are uniquely represented by their spectral estimates as seen in Figures 5.3.1 through 5.3.26. However, a single parameter defining the behavior of an individual spectral estimate was needed to correlate a particular estimate to its corresponding Manning "n" friction coefficient.

Various quantitative values within the spectral estimates were examined for this purpose. Among the variables considered were: the frequency at which the maximum

peak occurs, the magnitude of the maximum peak, the frequency of the third occurrences of a significant peak, and the frequency at which 90 percent of the power occurs under the spectral density curve. The latter frequency was called the cutoff frequency in this study and is given in Tables 5.3.1 and 5.3.2 for each estimate. When these parameters were plotted against corresponding Manning "n" friction coefficients, the graphs were so scattered that no linear functional relationships could be drawn between the variables involved. An example of this behavior is illustrated in Figure 5.5.1 which shows the graphical relationship between the Manning "n" friction coefficient and the cutoff frequency, fc.

Since a particular parameter for spectral estimates could not be obtained directly from the spectrum functions, an indirect method was used to obtain it. A close inspection of the figures reveals that the peaks of power spectral density function decay exponentially with respect to frequency. A model defining this phenomena was assumed to be:

$$G(f) = K_0 e^{-Kf}$$
 (5.5.1)

where

 $K_{O}$ , K = constants.

The constant, K, is termed the decay coefficient. The constants  $K_O$  and K were determined by a regression analysis. The peaks with magnitudes of less than 0.02 were not used

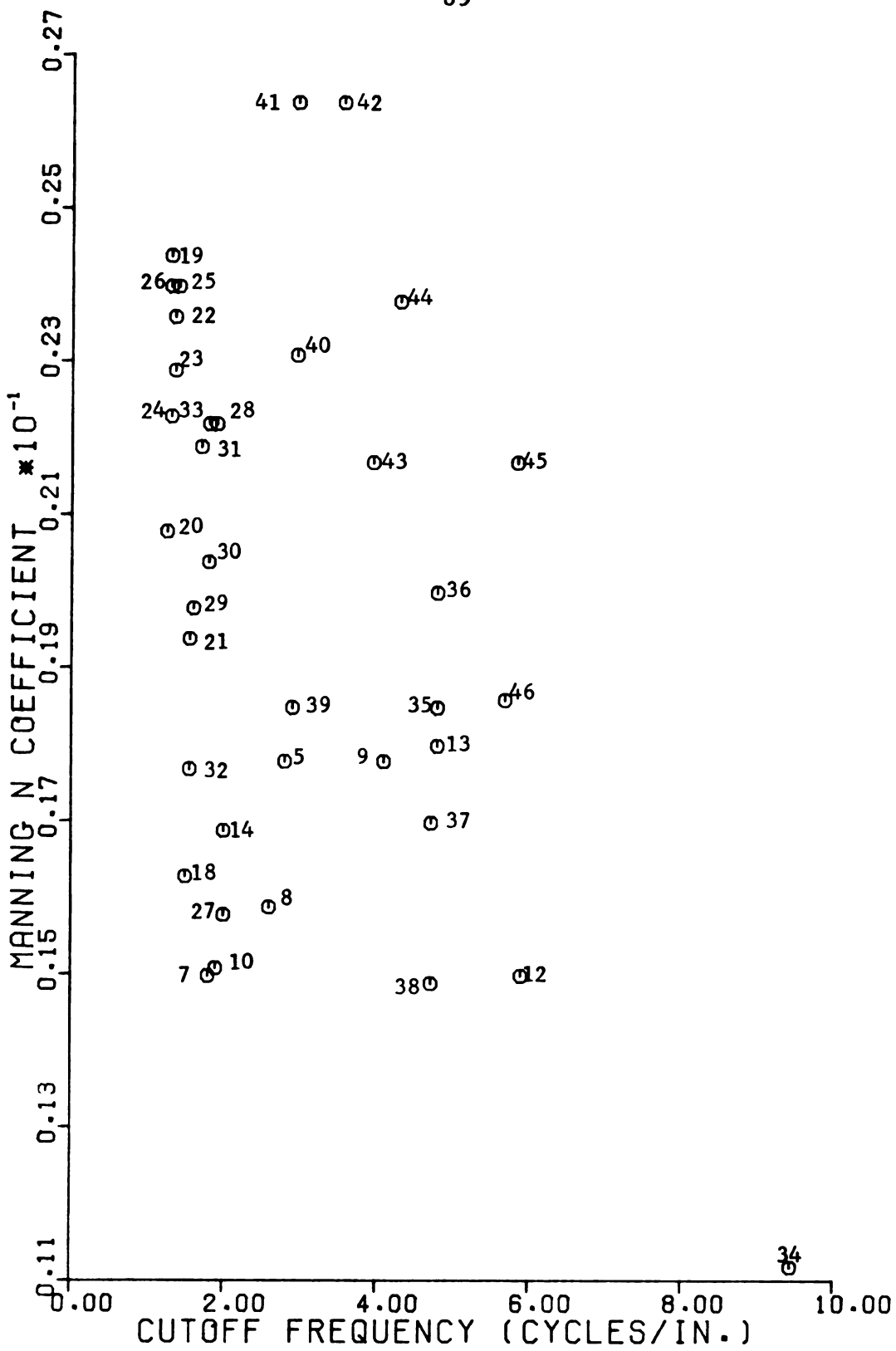


Figure 5.5.1.--Behavior of the Manning "n" friction coefficient with respect to the cutoff frequency.

in the regression. A FORTRAN IV computer program was developed to obtain  $K_O$  and K. The program and a sample output are given in Appendix C.

The calculated decay coefficients for each spectrum are given in Tables 5.3.1 and 5.3.2.

The decay coefficient, K, is assumed to represent the behavior of the spectral estimates. Figure 5.5.2 shows the behavior of the decay coefficients with respect to their Manning "n" friction coefficients. A parabolic relationship is hypothesized to exist between the variables involved. A FORTRAN IV library program was used to obtain the best-fitted curve through the data points. The resultant functional relationship between n and K is:

$$n = 0.0044 + 0.045 K - 0.024K^2$$
 (5.5.2)

The Manning "n" friction coefficient can be estimated from (5.5.2) once the decay coefficient of a given surface is determined.

### 5.6. Predicted Manning "n" Values

Equation (5.5.2) was used to predict the Manning "n" friction coefficients for surfaces whose actual friction coefficients were not known. Table 5.6.1 compares these values to the corresponding approximate values of "n" found in literature.

For gravel, the predicted "n" was obtained by averaging the K values of surfaces 1 and 2. For brick,

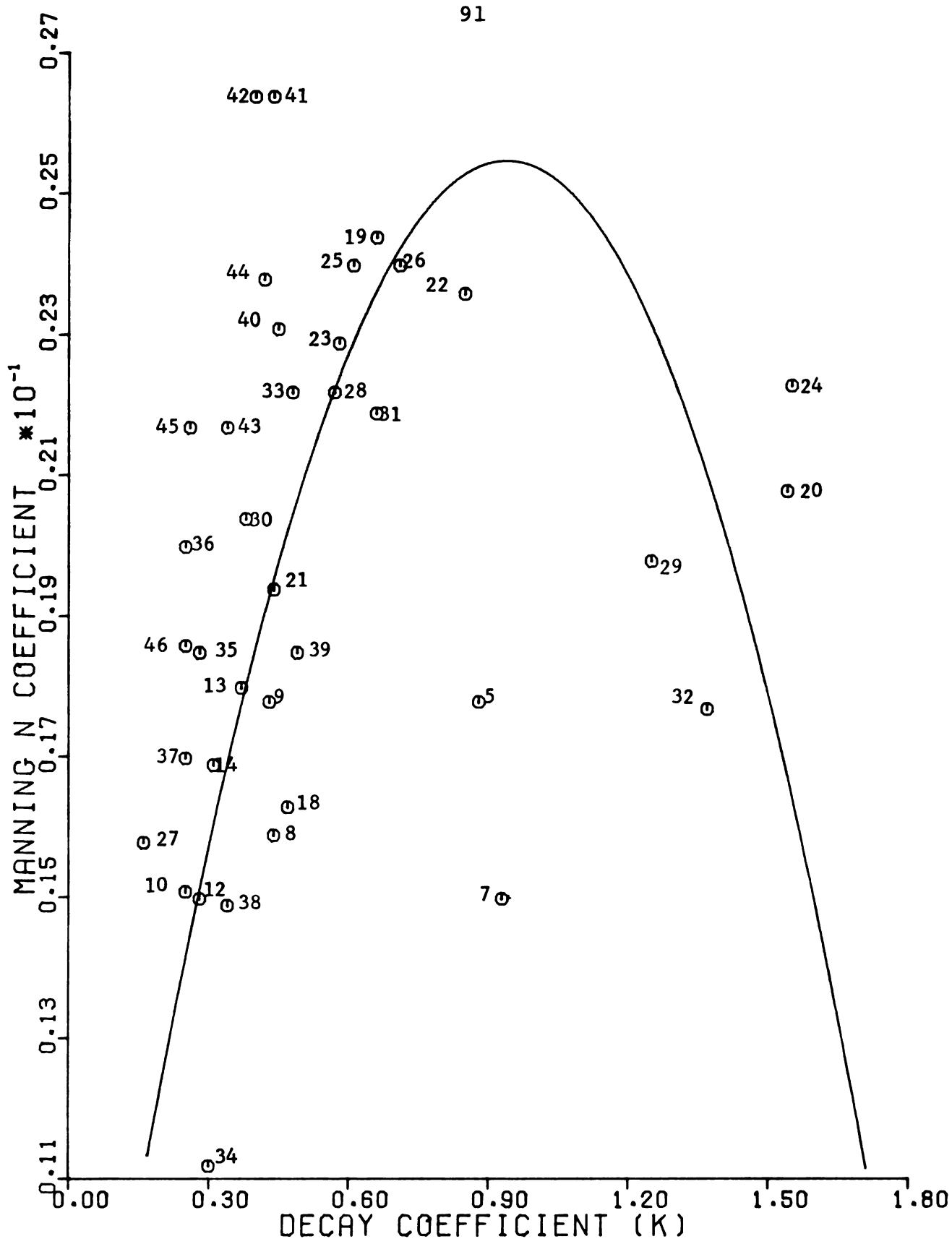


Figure 5.5.2.--Behavior of the Manning "n" friction coefficient with respect to the decay coefficients.

TABLE 5.6.1.--Comparison between predicted and literature values of Manning "n" friction coefficients.

	Predicted	In Literature
Plastic tubing	0.0213-0.0253	0.014
Gravel	0.0222	0.029
Fine gravel	0.0157	0.0162*
Corrugated metal tubing	0.020	0.022
Brick	0.0128	0.012-0.016

<sup>\*</sup>Calculated from the relationship,  $n = 0.031 d_1^{1/\sigma}$ ,  $d_1 = particle size$ ; average diameter of the gravel was 0.25 inches.

the K value obtained for surface 15 was used to get the predicted "n".

## 5.7. Theoretical Spectrum Functions for Surfaces With Rectangular Roughness Elements and Their Comparison With Estimated Spectrum Functions

In the preceding sections, spectrum functions of surfaces with rectangular roughness elements were obtained by a digital approximation method. The true spectrum functions of this type of surface can also be obtained from theoretical considerations.

The fixed sampling interval L of the sample function  $X_k(\ell)$  can be generalized as having n rectangular wave forms of width w and amplitude a, with spacing  $\lambda$  between the wave forms. We investigate only the case where  $\lambda$  is always greater than w. The general shape of function  $X_k(\ell)$  is illustrated in Figure 5.7.1.

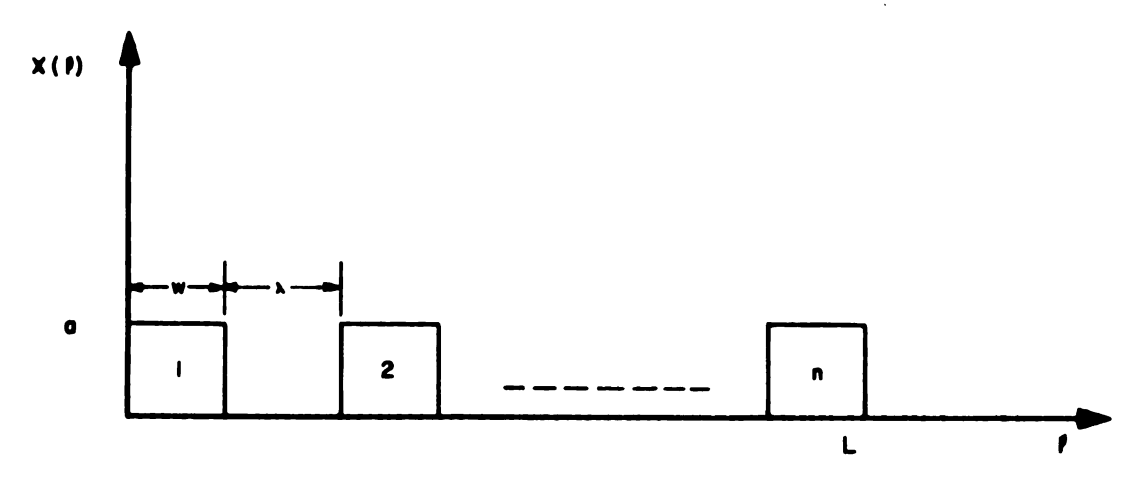


FIGURE 5.7.1.—SAMPLING FUNCTION,  $X_k$  (1)

Figure 5.7.1.--Sampling function,  $X_k(\ell)$ .

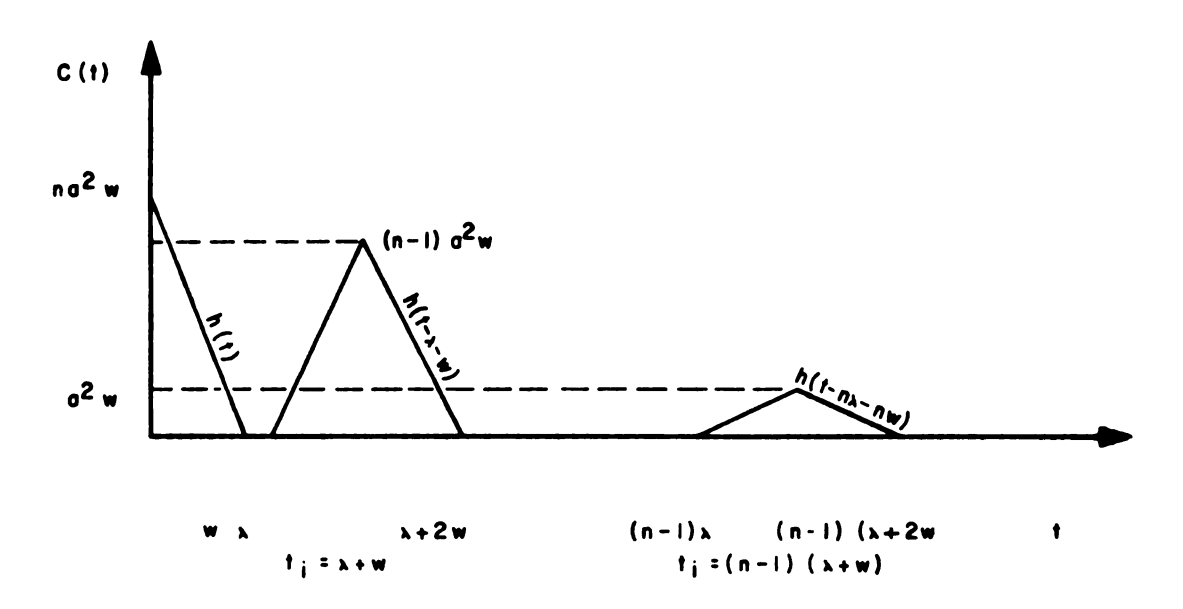


FIGURE 5.72.— GENERAL CORRELATION FUNCTION OF  $\mathbf{X_k}$  (1)

Figure 5.7.2.--General correlation function of  $\mathbf{X}_{\mathbf{k}}(\mathbf{l})$ .

The correlation function,  $C(\tau)$ , of the function  $X_k(\ell)$  is defined by the relationship

$$C(\tau) = \int_{-\infty}^{\infty} X_{k}(\ell) X_{k}(\ell + \tau) d\ell \qquad (5.7.1)$$

where  $X_k(\ell)$  is defined only on the interval 0 <  $\ell$  < n(w +  $\lambda$ ).

For n rectangular wave forms, the correlation function (5.7.1) becomes the piecewise function

$$C(\tau) = a^{2}n(w-\tau) \qquad 0 \le \tau < w$$

$$= 0 \qquad w \le \tau < \lambda$$

$$C(\tau) = a^{2}(n-1)(\tau-\lambda) \qquad \lambda \le \tau < \lambda + w$$

$$= a^{2}(n-1)(\lambda+2w-\tau) \qquad \lambda + w \le \tau < \lambda + 2w$$

$$= 0 \qquad \lambda + 2w \le \tau < 2\lambda + w$$

$$\vdots \qquad \vdots \qquad \vdots \qquad \vdots$$

$$C(\tau) = a^{2}2[\tau - (n-2)\lambda - (n-3)w] \qquad (n-2)\lambda + (n-3)w \le \tau < (n-2)\lambda + (n-2)w$$

$$= a^{2}2[(n-2)\lambda + (n-1)w - \tau] \qquad (n-2)\lambda + (n-2)w \le \tau < (n-2)\lambda + (n-1)w$$

$$= 0 \qquad (n-2)\lambda + (n-1)w \le \tau < (n-1)\lambda + (n-2)w$$

$$C(\tau) = a^{2}[\tau - (n-1)\lambda - (n-2)w] \qquad (n-1)\lambda + (n-2)w \le \tau < (n-1)\lambda + (n-1)w$$

$$= a^{2}[(n-1)\lambda + nw - \tau] \qquad (n-1)\lambda + (n-1)w \le \tau < (n-1)\lambda + (n-1)w$$

$$= a^{2}[(n-1)\lambda + nw - \tau] \qquad (n-1)\lambda + (n-1)w \le \tau < (n-1)\lambda + nw$$

$$= 0 \qquad (n-1)\lambda + nw \le \tau$$

The general shape of the correlation function  $C(\tau)$  is shown in Figure 5.7.2 (on page 93).

The energy spectrum of the sample function  $\mathbf{X}_{\mathbf{k}}^{(\ell)}$  is defined by

$$G(\omega) = \int_{-\infty}^{\infty} C(\tau) e^{-j\omega\tau} dt \qquad (5.7.3, a)$$

or

$$= 2 \int_{-\infty}^{\infty} C(\tau) \cos \omega \tau d\tau \qquad (5.7.3, b)$$

where

 $\omega$  = angular frequency.

The spectrum,  $H(\omega)$  of the first wave form h(t), in Figure 5.7.2 can be derived directly from (5.7.3, b) by using  $C(\tau)$  when  $\tau$  is between 0 and  $\omega$  (5.7.2).  $H(\omega)$  takes the form

$$H(\omega) = \frac{na^2}{\omega^2 w} (1 - \cos \omega 2w)$$
 (5.7.4, a)

or

$$= 2 \operatorname{na}^{2} w \left( \frac{\sin \omega w}{\omega w} \right)^{2}. \tag{5.7.4, b}$$

Then the energy spectrum of the function becomes

$$G(\omega) = \int_{-\infty}^{\infty} C(t) e^{-j\omega t} d\tau \qquad (5.7.5, a)$$

or, summing over all values of i,

$$= \sum_{i=0}^{n-1} \int_{-\infty}^{\infty} h(t - t_i) e^{-j\omega t} dt. \qquad (5.7.5, b)$$

Let us define a dummy variable  $x - t - t_i$ . We introduce this variable in (5.7.5, b) to obtain the form

$$G(\omega) = \sum_{-\infty}^{\infty} \int_{-\infty}^{\infty} h(x) e^{-j\omega(x+t_i)} dx \qquad (5.7.6, a)$$

or,

$$= \sum_{i=0}^{n-1} \int_{-\infty}^{\infty} e^{-j\omega t} \int_{-\infty}^{\infty} f(x)e^{-j\omega x} dx \qquad (5.7.6, b)$$

which becomes, through the use of the steps leading from (5.7.3, b) to (5.7.4, b),

$$= \sum_{i=0}^{n-1} e^{-j\omega t_i} H(\omega)$$
 (5.7.6, c)

Equation (5.7.6, c) is the general transformation function for true spectrum function,  $G(\omega)$ .

Consider the basic wave form h(t) in Figure 5.7.2: the amplitudes of the waves are  $na^2w$ ,  $(n-1)a^2w$ , . . . .  $[n-(n-2)]a^2w$ ,  $[n-(n-1)]a^2w$  and the peaks occur at values of  $t_i=i(\lambda+w)$ ,  $i=1,2,\ldots,(n-1)$ . By using the transformation function (5.7.6, c) the spectrum function  $G(\omega)$  becomes

$$G(\omega) = 2w \left(\frac{\sin \omega w}{\omega w}\right)^{2} \left[na^{2}w + (n-1)a^{2}w \left(e^{-j\omega(\lambda+w)} + e^{j\omega(\lambda+w)}\right)\right]$$

$$+ \cdot \cdot \cdot \cdot + [n - (n-2)]a^{2}w \left(e^{-j\omega[(n-2)\lambda+(n-2)w]}\right]$$

			-
			1
			1
			į
1			
			i

$$+ e^{j\omega[(n-2)\lambda+(n-2)w]}$$

$$+ [n - (n-1)]a^{2}w[e^{-j\omega[(n-1)\lambda+(n-1)w]}$$

$$+ e^{j\omega[(n-1)\lambda+(n-1)w]}$$

$$(5.7.7, a)$$

or,

$$= 2 a^{2}w^{2} \left[ \frac{\sin \omega w}{\omega w} \right]^{2} \left[ n + 2(n-1) \cos \left[ \omega (\lambda + w) \right] \right]$$

$$+ 2(n-2) \cos \left[ 2\omega (\lambda + w) \right] + \cdots$$

$$+ 2[n - (n-2)] \cos \left[ (n-2)\omega (\lambda + w) \right]$$

$$+ 2[n - (n-1)] \cos \left[ (n-1)\omega (\lambda + w) \right]. \qquad (5.7.7, b)$$

In order to compare the theoretical spectrum and the estimated spectrum functions of the surfaces, a normalization process for the theoretical spectrums was used, since the estimated power spectrum functions were obtained directly from the autocorrelation of the sample functions. The normalization is achieved by the following relationships:

$$C_{x}(\tau) = C(\tau) - \mu_{x}^{2}$$
 (5.7.8)

where

 $C_{\mathbf{x}}(\tau)$  = autocovariance function, and  $\mu_{\mathbf{y}}$  = expected value of the sample function.

The autocorrelation of the covariance function is therefore defined by

$$R(\tau) = \frac{C(\tau) - \mu_{x}^{2}}{C(0) - \mu_{x}^{2}}.$$
 (5.7.9)

By substituting  $\mu_{\mathbf{X}}$  and C(O), and dividing C(O) and C(\tau) by the sampling length to obtain functional terms having correct dimensions, (5.7.9) becomes

$$R(\tau) = \frac{\frac{C(\tau)}{n(\lambda+w)} - \left(\frac{aw}{\lambda+w}\right)^2}{\frac{na^2w}{n(\lambda+w)} - \left(\frac{aw}{\lambda+w}\right)^2}$$
(5.7.10, a)

or

$$= \frac{C(\tau)(\lambda+w)}{na^2\lambda w} - \frac{\omega}{\lambda}. \qquad (5.7.10, b)$$

Hence, the normalized power spectrum function  $G^{\, {}^{\prime}} \left( \omega \right)$  becomes

$$G'(\omega) = \frac{(w+\lambda)}{a^2w\lambda n} G(\omega) - \frac{w}{\lambda} \delta(\omega) . \qquad (5.7.11)$$

The last term in (5.7.11) is a delta function and affects the value of the spectrum only at  $\omega = 0$ . Since we seek the exponential decay function for the spectral peaks for  $\omega > 0$ , this term does not enter into the computations and hence can be disregarded.

Substituting the value of  $G(\omega)$  from (5.7.7, b) allows (5.7.11) to become

$$G'(\omega) = \frac{2(w+\lambda)}{\lambda n} \left( \frac{\sin \omega w}{\omega w} \right)^{2} \left( n + 2(n-1) \cos \left[ \omega (\lambda + w) \right] + 2(n-2) \cos \left[ 2\omega (\lambda + w) \right] + \cdots + 2[n - (n-2)] \cos \left[ (n-2)\omega (\lambda + w) \right] + 2[n - (n-1)] \cos \left[ (n-1)\omega (\lambda + w) \right] \right).$$
 (5.7.12)

Equation (5.7.12) was programed for the computer to obtain the spectrum functions of the rectangular surfaces for comparison with the functions obtained by digital approximation. The program and a sample output is given in Appendix D.

The theoretical and estimated spectrums of several surfaces representing high and low concentration roughness are plotted in Figures 5.7.3 through 5.7.6. The actual magnitude of the theoretical spectrum values shown in the figures was some constant multiple times greater than the estimated spectrum values. A different constant was obtained for the spectrums of each surface. The plotted theoretical spectrums were obtained by dividing the calculated values by the appropriate constant. The source of the constant appears to be in the normalized process of the theoretical spectrum.

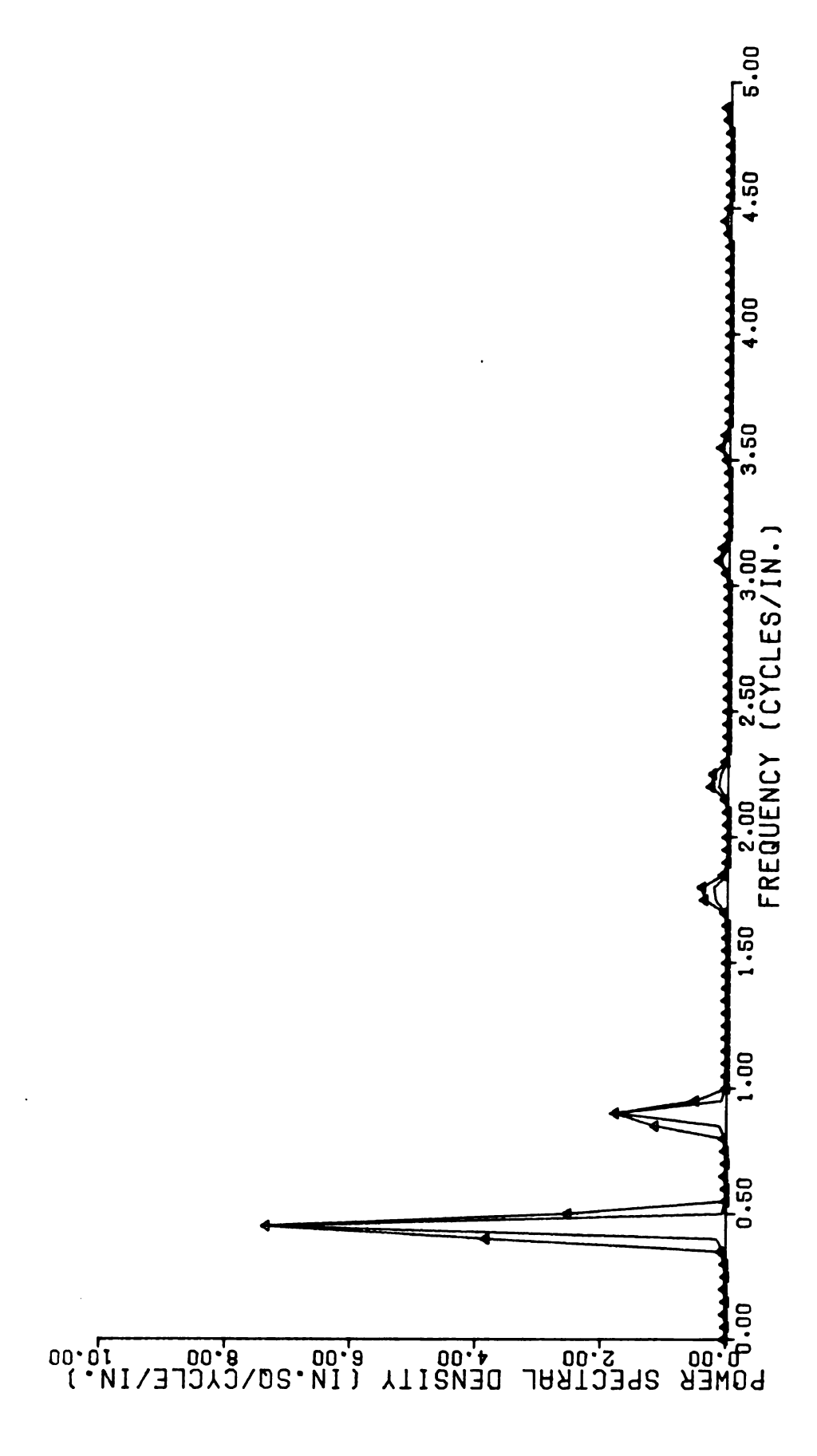


Figure 5.7.3.--The theoretical and estimated spectral density functions of surface 30. (The curve with triangular data points is the estimated spectral density function.)

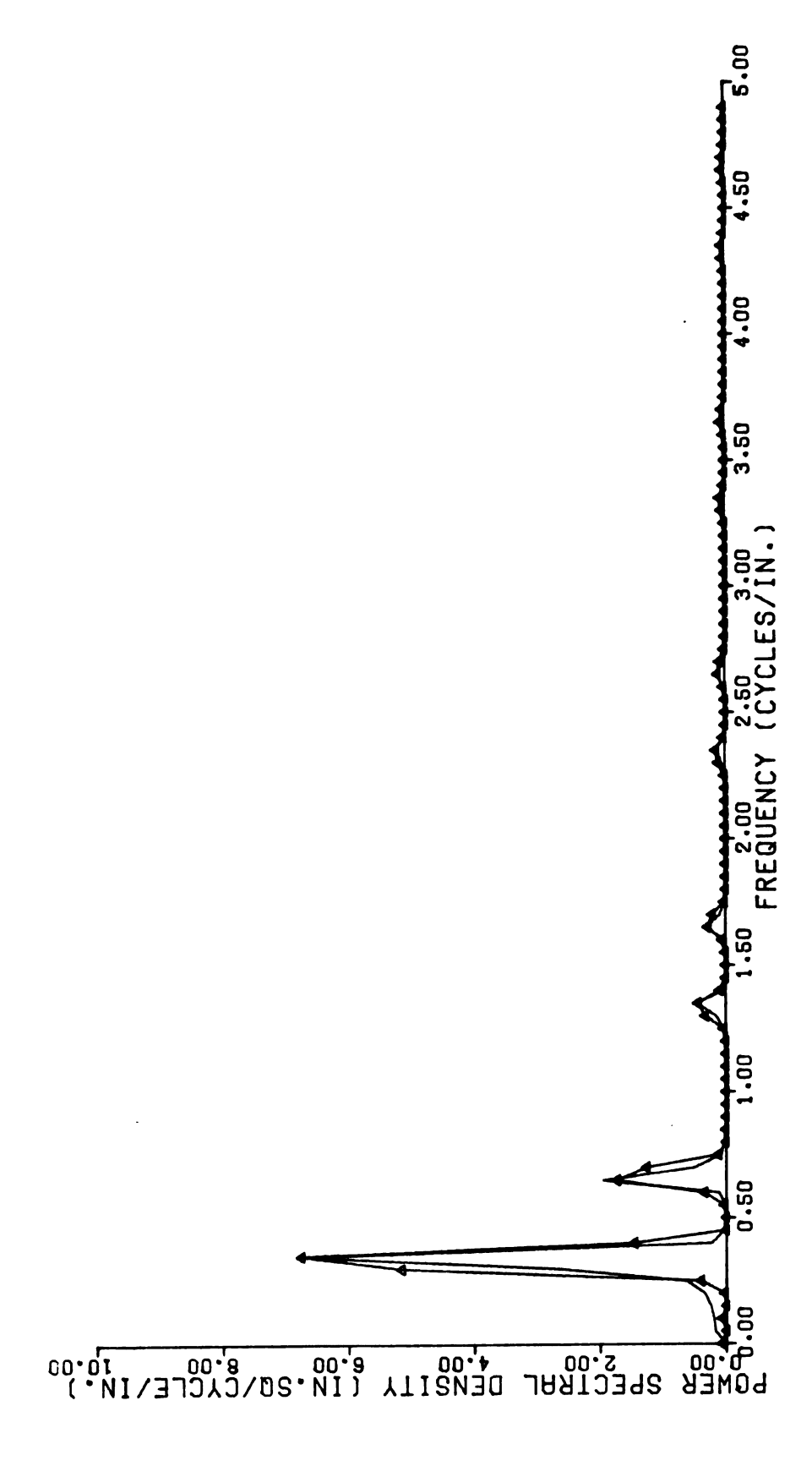


Figure 5.7.4.--The theoretical and estimated spectral density functions of surface 23. (The curve with triangular data points is the estimated spectral density function.)

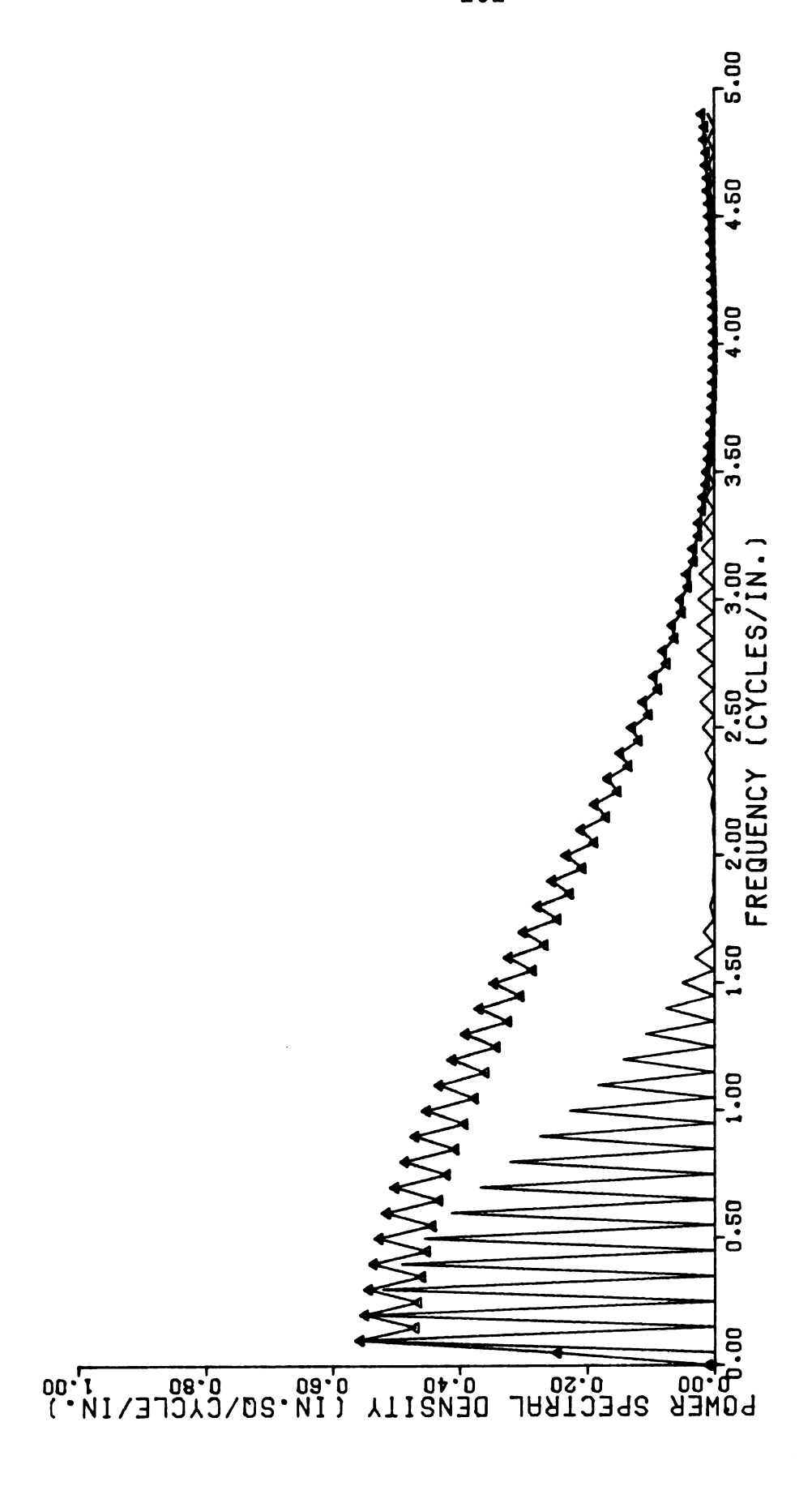


Figure 5.7.5.--The theoretical and estimated spectral density functions of surface 40. (The curve with triangular data points is the estimated spectral density function.)

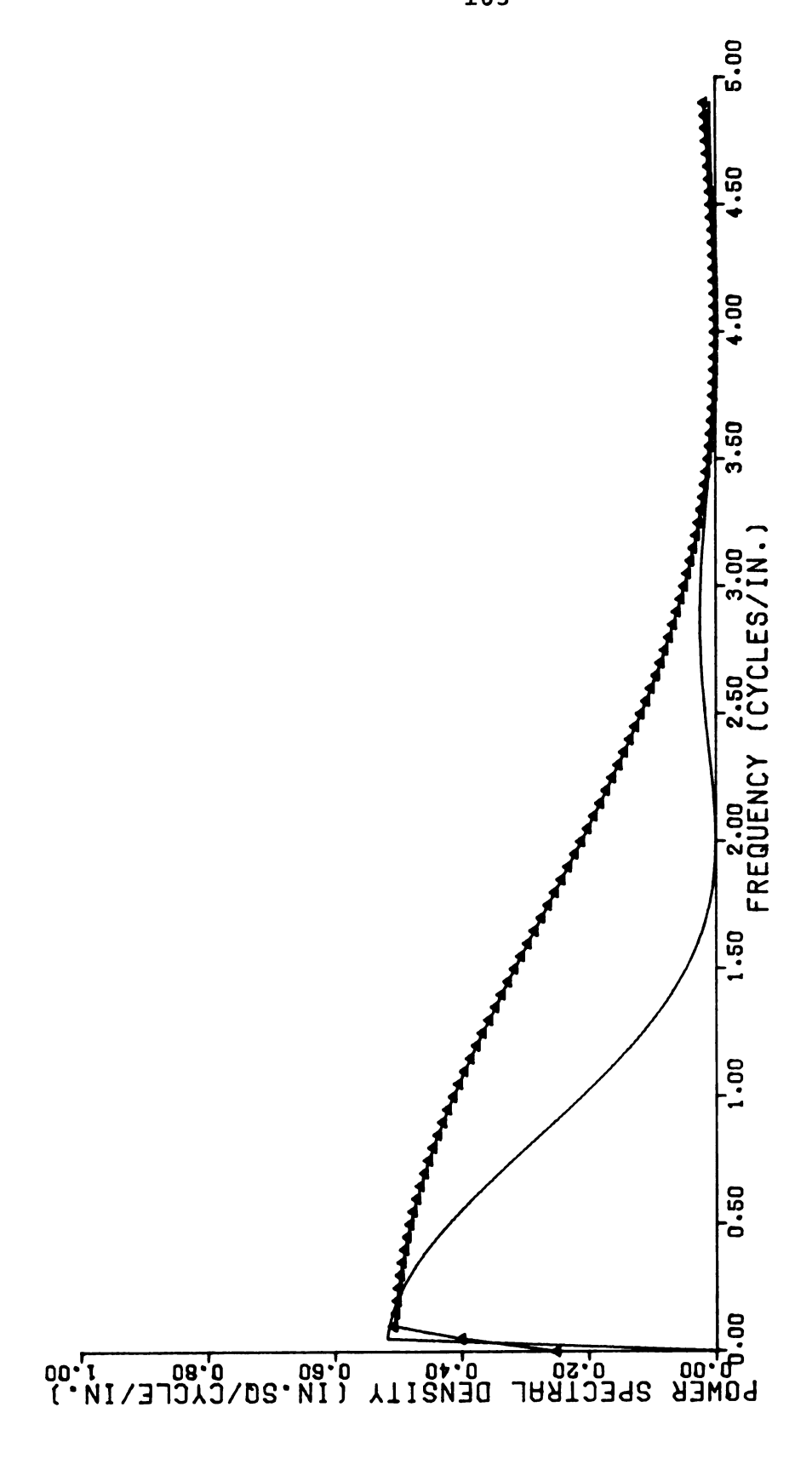


Figure 5.7.6.--The theoretical and estimated spectral density functions of surface 39. (The curve with triangular data points is the estimated spectral density function.)

Generally, the theoretical and estimated spectrum values agree well for high roughness concentrated surfaces. The agreement lessens for low roughness concentrated surfaces reflecting the need for an appropriate change on the coefficients of the window function (Hanning window) used in this study.

#### 6. DISCUSSION

As was pointed out in the literature review, many researchers have shown that for completely turbulent flow, the resistance to flow is dependent only upon the characteristic of the rough surface boundary. The surface roughness effect is attributed to the concentration of the elements which constitute such a surface. It is a postulate of this research that the concentration of the roughness elements may be defined functionally by considering the frequency decomposition of the variance of the roughness elements, as reflected in the autocorrelation function and power spectral density.

The roughness makeup of the surfaces is uniquely represented by the power spectral density functions as demonstrated in Figures 5.3.1 through 5.3.26. The spectrum contains most of its power at high frequencies when the surface roughness elements are close to each other; i.e., when the concentration of the elements is high. In particular, the peaks in the spectrum are dispersed toward higher frequencies, with increasing concentration. With decreasing concentration the peaks move slightly to the lower frequencies. At low roughness concentrations, almost all power is contained at low frequencies.

At very low roughness concentrations, however, information on the roughness makeup of the surfaces is lost. This is illustrated in Figures 5.3.12 and 5.3.15. When roughness elements are placed at 10-inch intervals no significant peak appears on the spectral estimate as demonstrated in Figure 5.3.15. When the size of the roughness elements is decreased but the elements are located at the same intervals (Figure 5.3.12), the peaks are nonexistent on the spectral estimate and the estimate itself shows a very smooth decay. A similar behavior of the estimate was obtained for roughness type 47. erroneous behavior of the spectral estimates for surfaces of low roughness concentration is due to the unsuitability of the window function used in the program for spectral estimates. It is felt that different weighting constants should be used to bring the estimated spectrums closer in agreement with the theoretically derived spectrum functions. This is illustrated in Figures 5.7.5 and 5.7.6 where the estimates for surfaces of high concentration of roughness agree well with the theoretical predictions, while in Figures 5.7.3 and 5.7.4 the estimates for surfaces of low roughness concentration contain considerably more power at high frequencies than do the theoretical spectrum functions.

The decay coefficient for surface 47, a surface with low roughness concentration, appeared to be so

erroneous that the value from this surface was not used to estimate the curve in Figure 5.5.2.

A parabolic relationship was fitted to the decay coefficients and corresponding friction coefficients with a correlation of 0.6 as seen in Figure 5.5.2. behavior is thought to accurately describe the mechanism involved between a rough surface and the Manning "n" friction factor associated with such a surface. It is a fundamental fact (Morris, 1955; Koleseus and Davidian, 1966; Robertson and Chen, 1970) that the main source of friction losses, in a fluid flowing over a rough surface, is the generation, spreading, and subsequent dissipation of vortices behind each roughness element. Each element is a source of vorticity and consequently the longitudinal spatial frequency of roughness elements is closely related to the creation of such vortices. If the roughness elements are highly concentrated, the flow skims the peaks of the roughness elements leaving some dead water regions between the elements. The relatively still water trapped in these spaces results in a lesser degree of vortex generation and consequently such a surface exhibits somewhat smaller friction factors. For this type of surface, the lower friction factors are defined by the lower lefthand side of the parabola in Figure 5.5.2.

If the spacing between roughness elements is increased the dead water regions between the elements no

longer exist and new vortices begin to develop between the elements. Vortex generation and dissipation associated with each element are not completed before the next element is encountered by the moving fluid particle. result is additional perturbation and greater friction losses. Increasing distance between the elements is thus associated with increasing friction losses up to a maximum intensity. Increasing the distance after a certain point results in decreasing friction losses since the elements are so far apart that individual elements act as isolated bodies. The intensity of vortex generation and associated dissipation is greatly reduced, thus resulting in less friction loss. For this reason the curve in Figure 5.5.2 makes a downward trend after it reaches a maximum value. The lower right side of the parabola reflects the lessened friction coefficients of such surfaces with low roughness concentrations.

The equation obtained for the parabola (5.5.2) would probably not prove to be a good estimator for surfaces with very low and high roughness concentrations, since the method used to obtain spectral estimates for these surfaces do not provide accurate spectral data points for very low or high roughness concentrations. Limits on roughness concentration for these surfaces is presently unknown. However, most surfaces encountered in practice fall within the validity range of (5.5.2).

As is seen in Figure 5.2.2, two data points behave erratically. These data points correspond to surface 5 (K = .88, n = 0.0178) and surface 7 (K = 0.93, n = 0.0150). Close inspection of surface 5 (Figure 5.3.24) indicates that it has almost the same surface configuration and spectral estimates, as well as equivalent Manning "n" friction coefficients. It is suspected that the erratic behavior of this data point resulted from the regression process of (5.5.1) since peaks on spectral estimates with magnitudes less than 0.02 were observed. Since the cutoff value for the peaks included in the regression analysis was 0.02, these peaks were not used.

Surface 7 could not be compared with any other surface because of its uniqueness. However, this surface was regenerated in the computer. The resulting K was 0.33, a value which falls on the appropriate section of the parabola. It is suspected that the number of data points used to describe the surface during the measurement process was insufficient, a property which yielded an erroneous spectral estimate. An unexpected result was also obtained for surface 6 but the cause is unknown to the author.

The comparison between predicted values of
Manning's "n" and values obtained from the literature
(Table 5.6.1) indicates that predicted "n" values differ
from literature values only for plastic tubing. This

			•

result is not unexpected since the wide variety of the corrugated plastic tubing, having different corrugation configurations, should not be expected to be accurately described with only one Manning "n" friction coefficient. It is worthwhile to mention that corrugated tubing with narrow corrugations was found to have "n" values as high as point 0.0178 (Dinc et al., 1971).

#### 7. CONCLUSIONS

The following conclusions may be drawn from this investigation.

- 1. The one-dimensional roughness composition of a surface can be concisely defined by its estimated spectral density function.
- 2. For surfaces with low and high roughness concentrations, the technique developed and reported on in this investigation is not adequate to obtain an accurate spectral density estimate.
- 3. Spectral density estimates of a surface can be characterized by a single parameter, decay coefficient K, defined by an exponential curve fit through the peak values of the spectral density estimates beginning with the largest values at the lowest frequency and fit through data points defined by spectral density estimates whose values are greater than 0.02.
- 4. A parabolic relationship can be used to relate the Manning "n" coefficient and the decay coefficient K in the equation  $n = 0.0044 + 0.045K 0.024K^2$ .
- 5. The proposed equation (5.5.2) can be used to predict the Manning "n" friction coefficients of most surfaces encountered in practice for which Manning's equation can be used to model flow.

#### 8. RECOMMENDATIONS FOR FUTURE WORK

Specific recommendations for future research are:

- 1. Additional one-dimensional artificial roughnesses should be investigated in order to increase the degree of accuracy of the proposed equation (5.5.2).
- 2. This work should be extended to two-dimensional roughness by utilizing multivariate spectral techniques.
- 3. Hydraulic measurements should be collected for each surface analyzed to add further validity to the method.
- 4. The coefficients of the window function should be adjusted to obtain more accurate estimates of spectrum functions for surfaces with low roughness concentrations.

APPENDICES

#### APPENDIX A

### IDENTIFICATION OF SURFACES OBTAINED FROM PREVIOUS INVESTIGATIONS

#### APPENDIX A

### IDENTIFICATION OF SURFACES OBTAINED FROM PREVIOUS INVESTIGATIONS

TABLE A-1.--The surfaces and their corresponding Manning "n" coefficients obtained from the investigations of Ding et al. (1971).

Surface Identification as Used in the Original Paper	Surface Identification as Used in This Study	Manning "n" Coefficient
Michigan Vitrified Tile Co. 5-in. I.D.	5	0.0178
Advance Drainage Systems, Inc., 8-in. ID (Set I)	7	0.0150
Springfield Plastics, Inc. 5.7-in. ID	8	0.0159
Michigan Vitrified Tile Co. 4-in. ID	9	0.0178
Advance Drainage Systems, Inc., 4-in. ID	10	0.0151
Advance Drainage Systems, Inc., 6-in. ID	12	0.0150
Advance Drainage Sys- tems, Inc., 8-in. ID (Set II)	13	0.0180
Canada Dominion Sugar Co., Ltd. 4-in. ID	14	0.0169

TABLE A-2.--The surfaces and their corresponding Manning "n" coefficients obtained from the investigations of Johnson (1944).

Surface Identification as Used in the Original Paper	Surface Identification as Used in This Study	Manning "n" Coefficient
A	18	0.0163
В	19	0.0244
С	20	0.0208
D	21	0.0194
E	22	0.0236
F	23	0.0229
G	24	0.0223
Н	25	0.0240
I	26	0.0240

Table A-3.--The surfaces and their corresponding Manning "n" coefficients obtained from the investigations of E. A. LeRoux, reported by Johnson (1944).

Surface Identification as Used in the Original Paper	Surface Identification as Used in This Study	Manning "n" Coefficient
J	27	0.0158
K	28	0.0222
L	29	0.0198
М	30	0.0204
N	31	0.0219
0	32	0.0177
P	33	0.0222

TABLE A-4.--The surfaces and their corresponding Manning "n" coefficients obtained from the investigations of C. A. Smith and C. Warren, reported by Johnson (1944).

Surface Identification as Used in the Original Paper	Surface Identification as Used in This Study	Manning "n" Coefficient
A	34	0.0112
В	35	0.0185
С	36	0.0200
D	37	0.0170
E	38	0.0149

TABLE A-5.--The surfaces and their corresponding Manning "n" coefficients obtained from the investigations of Powell (1946).

Surface Identification as Used in This Study	Manning "n" Coefficient
39	0.0185
40	0.0231
41	0.0264
42	0.0264
43	0.0217
44	0.0238
45	0.0217
46	0.0186
47	0.0156
	39 40 41 42 43 44 45

#### APPENDIX B

# FORTRAN IV PROGRAM FOR ESTIMATION OF AUTOCORRELATION AND POWER SPECTRUM DENSITY FUNCTIONS

#### APPENDIX B

## FORTRAN IV PROGRAM FOR ESTIMATION OF AUTOCORRELATION AND POWER SPECTRUM DENSITY FUNCTIONS

The following FORTRAN IV program is for the calculation of autocorrelation and power spectrum estimates.

The total program consists of the main program, MAIN, and subroutines, AUTO and POWER.

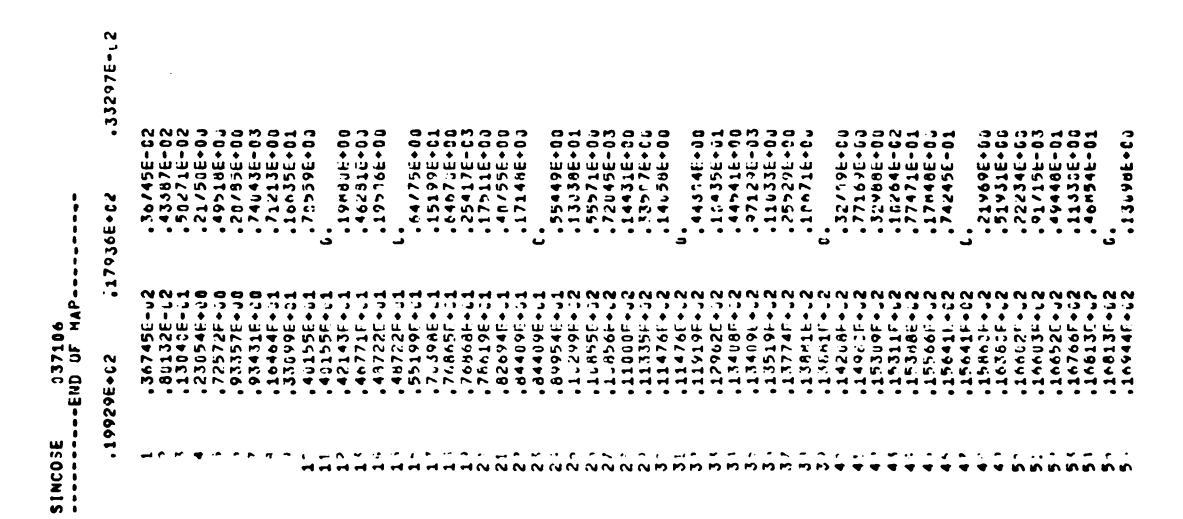
The main program, MAIN, defines the number of data points, N, and the maximum lag values, M. After the subroutines are called, it determines the cutoff frequency at which 90 percent of the power occurs under the spectral density curve.

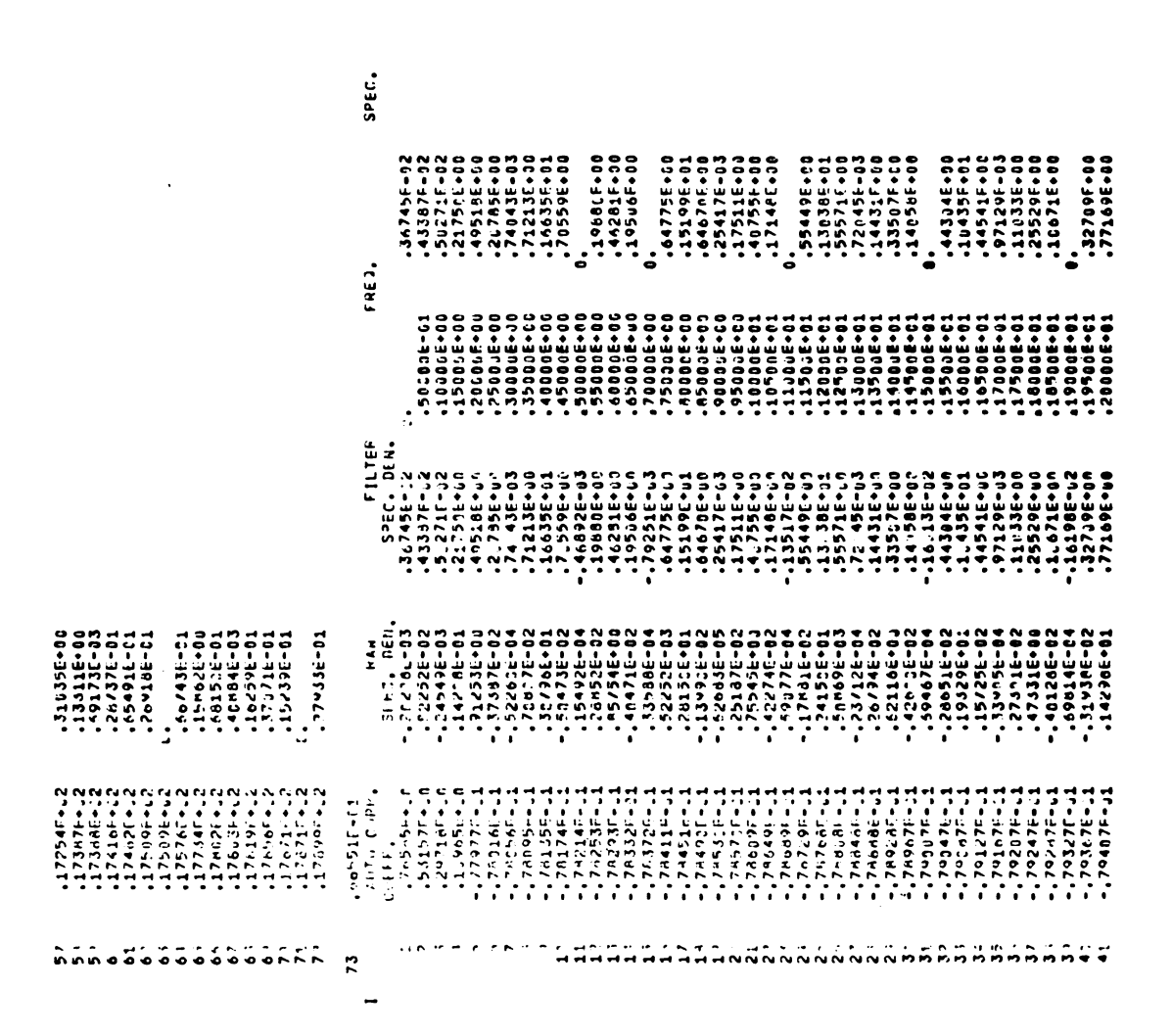
Subroutine AUTO calculates the expected values, AV, and the variance, RO, of the data. It then normalizes the initial data, Y(I). Finally, it determines the autocorrelation estimates R(J). R(J) is obtained by dividing autocovariance estimates, R(J), by the variance, RO.

Subroutine POWER defines the sampling interval, DELX; calculates the frequency, FR(J); the raw spectral estimates, S(J); and smoothed spectral estimates, U(J).

PROGRAM	HAIN CDC 6500 FTM V3.U-P376 OPT=1	17/30/74 .13,44.31.	PAGE
	PROGRAM PAIN (19PUT,CJTPJT,TAPE4,TAPE60*INPUT,TAPE61*UUTPUT)		
	D114 0-171, 17521) CHRIDIVA/4661), 4(461), 2(4, 1), M.N.RO		
	CHRINGH/P/5(261),U(241),FR(2(1)		
r.	• 7 H L L		
	HEZO		
10	IC KEASCOLUBES (1)		
	Calledon Andrew Control of the Calledon		
	174.41 H		
•	50 Y(K) 8Y(1)		
£	23 CHATIME 1100 F 110 F I10 F		
	כארו אחזי		
	CALL POSES		
20	90 1stel 90 00		
	P(1) x (1)		
	UF T		
;	SEMBO		
52	DO SOLUTION OF THE CONTRACT OF		
	EDICATO CHACOLIC		
	Paralle Second S		
	655 FURNAT (12X, 3E15,5,7)		
Ë	Trip & O.		
	30 55, lat.199		
	7.204.707.40.10 11.104.10.10.10.10.10.10.10.10.10.10.10.10.10.		
	G: 10 745		
3,5	746 PHINT 6, 3, 1, TUP, P(1)		
	Xale1		
	OLD FORMAT(* ** 10% ZELD*)		
	25.5 PHINT 7.0.K. (4)		
<b>-</b>	7.0 FORMAT(7,104,15,E15,5)		
	######################################		
	11 12 (01 ,000)		
,	W. TE(4.226) 1,4(1),5(1), J(1),FR(1),P(1)		
<b>4</b> 5	TO THE THEORY FORD THE CONTROL OF TH		
	,		
		•	
50	10-17/N-0-17 Cueff		
	X 9.		
SURMO - INF	Anth CDC 5503 F74 675-6276	17:5774 .13:44.31.	7 6 6 8
	Suppose that the second		
ď			
	(1) A+R CH = 5 11		

```
CDC 6500 FTN V3.6-P376 OPT=1 37/30/74 .13,44.31.
                                                                                                                                                                                                       SUBROUTINE POWER
COMMOW/A/Y(4001),R(401),X(4001),M,N,RO
COMMOW/R/S(201),U(201),FR(201)
                                                                                                                                                                                                                                                                                                                                                                                20 SHR=SUM+2.0+(I)+CUS(P+P,H)
FP(J)=P1/(2.+A+DELX)
10 S(J)=(1.+FUM+M(M1)+CUS(P1+P2))+DELX+2.
U(1)=U.46*S(2)+U.54*S(1)
30 J=2.M2
30 U(J)=U.73*S(J-1)+0.54*S(J)+[.23*S(J+1)
H(H)=U.46*S(H2)+0.54*S(H)
DO 15 I=1.h
                                                                   CJ=...
N2=N-J
DO 56 I=1.N2
IJ=J+I
DZ=CJ+Y(I)*Y(IJ)
                                                                                                                                     K(J)=CJ/J2
K(J)=K(J)/R7
RETUFL
E4D
                                                                                                                                                                                                                                                     P2=3.1415927
DELX=J..5
PH=P2/A"
M1=H
M2=H-1
H3=H+1
DN 10 J=1.H3
SVH=0.0
DN 20 I=1.H2
P1=J-1
                                    Pu 40 J=1.8
                       PO=SUNZAN
                                                                                                                                                                                                                                                                                                                                                                                                                                                                RETUR.
                                                                                                                                                                                                                                                                                                                                                                         P=P1+I
                                                                                                                                                                                                                                            AYER
                                                                                                                                                                                    POWER
                                                20
                                                                                                                  ر.
0
                                                                                                                                                                                  SUBRO IT 11E
                                                                     £1
                                                                                                                                                                                                                                                       ĸ.
                                                                                                                                                                                                                                                                                                                                                                       ۲.
۲.
             10
                                                                                                                            5
                                                                                                                                                                                                                                                                                                                10
                                                                                                                                                                                                                                                                                                                                                                                                                                20
```





<b>`</b>	-,79447F-31	3135E-0	2986E+3	.2050aE+01	2988E+0
ž	70487F-0	5/13E-0	1,264E-0	1000E+0	10264E
•;	.70528E-u	5354E-0	77471E-3	1500E+0	7471E-0:
<u>,</u>	.79568F-2	33092E+0	17848E+0	2000E-0	17648E+0
<u>.</u>	153375-0	34822E-0	74245E-0	2501E+C	.74245E-0
	11029F+	62463E-0	14534E-0	33036.0	
	29406F+5	29836E-0	21969E+0	3500E+C	219695+3
·	3-0-1C-0-0	10041100	21731E*B	45005-0	91 V 31 E + J
, in	38900F+.0	35v75E-04	.91715E-L3	25000E+01	.917156-93
ŗ.	20415E+	21074E-0	4944BE-	5500E+0	4044EF-5
ŭ,	10651F+	.210-9E+0	11330E+0	630JE+0	11339E+0
	137564-	27393E-0	46854E-U	6503E+0	46854E-0
, ^ "		. 49+35E-3	11575F-L	7000E+0	
, ,	1000	3-16:14:	13.70E**	/200E+0	13096k + 30
	01675	0/7 OF * 0	31.37E*U		0100110 11100110
, ic		15675E=0	13311E*E	9-10000	13311E+3
	0.445	2 - 1 - 2 - 4	247.75-1	040000	0-1217-0
٠.	0204F	12145E+0	654916-6	0.0000	654916-1
	ij	18748E-0	26918E-u	0503E+0	69146-3
•	03646-	34043E-P	79654E-L	1300E+C	
	- 350 bu	10498E-0	66743E-U	1503E+0	66743F-1
	04456-	294-3E+6	15862E+6	2000E+C	15862F+J
<u>.</u> .	04455	. 376.39E-D	66153E-0	2500E+0	.6815¢E-01
۰ ،	- 10/6	140346-6	4,634E-U	3430000	456841-3
		13338-0-1	16229E-U	30000	105291
		0-30040	101//2	45000	
	9637F	19241E-0	43503F-0	5.00E+C	114577
٠. ٢	コールをへいり	0/44E-0	.27933E-u	55036+6	27933E-0
	07635-	123476+0	66551F-6	600LE+0	66551F-3
	160464	.1456710	20553E-L	J+30050	.28583F-31
	706495	72.56.2E-C	127,86-0	70CCE+0	127ubf-3
.;	736.078-	14466-0	1.396E-L	750.00	113965-0
	70.77	77.476-0	14 125-5	1000 E	24 - 15 C = 17 C
. ~	121	(73451-7	1:7.45	9307E	
. ~	6. 5221	19/7:6-0	111996-0	9500Fe	111021-6
•	0-1986-0	.491476-8	2644BF-J	P303E+C	.2644rF-91
 c ·		94196-3	1:1991-0		111966-0
D 4		2-3720/	1, 234F • 6	1000	
	10.000	7-305-7-8	111111	1 1 2 2 2 2	0-116.71
		37106-6	1:5196-	2500E+6	12516F-31
٠,	8.33AF	2465£-B	91491E-U	320 JE+C	91401F-0
	0.378f	27265L-C	1.2.9E-L	STORES	102. VE-P
		. 437495	2:223E-J		23555-1-1
·		11/10/10/10	7.373E-C		0 - 17cc/6
	142	57647E-0	16442E-1	550 LE+C	164421-0
,. •	.543F	724274-0	305950	6.300k+r	392846-5
 • •	<u>'</u> .	.41164c-n	16971E-0	656JE+F	.166716-61
		17006-0	Z. 880E-U	/303E+0	20080F-3
	1/1/1	10101-3	A 7 4 5 HE - L	9441377	174366-7
	OF ME	747645-0	4. 222E	45005+0	46666
-	6408Fe.	142736-0	322516-1	930.6+0	0-100/64
- 01	J003F	49415E-0	21217E-	9502E+0	.21217E-3
. 01	4546F+L	33856E-0	5.635E-u	OOC UE+9	.50635F-01
. 01	176678	46>61E-0	2:847E-L	0-300-0	21647E-0

## APPENDIX C

# FORTRAN IV PROGRAM FOR ESTIMATION OF DECAY COEFFICIENTS

#### APPENDIX C

## FORTRAN IV PROGRAM FOR ESTIMATION OF DECAY COEFFICIENTS

The following FORTRAN IV program is for determining the decay coefficient of the estimated power spectral function. The program is composed of the main program, MAIN, and subroutines PEAK and LEASTSQ.

The main program, MAIN, defines only the number of different sets, N.

Subroutine PEAK searches the peaks in the spectrum function whose magnitudes are greater than FTLN (FTLN was assumed to be 0.02 in this study) after the highest peak in the data was found. First, the data is scanned and the highest peak is determined and stored. At this point, the following peaks, A(I), whose magnitudes are greater than 0.02 are found and stored along with the corresponding frequencies, B(I).

Subroutine LEASTSQ determines the standard deviation, STAND, of A(I), and then calculates the decay coefficient, S, and  $K_O$ , BE, in (5.5.1) by using the least square regression method.

PROGRAM	HAIN	CDC 6900 FTM V3.6-P366 OPT-1	18/06/74 +23.44.21.	E 4 0 E
	PROGRAM HAI'N COUTPUT,TAPE4,TAPE61mOUTPUT) COMMON K(203),Y(208) COMMON A(103),B(108),M1,NPT	001901)		
<b>s</b> r.	7 3 2 3 2 3 2 5 5 6 7 6 7 6 7 6 7 6 7 6 7 6 7 6 7 6 7			
10				
	10 [=]+1 READ(4,150) X([),Y([)			
	f(EOf(4)) 0,10 9 NPT=1-1			
15	CALL PEAK			
	100 FORMATCRAX, 2515, 5)			
20	202	3 2 3 3 4 4 4 4 4 4 4 4 4 4 4 4 4 4 4 4	9 B	
	TRAK	CDC 0300 716 45,017500 07111 18/062/4 548,44,41.	. 12.22. 4/20/21	
·	SUBROUTINE PEAK COHHOW KIZED, V(ZDD) COHHOW A(103), 04(130), 12,NPT DIMERSION S(107), 7(160)			
<b>e</b> n	A45xed.c			
	11 1 1 1 1 1 1 1 1 1 1 1 1 1 1 1 1 1 1			
10	IF(V(I),GE,AMAX) GO TO 30 20 CONTITUDE			
	30 10 40 80 80 80 80 80 80 80 80 80 80 80 80 80			
15	AMAXBY(1) GO TO 29			
	XATA OLIVIA			
,				
07				
	IFFENDAL'S GO TO SO OF SO TO SO TO SO OF SO TO SO TO SO OF SO TO SO OF SO TO S			
25				
	71 Neh+1 IF(V(N),GE,AHAK) GO TJ 46			
en.	GO TO BA			
	60 TO 71 89 Mer-1			
	X4148(1)5			
35	00 CO TO			
E T	Un 29 Jane 2			

```
PAGE
                                                                                                                                                                                                                                                                                                                                                                                                                                                                                                                                                            CDC 6900 FTN V3,0-P380 OPT#1 11/06/76 423,44,21.
                                                                                                                                                                                                                                                                                                                                                                                                                                                                                                                                                                                                                                                                                                                                                                                                                                                                                                                                                                                                                                                                                                                                                                                                                                                                                                                                                                                                                                                                                                                                                                                                                                                                      A(KH) = S(J)

B(KH) = T(J)

B(KH) = T(J)

B(KH) = T(J)

G(T) = T(T) = T(T) = T(T)

B(T) = T(T) = T(T
                                                                                                                                                                                                                                                                                                                                                                                                                                                                                                                                                                                                                                                                             COMMON X(205),Y(205)
COMMON A(105),B(100),M1,NPT
CALCULATION OF STANDARD DEVIATION
SUPED.
                                                                                                                                                                                                                                                                                                                                                                                                                                                                                                                                                                                                                                                                                                                                                                                                                                                                                                                                                                                                                                                                                 VARSUH/AN
STANDEVAR**0.5
CALCULATION OF LEAST SQJAHE FIT
SUHXYBO.
                                                                                                                                                                                                                                                                                                                                                                                                                                                                                                                                                                                                                                                                                                                                                                                                                                                                                                                                                                                                                                                                                                                                                                                                                                                                                       SCHWZEG

SCHWZEG

DO 1 11, M1

X(1) BP(1)

Y(1) BR(1)

Y(1) BR(1)

SCHWZESCHWY+Y(1)

SCHWZESCHWY+Y(1)

SCHWZESCHWY+Y(1)

SCHWZESCHWY+Y(1)
                                                                                                                                                                                                                                                                                                                                                                                                                                                                                                                                                                                                                                                                                                                                                                                                                                                                                                                                                                                                                                50 20 14 (41 1)-AV) +2)
                                                                                                                                                                                                                                                                                                                                                                                                                                                                                                                                                                                                                               SUBROUTINE LEASTSO
                                                                                                                                                                                                                                                                                                                                                                                                                                                                                                                                                                                                                                                                                                                                                                                                                                                                                                        SUMESUM+A(1)
AVESUM/AN
SUMED.
                                                                                                                                                                                                                                                                                                                                                                                                                                                                                                                                                                                                                                                                                                                                                                                                                                     AN=H1
D0 10 1=1.H1
25 GONTINUE
                                                               63 K'AKH+1
                                                                                                                                                                                                                                                                                                                                                                                                                                                                                                                                                            SUBROUTINE LEASTSO
                                                                                                                                                                                                                                                                                                                                                                                                                                                                                                                                                                                                                                                                                                                                                                                                                                                                                                                                                                                                                                                                                                                                                                                                                                                                                                                                                                                                                                                                                                                                                                                                                                                                                                                                                                                                                                                                            110
                                                                                                                                                                                                                                                                                                                                                                                                                                                                                                                                                                                                                                                                                                                                                                                                                                                                                                                                                                                                                                                            20
                                                                                                                                                                                                                                                                                                                                                                                                                                                                                                                                                                                                                                                                                                                                                          ပ
                                                                                                                                                                                                                                                                                                                                                                                                                                                                                                                                                                                                                                                                                                                                                                                                                                                                                                                                                                                                                                                                                                                                                                                ပ
                                                                                                                                                                                                                                                                                                                                                                                                                                                                                                                                                                                                                                                                                                                                                                                                                                                                                                                                                                                                                                                                                                                                                                                                                                                                                                                                                                                                                                                                                                                                                                                                                                                                                                                                                       30
                                                                                                                                             .
                                                                                                                                                                                                                                                                                                                                    20
                                                                                                                                                                                                                                                                                                                                                                                                                                                                                                                                                                                                                                                                                                                                                                                                                                                                                                                                                                                         10
                                                                                                                                                                                                                                                                                                                                                                                                                                                                                                                                                                                                                                                                                                                                                                                                                                                                                                                                                                                                                                                                                                                                                                                                                                                                                                                                                                                                                                                                                                                                                                   د.
                                                                                                                                                                                                                                                                                                                                                                                                                                                                                                                                                                                                                                                                                                                                                                                                                                                                                                                                                                                                                                                                                                                                                                                                                                                                                                                                                                               20
                                                                                                                                                                                                                                                                                                                                                                                                                                                                                                                                                                                                                                                                                                                                                                                                                                                                                                                                                                                                                                                                                                                                                                                                                                                                                                                                                                                                                                                                                                                                                                                                                                                                                                                                                                                                                                                                                                                                                  35
```

FREQUENCY	00 CC	001090	00	4.000	00	480	66 50 50	.0000	. 200	4000	00000	0000	2000	6009		0.00	.40.0	.6000	.000	.2000	900	2000
PEAK	300	950	288	583	750	410	284 643	101	363	150	213	454	559	695	7 9	648	576	387	286	161	162	.02328
	~ev	ne	w∙o	<b>7</b> 80	<b>~</b> =	ч <b>і</b> лі	154	w.	<b>6</b> 6	<b>80</b> ,0×	94	! 2	<b>5</b>	Ē,	0.5	. 60	<b>o</b> .	<u> </u>	2	m 4	ino	7.00

## APPENDIX D

# FORTRAN IV PROGRAM FOR CALCULATION OF THEORETICAL POWER SPECTRUM DENSITY FUNCTIONS

### APPENDIX D

# FORTRAN IV PROGRAM FOR CALCULATION OF THEORETICAL POWER SPECTRUM DENSITY FUNCTIONS

The following FORTRAN IV program is for the calculation of theoretical power spectrum density functions.

The program MAIN first defines the width W and the height A of a rectangular surface element.

D is defined as the distance between two rectangular elements.

CF is the constant which is used to correlate theoretical spectrum with estimated spectrum values.

S(M) is the theoretical spectrum values calculated from equation (5.7.7, b).

SN(M) is the normalized theoretical spectrum values [equation (5.7.12)].

Property of the Paris	我也也不能也有我们有什么,我们是一个一个一个一个一个一个一个一个一个一个一个一个一个一个一个一个一个一个一个	4014100	A STATE OF A STATE OF	COC COC FIN VG.OFFFFFFFFFFFFFFFFFFFFFFFFFFFFFFFFFFFF
	dt1)	の)102.1    AIM   (14PUT.01P)  T.474PE4) 以内に引き、3209)。S+(300)。P(3m5)。SS(40)。FR(305)	นีว) "FR (จิญกิ)	
Ľ.	C 1 + 12 C C C C C C C C C C C C C C C C C C			
	(829 To 1 1 1 1 1 1 2 2 3 3 3 3 3 3 3 3 3 3 3 3			
	大学 ない かいました はない かんかい かんかい かんかい かんかい はんかい はんかい はんかい はんか			
E ,1	1000 mg / mg			
	11			
ىد . •	12			
	7×=×7×1 7×(×7)=1			
	Output to Control			
2r	)+(1495-1461)+(	このではもこのもつもしいのこととではない。 ではない		
	1 1 1 1 2 2 1 1 4 4 1 1 2 2 3 4 (a)	HNS+(6++((F+C)/((F+C))(I()))+(8++)	J+4))++2)+S(IH	
<b>5</b> .	(C+F)   CH   CH   CH   CH   CH   CH   CH   C	((tarena(2**V)))/(r		
	Sent of the factor of	1, Sugar, 50, 135011		
	71 - 71 Tate 27 1 4 (1)	(1)38*(1)		
د. ع	THE TOTAL STATES AND SELECT THE S	.5} 4623.5)		
٠,	T 42 35 C.	* 32249E+73	50-305166.	,737105-92
¥. 4.*		57-3169-2	550725-03	.79555-62
.,		. 394746- 3	.13012F-32	. 894365-122
1.32	€ 2 € B € 7 € 5 € 6	S. 450 641.	3145F-02	10-3478-61
1.97	\$1+84-34F	.617485-13	.171725-02	. 142365-01
1.33		.928425-73	.25622F-62	.213539-01
er er ev	40 - C C C C C C C C C C C C C C C C C C	.1782JE-[2	.49543F-92	.419458-112

LIST OF REFERENCES

#### LIST OF REFERENCES

- Basha, M. A. (1961). Resistance Characteristics of Artificially Roughened Open Channels in Relation to those of Alluvial Channels, Thesis submitted to the University of Roorkee in partial fulfillment of the requirements for the degree of Master of Engineering.
- Bazin, H. E. (1865). Recherches Hydrauliques, Memoires presentes par divers savants, Science, Mathematiques et Physiques, Series 2, Vol. 19.
- Bendat, J. S., and Piersol, A. G. (1966). Measurements and Analysis of Random Data, Wiley and Sons, New York
- Blackman, R. B., and Tukey, J. W. (1958). The Measurements of Power Spectra from the Point of View of Communications Engineering, Dover Publications, Inc., New York.
- Blasius, H. (1913). Das Ahnlichkeitsgesetz bei Reibungsvorgangen in Flussigkeiten, Forsch-Arb., Ing.-Wes. Heft 131, Berlin.
- Burney, J. R., and Higgins, L. F. (1973). Hydraulics of Shallow Flows Over Stable Eroded Sand Surfaces Defined by Aerial Spectra, Technical Report No. 36, Purdue University Water Resources Center, Lafayette, Indiana.
- Chang, F. F. M. (1970). Ripple Concentration and Friction Factor, Journal of the Hydraulics Division, ASCE, Vol. 96, HY2, pp. 417-429.
- Chiu, C. (1968). Stochastic Open Channel Flow, Journal of the Engineering Mechanics Division, ASCE, Vol. 94, EM3, pp. 811-822.
- Chow, Ven-Te (1955). Open Channel Hydraulics, McGraw-Hill Book Co., New York.

- Colebrook, C. F. (1939). Turbulent Flow in Pipes with Particular Reference to the Transition Region Between the Smooth and Rough Pipe Laws, Journal, Ins. of Civ. Engrs., Vol. 11, pp. 133-156.
- Colebrook, C. F., and White, C. M. (1937). Experiments with Fluid Friction in Roughened Pipes, Proceedings, Royal Soc. of London, Series A, Vol. 161, pp. 367-381.
- Dinc, G., Merva, G. E., and Kidder, E. H. (1971).

  Hydraulic Roughness of Corrugated Plastic Drain
  Tubing, National Drainage Symposium Proceedings,
  ASAE.
- Einstein, H. A., and Banks, R. D. (1950). Fluid Resistance of Composite Roughness, Transactions, Amer. Geoph. Union, Vol. 31, No. 4, pp. 603-610.
- Herbich, J. B., and Shulits, S. (1964). Large-Scale Roughness in Open-Channel Flow, Journal of the Hydraulics Division, ASCE, Vol. 90, No. HY6, pp. 203-230.
- Houbolt, J. C. (1961). Runway Roughness Studies in the Aeronautics Field, Journal of the Air Transport Division, ASCE, Vol. 87, No. AT1, pp. 11-31.
- Houbolt, J. C., Walls, J. A., and Smiley, R. F. (1955).
  On Spectral Analysis of Runway Roughness and Loads
  Developed During Taxiing, NACA TN 3484.
- Houk, I. E. (1918). Calculation of Flow in Open Channels, Miami Conservancy District Technical Reports, Part IV.
- Hutchinson, G. B. (1965). Analysis of Road Roughness Records by Power Spectral Density Techniques, Report No. 101, Dept. of Highways, Ontario, Canada.
- Jenkins, G. M., and Watts, D. G. (1969). Spectral Analysis and Its Applications, Holden-Day, San Francisco.
- Johnson, J. W. (1944). Rectangular Artificial Roughness in Open Channels, Trans. Amer. Geophys. Union, pp. 906-914.
- Keulegan, G. H. (1938). Laws of Turbulent Flow in Open Channels, Journal, Nat'l. Bureau of Standards, Washington, D.C., Research Paper 1151, Vol. 21, pp. 707-741.

- Koleseus, H. J., and Davidian, J. (1966). Free Surface Instability Correlations and Roughness-Concentration Effects on Flow Over Hydrodynamically Rough Surfaces, Geological Survey Water-Supply Paper 1592-C.D., U.S. Gov't. Printing Office.
- Lee, Y. W. (1960). Statistical Theory of Communication, John Wiley & Sons, Inc., New York.
- Leopold, L. B., and Wolman, M. G. (1957). River Channel Patterns: Braided, Meandering and Straight, Geological Survey Prof. Paper 282-B, U.S. Gov't. Printing Office.
- Limerinos, J. T. (1970). Determination of the Manning Coefficient From Measured Bed Roughness in Natural Channels, Geological Survey Water-Supply Paper 1898-B, U.S. Gov't. Printing Office.
- Manning, R. (1891). On the Flow of Water in Open Channels and Pipe, Transaction, Inst. of Civ. Engr., Ireland, Vol. 20, pp. 161-207.
- Martinelli, R. C. (1947). Trans. ASME, Vol. 69.
- Mirajgauker, A. G., and Charlu, K. L. N. (1963). Natural Roughness Effects in Rigid Open Channels, Journal of the Hydraulics Division, ASCE, Vol. 89, No. HY5, pp. 29-44.
- Morris, H. M. (1955). A New Concept of Flow in Rough Conduits, Transactions, ASCE, Vol. 120, pp. 373-410.
- Neil, C. R. (1962). Hydraulic Roughness of Corrugated Pipes, Journal of the Hydraulics Division, ASCE, Vol. 88, No. HY3, pp. 23-44.
- Nikuradse, J. (1933). Stromungsgezetze in Rahhen Rohren, Vein Deutscher Ingenieure, Forschumagasheft 361 (English translation: Laws of Fluid Flow in Rough Pipes, The Petroleum Engineer), Part 1, March 1940, pp. 164-166; Part 2, May 1940, pp. 75-82; Part 3, June 1940, pp. 124-130; Part 4, July 1940, pp. 38-42; Part 5, August 1940, pp. 83-87.
- Nordin, C. F., and Algert, J. H. (1966). Spectral Analysis of Sand WAves, Journal of the Hydraulics Division, ASCE, Vol. 92, No. HY5, Proc. Paper 4910, pp. 95-114.

- Potter, D. M. (1957). Measurements of Runway Roughness of Four Commercial Airports, NACA RM L56126.
- Powell, Ralph W. (1946). Flow in a Channel of Definite Roughness, Transactions, ASCE, Vol. 111, pp. 531-566.
- Powell, Ralph W. (1950). Resistance to Flow in Rough Channels, Transactions, Amer. Geophys. Union, Vol. 31, pp. 575-582.
- Powell, Ralph W. (1968). The Origin of Manning's Formula, Journal of the Hydraulics Division, ASCE, Vol. 94, No. HY4, pp. 1179-1181.
- Prandtl, L. (1904). Heber Flussigheit, Shewegung bei sehr kleiner Reibung, Verhandlungen, 3rd Internat'l. Mathematiker Kongresses, Heidelberg.
- Raju, K. G. R., and Garde, J. G. (1970). Resistance to Flow Over Two-Dimensional Strip Roughness, Journal of the Hydraulics Division, ASCE, Vol. 96, No. HY3, pp. 815-833.
- Roberson, J. A., and Chen, C. K. (1970). Flow in Conduits with Low Roughness Concentration, Journal of the Hydraulics Division, Vol. 96, No. HY4, pp. 941-957.
- Robinson, A. R., and Albertson, M. L. (1952). Artificial Roughness Standard for Open Channels, Trans. Amer. Geophys. Union, Vol. 33, No. 6, pp. 881-888.
- Rouse, H., and Ince, S. (1957). History of Hydraulics, Iowa Inst. of Hydraulic Research.
- Rouse, Hunter (1965). Critical Analysis of Open-Channel Resistance, Journal of the Hydraulic Division, ASCE, Vol. 91, No. HY4, Proc. Paper 4387, pp. 1-25.
- Sayre, W. W., and Albertson, M. L. (1961). Roughness Spacing in Rigid Open Channels, Journal of the Hydraulics Division, Vol. 87, No. HY3, May, 1961, pp. 121-149.
- Schlichting, H. (1968). Boundary Layer Theory. McGraw-Hill Book Co., Inc., New York. 6th Edition.
- Skoglund, V. S. (1936). Effect of Roughness on the Friction Coefficient of a Closed Channel, Journal of the Aeronautical Sciences, pp. 28-29.

- Squarer, D. (1970). Friction Factors and Bed Forms in Fluvial Channels, Journal of the Hydraulic Division, ASCE, Vol. 96, No. HY4, pp. 995-1017.
- Streeter, V. L. (1936). Friction Resistance in Artificially Roughened Pipes, Transactions, ASCE, Vol. 101, 1936, pp. 681-713.
- Task Force Report (1963). Friction Factors in Open Channels, Progress Report, Journal of the Hydraulics Division, ASCE, Vol. 89, No. HY2, pp. 97-143.
- Taub, H., and Schilling, D. L. (1971). Principles of Communication Systems, McGraw-Hill Book Co., New York.
- Thompson, W. E. (1958). Measurements and Power Spectra of Runway Roughness at Airports in Countries of the North Atlantic Treaty Organization, NACA TN 4303.
- Vanoni, V. A. (1953). Some Effects of Suspended Sediment on Flow Characteristics, Proceedings, 5th Hydraulics Conf., Iowa State University, Iowa City, Iowa, pp. 137-158.
- Vanoni, V. A., and Hwang, L. (1967). Relation Between Bed Forms and Friction in Streams, Journal of the Hydraulic Division, ASCE, Vol. 93, No. HY3, pp. 417-429, Proc. Paper 5243, pp. 121-144.
- Walls, J. H., Houbolt, J. C., and Press, H. (1954). Some Measurements and Power Spectra of Runway Roughness, NACA TN 3305.
- Williams, G. P. (1970). Manning Formula A Misnomer?

  Journal of the Hydraulics Division, ASCE, Vol. 96,

  No. HY1, pp. 193-200.

